



UNIVERSITAT
POLITÈCNICA
DE VALÈNCIA



ESCUELA TÉCNICA
SUPERIOR INGENIEROS
INDUSTRIALES VALENCIA

MASTER THESIS FOR THE MASTER OF POLYMERS AND PROCESSES WITH IFP SCHOOL (IFP SCHOOL) AND FOR THE MASTER OF CHEMICAL ENGINEERING IN THE POLYTECHNIC UNIVERSITY OF VALENCIA (UPV)

ANALYSIS AND STUDY OF DATA CONSISTENCY FOR ELECTROLYTE SYSTEMS WITH PURE WATER AND MIXED SOLVENTS.

Direction of Physico-Chemistry and Applied Mechanics

Department of Thermodynamics and Molecular Modelling

AUTHOR: SANTIAGO VAQUÉ AURA

SUPERVISOR: JEAN-CHARLES DE HEMPTINNE

Academic Course: 2019-2020

RESUMEN

Durante los últimos años, la necesidad de mejorar los modelos termodinámicos, haciéndolos más precisos y predecibles para sistemas complejos, ha aumentado [1]. La complejidad de los sistemas electrolíticos se debe principalmente a las fuertes interacciones entre los iones, las fuerzas de hidratación generadas durante la disociación de la sal y las fuerzas físicas a altas concentraciones de soluto. Estas fuerzas dificultan la precisión en los cálculos del equilibrio de fases en las mezclas electrolíticas. En consecuencia, los modelos termodinámicos de electrolitos existentes muestran algunas limitaciones y están lejos de estar completamente optimizados para las simulaciones industriales. La termodinámica basada en mezclas de electrolitos y disolventes mixtos requiere un mayor desarrollo e investigación [2].

Para hacer frente a ese problema, en el presente trabajo se presenta una estrategia para analizar la coherencia interna y externa de los datos experimentales en las mezclas de electrolitos. La coherencia interna es la identificación de datos inconsistentes para un sistema específico. Para ello, se establece una metodología sencilla para analizar las desviaciones entre los datos experimentales de las diferentes propiedades termodinámicas, y el modelo termodinámico "Electrolyte Non-Random Two-Liquid" (eNRTL). El objetivo es analizar las desviaciones de los datos disponibles e identificar las causas de las desviaciones más relevantes.

Por otro lado, el objetivo de la coherencia externa es identificar las posibles relaciones lógicas entre las propiedades físicas de los sistemas y el parámetro de un modelo termodinámico. El análisis correcto de estas relaciones proporciona información sobre el comportamiento de los sistemas electrolíticos y también puede ser útil para la predicción y la extrapolación de los parámetros. Para una interpretación simplificada y precisa de los resultados, la coherencia externa requiere la selección de un modelo electrolítico con un bajo número de parámetros. El modelo de Bromley, que sólo depende de un parámetro ajustable [3], ha sido seleccionado después de ser comparado con otros modelos simplificados. El parámetro ajustable B de Bromley ha sido optimizado y estudiado para diferentes sistemas electrolíticos y para diferentes condiciones. El parámetro se relacionó con las propiedades físicas de los componentes para definir posibles relaciones lógicas entre ellos.

Los sistemas electrolíticos representan una mezcla entre sales y disolvente a diferentes condiciones (temperatura, presión, concentración de sales). Los sistemas estudiados están compuestos por las sales monovalentes más comunes, agua pura y un alcohol primario (metanol, etanol, 1-propanol, 1-butanol). Los datos disponibles de los sistemas descritos se han resumido y analizado en función de las diferentes propiedades termodinámicas estudiadas.

Palabras clave: **Coherencia de datos; Modelos termodinámicos electrolíticos; Modelo de Bromley; Modelo eNRTL; Sistemas electrolíticos; Disolventes mixtos; Propiedades termodinámicas.**

ABSTRACT

In the recent years, the need to improve the thermodynamic models, making them more precise and predictable for complex systems, has increased [1]. The complexity of electrolyte systems is caused by the strong interactions between ions, the hydration forces that take place during salt dissociation, and the physical forces at high concentrations of solute. These forces make difficult the calculations of phase equilibrium in electrolyte mixtures. Consequently, the existing thermodynamic electrolyte models show some limitations and are far from being completely optimized for industrial simulations. Thermodynamics based on electrolyte mixtures and mixed solvents requires further development and research [2].

To deal with that problem, the present work presents a strategy to analyze the internal and external consistency of experimental data in electrolyte mixtures. Internal consistency is the identification of inconsistent data in a specific system. For that purpose, a simple methodology to analyze the deviations between the experimental data of different thermodynamic properties, and the Electrolyte Non-Random Two-Liquid (eNRTL) thermodynamic model, is established. The objective is to analyze the deviations for the available data and to identify the causes of the more relevant deviations.

On the other hand, the objective of external consistency is to identify logical relations between the physical properties of systems and the parameter of a thermodynamic model. The correct analysis of these relations gives information about the behavior of electrolyte systems and may also be useful for parameters predictions and extrapolation. For a simplified and precise interpretation of results, external consistency requires the selection of an electrolyte model with low number of parameters. The Bromley model, which only depends on one adjustable parameter [3], has been selected after being compared to other simplified models. The adjustable parameter B of Bromley has been optimized and studied for different electrolyte systems. The parameter was related to the physical properties of components in order to define potential logical relations between them.

Electrolyte systems represent a mixture between salts and solvent at different conditions (temperature, pressure, concentration of salts). The systems studied are composed by the most common monovalent salts, pure water, and a primary alcohol (methanol, ethanol, 1-propanol, 1-butanol). The available data of the described systems have been summarized and analyzed for the different thermodynamic properties studied.

Key words: Data consistency; Electrolyte thermodynamic models; Bromley model; eNRTL model; Electrolyte systems; Mixed solvents; Thermodynamic properties.

TABLE OF CONTENTS

1.	INTRODUCTION	4
1.1	SCOPE OF THE WORK	5
1.2	APPLICATIONS OF ELECTROLYTES	8
1.3	OBJECTIVES.....	12
1.4	METHODOLOGY FOR DATA CONSISTENCY ANALYSIS	13
2.	DEFINITIONS AND PROPERTIES IN ELECTROLYTE SYSTEMS	15
2.1	CONCENTRATION UNITS FOR ELECTROLYTE SYSTEMS	15
2.1.1	Molarity (mol of solute/volume (L) of solution).....	15
2.1.2	Molality (mol of solute/kg of solvent).....	15
2.1.3	Molar fraction.....	17
2.2	THERMODYNAMIC PROPERTIES IN ELECTROLYTE SYSTEMS.....	19
2.2.1	Definition of chemical potential.....	19
2.2.2	Definition of fugacity in relation with chemical potential.....	20
2.2.3	Activity coefficient.....	23
2.2.4	Osmotic coefficient and osmotic pressure.....	27
2.2.5	Vapor-liquid equilibrium	31
2.2.6	Solid-liquid equilibrium	32
2.2.7	Definitions of enthalpies	33
3.	THERMODYNAMIC MODELS FOR ELECTROLYTE SYSTEMS.....	37
3.1	TYPES OF INTERACTIONS IN ELECTROLYTE SYSTEMS.....	37
3.2	MODELS FOR LONG RANGE INTERACTIONS.....	38
3.2.1	The Debye-Hückel theory.....	38
3.2.2	Debye Hückel limiting law	40
3.2.3	Extended Debye-Hückel	41
3.3	EMPIRICAL MODELS FOR SHORT RANGE INTERACTIONS	42
3.3.1	Hückel model description.....	42
3.3.2	Bromley model description	42
3.3.3	Pitzer Debye-Hückel	43
3.4	LOCAL COMPOSITION MODELS	45
3.4.1	Extended UNIQUAC.....	45
3.4.2	Electrolyte Nonrandom two-liquid (eNRTL).....	45

3.5	ADVANCED EQUATIONS OF STATE	46
4.	EXISTING DATA	47
4.1	GLOBAL VIEW OF ALL DATA	47
4.2	ACTIVITY COEFFICIENTS DATA.....	50
4.3	ANALYSIS OF DATA VERSUS SOLUBILITY	52
5.	ANALYSIS OF RESULTS FOR INTERNAL CONSISTENCY	54
5.1	PROCEDURE FOR INTERNAL CONSISTENCY ANALYSIS	54
5.2	SELECTION OF THE MODEL FOR INTERNAL CONSISTENCY ANALYSIS	55
5.3	RESULTS OF INTERNAL CONSISTENCY	57
5.3.1	Analysis and interpretation of the deviations with NaCl	57
5.3.2	Analysis and interpretation of the deviations with LiCl	62
5.4	CONCLUSION ON INTERNAL CONSISTENCY	66
6.	ANALYSIS OF RESULTS FOR EXTERNAL CONSISTENCY.....	67
6.1	SELECTION OF THE MODEL FOR EXTERNAL CONSISTENCY ANALYSIS.....	67
6.2	EVALUATION OF THE BROMLEY MODEL	69
6.2.1	Analysis and influence of the parameters of the Bromley model.....	69
6.2.2	Computation and relation of properties with Bromley model	70
6.2.3	Different behavior of salts.....	72
6.3	EXTERNAL CONSISTENCY FOR PURE WATER SOLVENT	75
6.3.1	Variation of the parameter B of Bromley with the Free Energy of Solvation	75
6.3.2	Variation of the parameter B of Bromley with the size of ions.....	77
6.3.3	Variation of the parameter B with the solubility of salts	79
6.3.4	Variation of the parameter B of Bromley with the temperature.....	80
6.4	EXTERNAL CONSISTENCY FOR MIXED SOLVENTS.....	82
6.4.1	Computation and analysis of properties for mixed solvents	82
6.4.2	Variation of the parameter B of Bromley with the concentration of solvent.....	85
6.4.3	Variation of the parameter B of Bromley with the size of ions.....	87
6.4.4	Variation of the parameter B of Bromley with the dielectric constant	88
7.	EXTRAPOLATION CALCULATIONS.....	89
7.1	EXTRAPOLATION TO LOW TEMPERATURE	89
7.2	EXTRAPOLATION FOR MIXED SOLVENTS PREDICTIONS	91
8.	CONCLUSIONS	93
	References.....	95
	APPENDIX	99

1. INTRODUCTION

The population worldwide suffer a substantial growth over the last century. This growing population causes an increase in production and consumption [4]. The improvement in the quality of life causes the necessity to develop advanced engineering materials, chemical products and improve processes efficiency.

In separation processes, the mixture of fluids are separated normally by distillation, absorption or extraction through diffusional techniques. Those processes require a good understanding and modeling of thermodynamics. The separation of compounds cannot be properly understood without the inclusion of validated thermodynamic models. The equilibrium properties of the fluids and the thermodynamic models need to be optimized to deal with the design of the separation processes. In addition, thermodynamic models have to be reliable and representative of the experimental data [5]. Research and applications of new industrial technologies and new methods of energy production and storage are directly followed by the need of more precise thermodynamic models. Consequently, the need of improving the thermodynamic models for a better description of the industrial applications has strongly increased.

Thermodynamics of systems with strong and weak electrolytes has taken a high importance in the last years, however, the capabilities of the thermodynamics model are far to be completely optimized because of the complexity of the molecular interactions [2]. Long range and short range interactions taking place in electrolyte systems make difficult the precise calculations of phase equilibrium. Consequently, thermodynamics models based on electrolyte systems required more development and research.

This introduction chapter defines the scope of the work and the main necessity and applications of electrolyte systems. It describes the main objectives of the present work and the methodology followed for the analysis of internal consistency and external consistency.

1.1 SCOPE OF THE WORK

IFPEN is a French company whose objective is to produce research, innovations and training for industrial applications in the fields of energy, transport and environment. The present work has been performed in the physico-chemistry and applied mechanics direction at IFP Energies Nouvelles (IFPEN), in the department of Thermodynamics and Molecular Modeling. IFPEN is a French company whose objective is to produce research, innovations and training for industrial applications in the fields of energy, transport and environment. The main purpose of the company and its mission is to achieve technological and innovative solutions in order to contribute in the energy sector and in climate change challenges [6]. Consequently the research center priority is to provide solutions to the society challenges of energy and climate by adapting the transition through a sustainable mobility and the necessity of a more diversified energy mix worldwide. The following table 1 summarizes the sectors of activity in IFPEN.

Table 1. Description of the main activity sector in IFP Energies Nouvelles [6].

ACTIVITY SECTORS	MAIN DEVELOPMENT ACTIVITIES
SUSTAINABLE MOBILITY	<ul style="list-style-type: none"> - Hybrid and electric drives: Development of efficient and high power electrical machines. - Thermal engines: Improving thermal engines on energy efficiency, reduction of pollutant emissions and optimization in fuels uses.
RENEWABLES ENERGIES	<ul style="list-style-type: none"> - Biogas: Eco-efficient processes for purification of biogas before reinjection into the network. - Hydrogen: Development of economically sustainable technologies to insert hydrogen into the energy mix. - Energy storage: The improvement of surface storage processes of electrical energy.
RESPONSIBLE HYDROCARBONS	<ul style="list-style-type: none"> - Fuels: Development of catalysts and hydrodesulfuration processes, hydro treatments, catalytic reforming and isomerization of paraffins, aiming more environmentally fuels. - Petrochemistry: Developing catalysts and processes for olefins and aromatics production, to improve the performance of existing technologies, and the purity. - Gas treatment: Studying the conversion of natural gas for the hydrogen production through the development of processes with high energy efficiency.
ENVIRONMENT AND CLIMATE	<ul style="list-style-type: none"> - CO2 capture, storage and uses: Investigation in CO2 capture processes, CO2 storage technologies and monitoring of storage sites in order to ensure their safety and sustainability over long periods of time. - Plastic recycling: Playing a role in chemical recycling technologies, in order to upgrade used plastics. - Environmental monitoring: Development of methods of exploration, characterization, exploitation and monitoring allowing the safe development of new energy technologies based on the use of the subsoil

The main objective of the physico-chemistry and applied mechanics direction is to design innovative technological systems and to contribute in the development of products and processes for energy transition and sustainable mobility. It develops the knowledge, tools of calculations and experimental means adapted to the different needs to implement them in the applied projects. One branch of the direction is specialize in thermodynamic processes and molecular modeling. These competences, complementary to one another, make it possible to approach at the relevant scales, the analysis, the characterization and the qualification of the behavior

The present work in IFPEN is associated with the Elether project. This project is defined as a thermodynamic Joint Industrial Project (JIP) which constitutes an industrial community on electrolyte thermodynamics. The figure 1 shows the industrial communities representing Elether Joint Industrial project.



Figure 1. Industrial communities composing the JIP of Elether

Industrial applications require good description of several properties of mixtures that contain electrolytes. Electrolytic systems pose two particular problems: the inclusion of long-distance interactions and the reactivity of species. The existing industrial models are not good at extrapolating the few existing data and the JIP aims to create an industrial community for electrolyte systems foresting best practices concerning:

- Communicating regarding the challenges.
- Elaborate a methodology to analyze the data in view of identifying trends that can be used to extrapolate.
- Extrapolation methods and identification of most significant lacks
- Parameterization of industrial models for mixed solvents including acids, alcohols, and aprotic solvents.
- Propose a Best Practice workflow.

The methodology of the project is organized in three steps. Elether project requires the representation of a number of case studies for electrolyte systems. Each of these categories will be investigated through some typical examples. In all examined cases, the three steps methodology are represented in the figure 2.

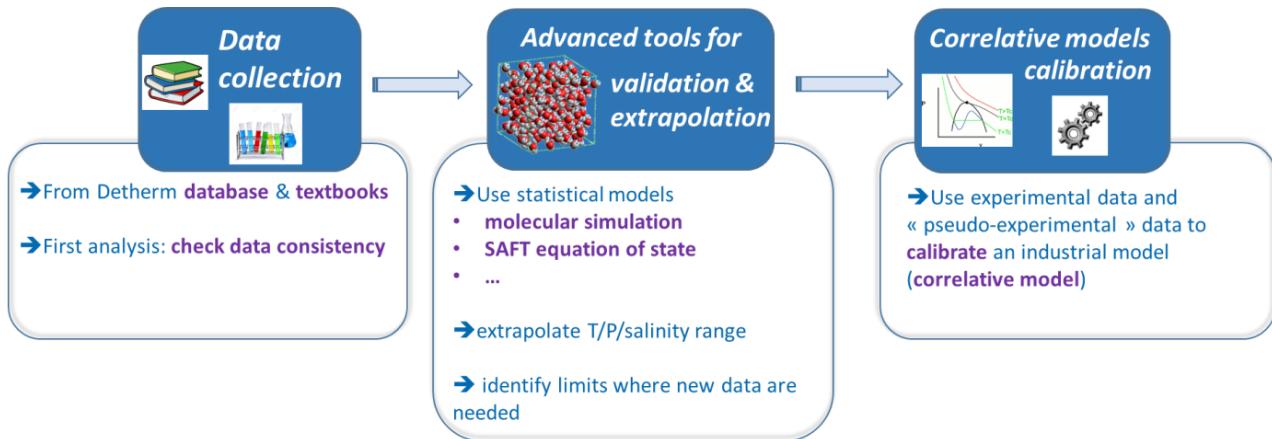


Figure 2. Methodology for ELEther Project

At first, data availability and consistency are evaluated. Data consistency means evaluation of the quality of the data when confronted with each other considering the thermodynamic relationships. External consistency means evaluating the quality of the trends within a given family. Partners have access to the references of the data used for each of the systems examined. Second, advanced tools are used to extrapolate the data to domains of interest to the applications, but where no such data are available. At last, a classical industrial model that is available in a process simulators is calibrated for the system of interest.

1.2 APPLICATIONS OF ELECTROLYTES

Electrolyte applications are present in a great deal of industrial processes. The optimization of the processes and the property calculations for the systems requires a proper understanding of the electrolyte effects in the process concerned. In some cases, the presence of salts is problematic and some techniques are needed in order to remove the salts from the mixture. In other cases, salts change the thermodynamic properties of mixture and can be added to help with the removal of other undesirable compounds [7]. Some of the main applications of the electrolytes system are represented in the figure 3.

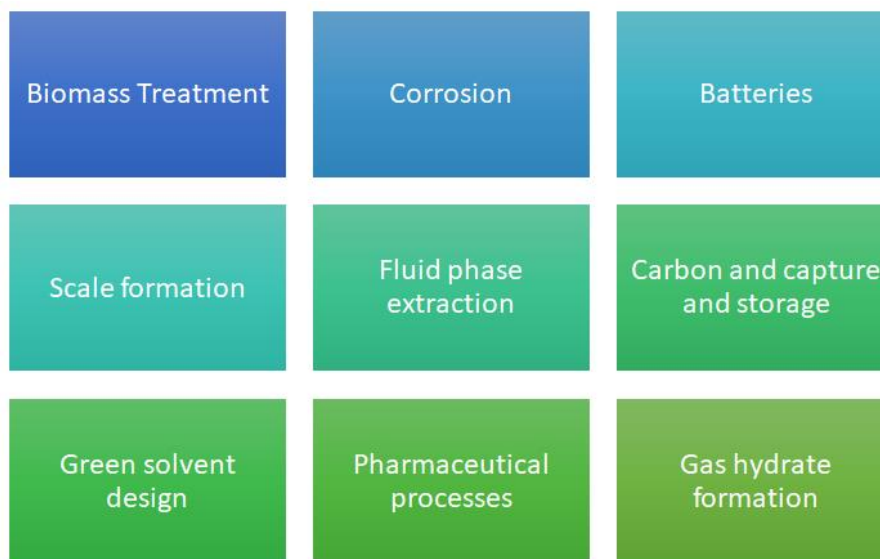


Figure 3. Main industrial applications of the electrolytes systems

Some of the main applications involving electrolytes systems are described with more details. These processes involve environmental constraints in water treatment, pharmaceutical processes using polymer electrolytes, batteries applications, scaling in heat exchangers that damage the equipment, and gas hydrates inhibitors

1- Environmental

Environmental applications include wastewater treatment. In some processes, such as petroleum, leather or food-processing, industry wastewater recovered contains high salts concentration. The water needs an important treatment before the release in the environment. The aim of the treatment is to reduce its content on dissolved hydrocarbons and salts [8]. High concentration of salt in the water has a negative impact in the aquatic life, water quality and agriculture. Various techniques are currently used for salts removal. Some examples of these processes are reverse osmosis, ion exchange, electrodialysis or biological treatments [9].

2- Pharmaceutical

Electrolyte systems play also an important role in the pharmaceutical industry. One example of the application of electrolytes can be found in drug delivery and solubility. The skin is the largest organ in the human body and it is considered an extremely important organ for all the functions of our body. The organ it is composed by a tissue organize into different layers: the dermis, epidermis and the hypodermis. One of the main functions of the skin is to protect, it is the first protection from infections and bacteria. The skin acts also as a physical and biochemical barrier. As a consequence, the pharmaceutical industry looks for new techniques to improve the wound of skin injuries and burns. Control drug delivery in the damage area is one of the most used techniques to support skin injuries [10]. Some tissue engineering techniques facilitate the transport of ionic drugs in the different skin layers using an electric current. Polymer electrolytes are polymers capable of conducting ions [11]. In addition, some polymers are highly biocompatible and are adequate to reduce rejection. They are as a consequence potential candidates to host the drugs for the delivery on the affected area . For instance, some pharmaceutical processes require to predict or provide knowledge of the solubility in mixture of solvents in presence of salts.

3- Batteries:

As it can be seen in figure 4, the main elements that form a lithium battery are a cathode, an anode, an electrolyte, and a separator. During the charge process, lithium ions move from the cathode to the anode. The movement is done under a the electric field via the Li^+ -conductive electrolyte. Electrons are simultaneously donated by the cathode host, in order to maintain electric neutrality, and flow to the anode via an external electrically conductive circuit.

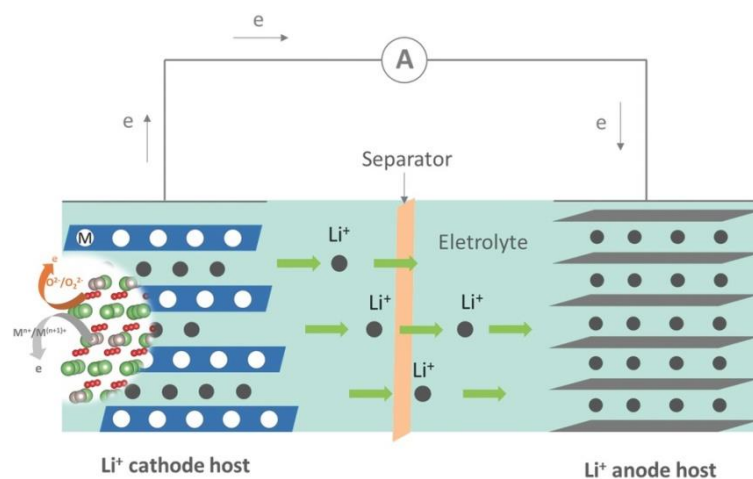


Figure 4. Mechanism of lithium-ion batteries [12].

Recent studies of rechargeable batteries use polymer electrolyte. The mentioned polymers are composed by a membrane which possess ionic conductivity. That material might improve lithium-battery technologies as it can be used to replacing the liquid electrolyte in the batteries. They allow the fabrication of flexible, compact, laminated solid-state materials free from leaks [13]. The latest research based on batteries has been specially oriented to the technology based on polymers electrolyte for batteries [14]. Lithium is the lightest of all metals and it can provide the conductivity.

When lithium is used as anode in contact with ionic lithium salt electrolytes, it can provide a wider electropositive potential window. These batteries can facilitate a very high energy density. In fact, these batteries are being manufactured presently on a large scale and used as rechargeable power packs in a wide variety of applications [15].

4- Scale in heat exchangers:

Scaling in heat exchangers is caused by some salts for which the solubility decrease with increasing temperature or with a change in the pressure of the system. The increase of resistance to heat, caused by scaling of the heat transfer surface, reduces the efficiency of the heat exchanger. Other consequences of the scaling phenomena are energy losses, excessive cleaning operations causing interruptions in the production. For heat exchangers applied in industry, a continuous or periodical mechanical cleaning of the heat transfer surfaces is often required. In special cases, addition of chemicals to the liquid prevents or reduces fouling [16]. However, mechanical cleaning systems require investment and additional operating cost. The nature of the fluid and the salt concentration, the velocity, the surface material, the temperature and the pressure are properties that define rate of formation of the fouling layer. In cooling water systems, calcium carbonate is a major component of fouling deposits [17]. Design of heat exchangers usually takes into account the decrease of heat transfer during operation and compensates for it by an increase of the heat transfer area. Tubes geometry can be modified in order to improve the heat exchange area and improve the heat transfer coefficients [18]. Figure 5 shows a picture from a shell and tube heat exchanger with the precipitation of salts due to scaling.



Figure 5. Image of scaling in a shell and tube heat exchanger [19].

5- Gas hydrates

Gas hydrate formation has taken an important role worldwide. The combination of small molecules such as methane, carbon dioxide, nitrogen or hydrogen, with water under specific conditions (low temperature and high pressure) is the cause of crystalline solid structures formation [20]. These structures are known as gas hydrates. Therefore, gas hydrates can be defined as a structure composed of water and small gas molecules trapped inside the solid structure. In some cases the solid structures are studied for positive applications such as carbon dioxide capture, gas storage, water treatment technologies or even separation processes [20]. However, the oil and gas transportation processes aim to avoid this phenomena, because it can deal on pipeline plugging and efficiency problems [21]. Inhibitors are a possible solution to prevent the gas hydrate formation. Electrolytes can be used to change the phase transition conditions thus preventing the gas hydrate formation [22]. The picture in figure 6 shows the gas hydrate formation in a pipe.



Figure 6. Gas hydrate formation in a pipe [23].

6- Carbon capture

One of the potential solutions of carbon dioxide emission to the atmosphere is based on carbon capture [24]. Several techniques exist for carbon capture processes. Post-combustion capture via chemical absorption is one of the most interesting and innovative techniques [25]. The process using an aqueous mono-ethanol-amine (MEA) solution has been highly tested and investigated during the last decades. However, the use of this solvent entails large heat requirements, degradation and corrosion issues and risks of emissions of degradation products. Hence, alternatives are being investigated, among which aqueous ammonia is a valid candidate. The inclusion of the systems involves the uses of electrolyte properties. In order to evaluate the complex $\text{CO}_2\text{-NH}_3\text{-H}_2\text{O}$ system, a thermodynamic model capable of describing solid–liquid–vapor equilibrium and thermal properties, over the wide temperature range from 0 to 150 °C, is necessary [26].

1.3 OBJECTIVES

The first steps for the development of a thermodynamic model in view of process simulation is data gathering and evaluation. This is also the first step in the EleTher workflow. This work focuses on this step by proposing a consistency analysis. For that purpose, the study has been divided into two different data analysis: The internal consistency and the external consistency.

Internal consistency is the analysis of the quality of data for different properties in a system. According to thermodynamics, there exist relationships between properties. Thermodynamic models incorporate these relationships. The objective of internal consistency is to make sure that all the data of a given system form an internally consistent body. This is then performed by analyzing the deviations between model calculations and the available experimental data. The purpose of the study is to analyze the trends followed by the deviations and to identify inconsistent data series. Each system requires the study of different properties at different conditions such as temperature, pressure or high concentration electrolytes. An analysis, a comparison and a summary of the available data for all the properties has to be done for the different systems.

External consistency refers to the relation between different systems and at different conditions. The objective of external consistency is also to evaluate whether trends can be made visible among the many data. To that end, a simple model is used, with a single parameter. This parameter is then correlated with physical properties for extrapolation to other conditions and systems. The objective of external consistency is also the analysis of the trends which makes it possible to identify outliers and possibly domains in need of additional experimental measurements. The observed trend may make it possible to find a predictive approach allowing to evaluate the physical properties of systems for which no data exist.

In the present work, these two types of consistency analyses will be performed on systems composed by non-reactive monovalent salts with water as pure solvent as well as with mixed solvents. Mixed solvents involve pure water with a primary alcohol (methanol, ethanol, 1-propanol, 1-butanol). The properties concerned by the present work are: The mean ionic activity coefficients (γ), the vapor-liquid equilibrium (VLE), the osmotic coefficient (ϕ), the enthalpies of solution and the solid-liquid equilibrium (SLE).

The figure 7 represents the different systems studied. It shows the monovalent salts studied, classified by cations and anions and the and the type of solvents used.

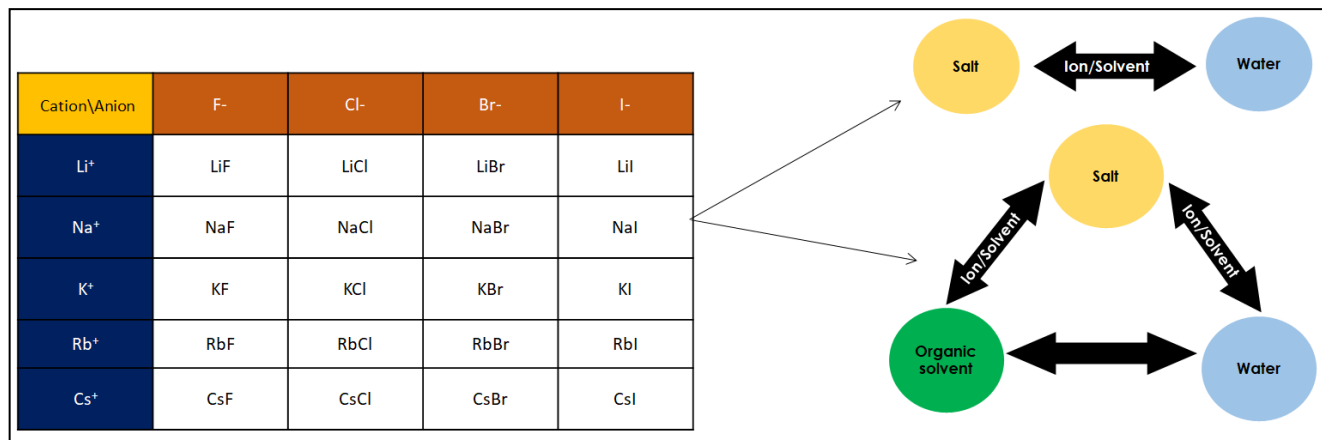


Figure 7. Representation the systems studied composed by monovalent salt and different solvents

1.4 METHODOLOGY FOR DATA CONSISTENCY ANALYSIS

The methodology followed in order to achieve the objectives mentioned is explained in figure 8. The representation shows a schematic diagram that summarizes the steps followed for external and internal consistency analysis.

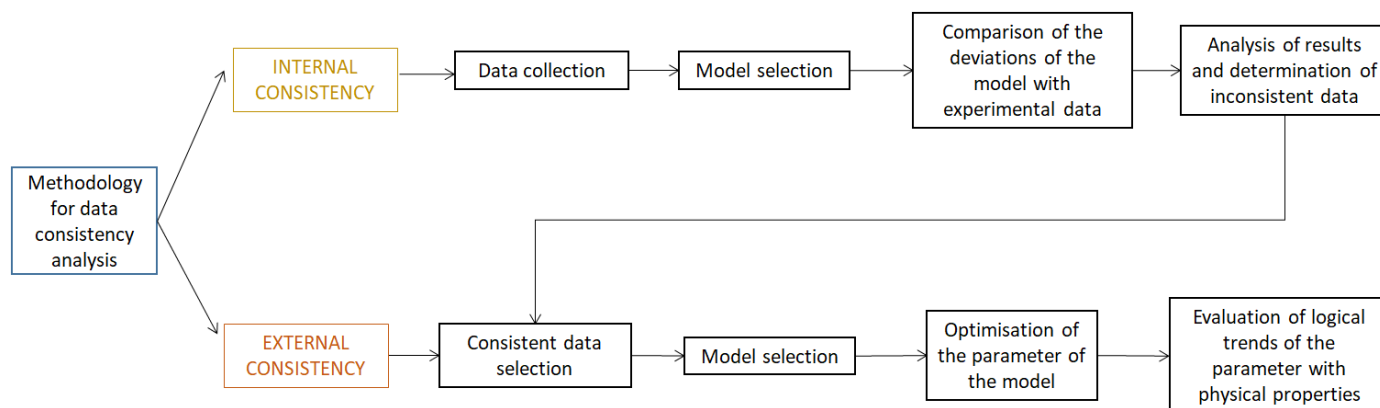


Figure 8. Scheme of the methodology used to analyze internal and external consistency

Internal consistency starts with data collection. All the data available in Detherm IFPEN data base have been classified and organized in function of the properties for all the systems. After the collection, a model has to be selected. As mentioned before, for internal consistency an advanced/accurate model is needed. It is important to have the lowest deviations possible to correctly visualize the outliers. After the selection of the model, the deviations between the model and experimental data are calculated for a specific property. The last step consists in evaluating the deviations and in identifying inconsistent data. In order to make sure that no unexpected but real phenomenon is detected, further study of these data is needed so as to be able to justify their rejection.

In the external consistency analysis, the data used in this type of consistency must have been validated previously through the internal consistency analysis. After classification, external consistency requires the selection of a simple model with one adjustable parameter. The methodology requires the regression of this parameter. Moreover, the model has to be evaluated for the different fundamental properties studied. The last part of this evaluation is the presentation and analysis of results. The optimized parameter is represented as a function of several physical properties and conditions. The trends and logic of this representations in comparison to electrolyte interactions are analyzed and tested to other systems.

2. DEFINITIONS AND PROPERTIES IN ELECTROLYTE SYSTEMS

Historically, in the field of electrolyte thermodynamics, a concentration unit different from the mole fraction is often used, such as the molarity or the molality. For modern simulation programs and thermodynamic models equations, the composition is described in mole fraction. Consequently, it is essential to define the relation between the molality of the salts in the solvent and the mole fraction. The following paragraphs describe the existing mathematical relations between the properties and a concrete definition. It also describes the properties studied in the present work for electrolyte systems.

2.1 CONCENTRATION UNITS FOR ELECTROLYTE SYSTEMS

The definitions and equations of the main concentration units used in electrolyte systems are described

2.1.1 Molarity (mol of solute/volume (L) of solution)

The molarity gives the number of moles of a solute in one liter of solvent. This unit is not recommended for thermodynamic applications because it is dependent on temperature and on pressure. The volume is not conserved when changing operating conditions (pressure, temperature, composition) and there is an excess volume that is not taken into account. Moreover, it is not a practical unit due to the fact that experimental data in electrolytes mixtures is calculated in molality. In order to convert molarity to molality units or mole fraction units, the density needs to be known. The density of the solution is also highly influence by the temperature or the pressure. The definition of the molarity is written as:

$$\text{Molarity} = \frac{n_{\text{salt}}(\text{mol})}{\text{Volume}_{\text{solution}}(\text{L})} \quad (2.1.1)$$

2.1.2 Molality (mol of solute/kg of solvent)

The molality is the most common concentration unit for the description of electrolyte solutions. That concentration unit is very often used in the presentation of experimental data. The molality m_i of an ion i , is the number of moles n_i , of the ion per kg of solvent. It is very common to evaluate the water as solvent at normal conditions (i.e. 25°C and 1 bar). Molality is a popular unit for salt solutions due to the fact that the concentrations in molality units give practical numbers (often between 0 and 20 for most salts), while the concentrations in mole fraction units are very small.

The molality (m_s) is defined as:

$$m_s = \frac{n_{\text{salt}}(\text{mol})}{\text{Mass}_{\text{solvent}}(\text{kg})} \quad (2.1.2)$$

It can be seen that the molality concentration unit is only dependent on the amount of the relevant solute and the amount of solvent (it is important to define exactly what is a solvent; often this is water). The mole fraction unit and the molarity units on the other hand, are also dependent on the amount of other solutes present. Nevertheless, it is highly interesting to relate the molality with the molarity. That relation is calculated with the relation between the mass of the solvent and the density of the solution. The mass of the solvent is first divided into:

$$\text{Mass}_{\text{solvent}} = \text{Mass}_{\text{solution}} - \text{Mass}_{\text{salt}} \quad (2.1.3)$$

The mass of the solution can be calculated as the volume of the solution multiplied by the density:

$$\text{Mass}_{\text{solution}} (\text{kg}) = V_{\text{solution}} (\text{m}^3) \cdot \rho_{\text{solution}} \left(\frac{\text{kg}}{\text{m}^3} \right) \quad (2.1.4)$$

The mass of the salt can also be calculated as:

$$\text{Mass}_{\text{salt}} = n_{\text{salt}} \cdot \text{Mw}_{\text{salt}} \quad (2.1.5)$$

Replacing the equation (2.1.4) and (2.1.5) in the equation (2.1.3) and then in equation (2.1.2), the last one remains:

$$m_s = \frac{n_{\text{salt}}}{V_{\text{solution}} \cdot \rho_{\text{solution}} - n_{\text{salt}} \cdot \text{Mw}_{\text{salt}}} \quad (2.1.6)$$

The equation is arranged in order to replace the moles of the salt and the volume by the molarity. The molality is then isolated in order to have the concentration unit in function of the molarity. The following final equation is deduced.

$$m_s = \frac{\text{Molarity}}{\rho_{\text{solution}} - (\text{Molarity} \cdot \text{Mw}_{\text{salt}})} \quad (2.1.7)$$

2.1.3 Molar fraction

The mole fraction unit most often is used in thermodynamic models for electrolytes. It is defined as the number of moles of a component in a system divided by the total number of moles. Molar fractions are described by x_i in the liquid phase and are defined as:

$$x_i = \frac{n_i}{n} \quad (2.1.8)$$

Where n is the mole number.

Most thermodynamic models use the molar fraction as concentration unit. It is important to find the relation between the molar fraction and the molality. The deduction of the relation is the following:

$$m_s = \frac{n_{\text{salt}}}{n_{\text{solvent}} \cdot \text{MW}_{\text{solvent}}} \quad (2.1.9)$$

The number of moles can be divided by the total number of moles in the denominator and the numerator. The relation can then be written depending in the molar fraction of salt and solvent:

$$m_s = \frac{x_{\text{salt}}}{x_{\text{solvent}} \cdot \text{Mr}_{\text{solvent}}} \quad (2.1.10)$$

As the system is defined with salt and solvent, the molar fraction of solvent can be express as the one minus the molar fraction of the salt.

$$m_s = \frac{x_{\text{salt}}}{(1 - x_{\text{salt}}) \cdot \text{Mr}_{\text{solvent}}} \quad (2.1.11)$$

Isolating the molar fraction of the salt, the final relation is found

$$x_{\text{salt}} = \frac{\text{Molality} \cdot \text{Mr}_{\text{solvent}}}{1 + \text{Molality} \cdot \text{Mr}_{\text{solvent}}} \quad (2.1.12)$$

In some cases it is interesting to define the molar fraction of the salt in function of the molar fraction of the solvent. The sum of the mole fraction of solvent plus the mole fraction of water is equal to one, it can be deduced also that:

$$x_{\text{salt}} = \text{Molality} \cdot x_{\text{solvent}} \cdot \text{Mr}_{\text{solvent}} \quad (2.1.13)$$

Often, the **ionic concentration** is used rather than that of the salt. It is important to understand that for monovalent salts the molality of the salt is always equal to the molality of each ion due to the fact that the moles of salt are the same as the moles of anion and the moles of cation. However, based on the molar fractions, the total amount of moles is different after the dissociation of the salt into electrolytes. As a consequence the molar fraction of salt is different from those of dissociated ions. The following demonstration is based on the sodium chloride salt but can be applied for any type of salt.

$$m_{\text{NaCl}} = \frac{n_{\text{NaCl}}}{\text{kg}_{\text{solvent}}} = \frac{n_{\text{Na}^+}}{\text{kg}_{\text{solvent}}} \quad (2.1.14)$$

The expression is represented within the mole fraction dependency:

$$m_{\text{NaCl}} = \frac{x_{\text{Na}^+}}{x_{\text{water}} \cdot M_{\text{r,water}}} \quad (2.1.15)$$

The molar fraction of the water can be expressed from the molar fraction of the sodium cation. The sum of the molar fraction of water plus sodium cation plus chloride anion has to be equal to one. As the moles of cation and anion are the same because the reaction is 1:1, the expression can be written as:

$$x_{\text{water}} = 1 - 2 \cdot x_{\text{Na}^+} \quad (2.1.16)$$

So the molality equation is directly related to molar fraction of sodium cation as:

$$m_{\text{NaCl}} = \frac{x_{\text{Na}^+}}{(1 - 2 \cdot x_{\text{Na}^+}) \cdot M_{\text{r,water}}} \quad (2.1.17)$$

Isolation now the molar fraction of sodium cation:

$$x_{\text{Na}^+} = \frac{\text{Molality}_{\text{NaCl}} \cdot M_{\text{r,water}}}{1 + (2 \cdot \text{Molality}_{\text{NaCl}} \cdot M_{\text{r,water}})} \quad (2.1.18)$$

The equation can be simplified to:

$$x_{\text{Na}^+} = \frac{1}{2 + \frac{1}{\text{Molality}_{\text{NaCl}} \cdot M_{\text{r,water}}}} \quad (2.1.19)$$

2.2 THERMODYNAMIC PROPERTIES IN ELECTROLYTE SYSTEMS

Before the study of the different models and the analysis of experimental data, the fundamental equations in electrolyte systems have to be described. The properties for ideal and real solutions are extremely important as the thermodynamic models are often based on the distinction between an 'ideal' contribution and an 'excess' contribution. The excess can never be properly understood if the 'ideal' contribution is not well defined. In the present chapter the thermodynamic properties of electrolyte systems are defined. The properties studied in the present work are: The chemical potential in electrolyte systems, the activity coefficients, the osmotic coefficient, the vapor-liquid and solid-liquid equilibrium and the enthalpies.

2.2.1 Definition of chemical potential

One of the most fundamental thermodynamic properties is the chemical potential. The chemical potential is defined as the Gibbs energy changes (absorbed or released) caused by the change of the particle number of a given component. The chemical property represents the contribution of the component to the total Gibbs Energy. The chemical potential defines the variation of the Gibbs energy with respect to the amount of a component i when the pressure, the temperature and the amount of the other components remain constant. The definition of the chemical potential and its relation with the Gibbs energy is established by the following equation:

$$\mu_i = \left[\frac{\partial G}{\partial n_i} \right]_{P,T,n_j} \quad (2.2.1)$$

The chemical potential is used to determine the equilibrium of a system. When equilibrium is reached, the chemical potential of each substance in one phase will be equal to the chemical potential of the substance in the other phases of the system.

2.2.2 Definition of fugacity in relation with chemical potential

The chemical potential may also be expressed in terms of fugacity. The fugacity represents the tendency of the component to escape from a phase. The relation between the chemical potential and the fugacity is defined in the following equation:

$$\mu_i = \mu_i^{\text{ref}} + R \cdot T \cdot \ln \left(\frac{f_i}{f_i^{\text{ref}}} \right) \quad (2.2.2)$$

f_i stands for the fugacity and f_i^{ref} represents the reference fugacity of the component i .

The chemical potential is a state function that requires a reference state in order to be computed. The reference state is arbitrary and may be different according to the compound studied. Four pieces of information define a reference state: temperature, pressure, composition and physical state. In all the reference states, the use of the equation implies that the temperature of the reference state is equal to that of the studied fluid. The remain three pieces of information have to be defined. Several choices can be made: ideal gas, pure liquid, infinite dilution or one molal (see tables below).

Table 2 shows the definition of the ideal gas as reference state.

Table 2. Conditions for ideal gas reference state

Symbol reference	Definition	Pressure	Temperature	Physical state	Composition
(#)	Ideal Gas	1 atm	Temp	Ideal gas	Pure component

This is what is often used for neutral molecules. Data of formation properties are available in the DIPPR database. The fugacity in the reference state is 1 atm, which means that:

$$\mu_i = \mu_i^{\#} + R \cdot T \cdot \ln \left(\frac{f_i}{1 \text{ atm}} \right) \quad (2.2.3)$$

f_i expressed in atmospheres.

The table 3 collects the conditions used for the pure liquid reference state.

Table 3. Conditions for pure liquid reference state

Symbol reference	Definition	Pressure	Temperature	Physical state	Composition
(°)	Pure liquid	P^σ	Temp	Liquid	Pure component

This case is used for liquid phase mixtures. The fugacity is then expressed as

$$f_i = x_i \cdot f_i^* \cdot \gamma_i \cdot \phi_i \quad (2.2.4)$$

Where γ_i is the activity coefficient that describes the deviation from the ideal mixture, which is a linear relationship between fugacity and mole fraction. ϕ_i is a correction to the pressure. It is the Poynting correction, represented by:

$$\begin{aligned} \phi_i &= \exp\left(\frac{1}{RT} \int_{P_i^\sigma}^P v_i^L dp\right) \\ &\approx \exp\left(\frac{v_i^L \cdot (P - P_i^\sigma)}{RT}\right) \end{aligned} \quad (2.2.5)$$

In the last equation v_i^L is the liquid molar volume of the component i

Therefore the chemical potential remains:

$$\mu_i = \mu_i^* + RT \cdot \ln\left(\frac{f_i}{f_i^*}\right) = \mu_i^* + RT \cdot \ln(x_i \cdot \gamma_i \cdot \phi_i) \quad (2.2.6)$$

The table 4 collects the conditions used for the infinite dilution reference state.

Table 4. Conditions for infinite dilution reference state

Symbol reference	Definition	Pressure	Temperature	Physical state	Composition
(*)	Infinite dilution	$P_{\text{solvent}}^\sigma$	Temp	Ideal liquid defined with the Henry convention, in a given solvent (often water): $f_i^{\text{ideal}} = x_i \cdot H_i$ Where $H_i = \lim_{x_i \rightarrow 0} \frac{f_i}{x_i}$	Pure

This case is used for solutes (neutral gases or very dilute compounds), generally in combination with solvents where the pure component reference state is used.

The fugacity is then written as:

$$f_i = x_i \cdot H_i \cdot \gamma_i^* \cdot \phi_i^* \quad (2.2.7)$$

Note that both Poynting and activity coefficient now refer to the infinite dilution reference state. The chemical potential is computed as:

$$\mu_i = \mu_i^\infty + RT \cdot \ln \left(\frac{f_i}{f_i^\infty} \right) = \mu_i^\infty + RT \cdot \ln(x_i \cdot \gamma_i^* \cdot \phi_i^*) \quad (2.2.8)$$

The table 5 collects the conditions used for the molality base reference state.

Table 5. Conditions for molality base reference state

Symbol reference	Definition	Pressure	Temperature	Physical state	Composition
(m)	Molality	$P_{\text{solvent}}^\sigma$	Temp	Ideal liquid defined as: $f_i^{\text{ideal}} = m_i \cdot H_i^m$ Where $H_i^m = \lim_{x_i \rightarrow 0} \frac{f_i}{m_i}$	Unit molality in water $m_i^0 = 1 \text{ mol/kg}$

The last case is most often used for electrolytes. Note that here a different reference state is used for the definition of the activity coefficient and reference state chemical potential.

The fugacity is now written as:

$$f_i = m_i \cdot H_i^m \cdot \gamma_i^m \cdot \phi_i^m \quad (2.2.9)$$

In the case of the molality scale, the Henry constant is defined differently:

$$H_i^m = \lim_{m_i \rightarrow 0} \frac{f_i}{m_i} \quad (2.2.10)$$

Again, the activity coefficient, that carries an (m) as superscript, is still defined as deviation from the ideal behavior, but since this ideality is different, its meaning is not the same. The correspondence between activity coefficients will be discussed in the next section. The Poynting correction can be neglected for low pressure systems. At the reference state for chemical potential, the fugacity is written as:

$$f_i^m = m_i^0 \cdot H_i^m \quad (2.2.11)$$

Introducing the terms for the molality activity coefficient and the term for the molality based standard state, the chemical potential in molality base can be written:

$$\mu_i = \mu_i^m + RT \cdot \ln\left(\frac{f_i}{f_i^m}\right) = \mu_i^m + RT \cdot \ln\left(\frac{m_i \cdot \gamma_i^m}{m_i^0}\right) \quad (2.2.12)$$

μ_i^m stands for the chemical potential of solute i in a hypothetical, ideal solution. The term m_i^0 is equal to 1 mol/kg and it is usually omitted from the equation thus remaining:

$$\mu_i = \mu_i^m + RT \cdot \ln(m_i \cdot \gamma_i^m) \quad (2.2.13)$$

2.2.3 Activity coefficient

The activity coefficient represent the deviation from an ideal behavior. It can be defined as:

$$\gamma_i = \frac{f_i}{f_i^{\text{ideal}}} \quad (2.2.14)$$

In electrolyte systems, several concentration units and several definitions of ideal solutions can be used. This leads to different definition of the activity coefficient. Most often, the ideal behavior is taken as a fugacity that behaves proportionally with the mole fraction.

$$f_i^{\text{ideal}} = x_i \cdot f_i^{\text{ref}} \quad (2.2.15)$$

The proportionality factor f_i^{ref} depends on the reference selected. Often, the reference state stands for the Lewis convention or the so-called symmetric convention takes the proportionality factor as the pure component fugacity.

$$f_i^{\text{ref}} = f_i^* = \lim_{x_i \rightarrow 1} f_i \quad (2.2.16)$$

Taken into consideration this convention, the ideal fugacity is:

$$f_i^{\text{ideal}} = x_i \cdot f_i^* \quad (2.2.17)$$

So the real fugacity can be calculated as:

$$f_i = x_i \cdot f_i^* \cdot \gamma_i \quad (2.2.18)$$

The activity coefficient γ_i in that case is known as the symmetrical activity coefficient.

The fugacity can be also computed with the proportionality factor taken as the infinite dilution limit in the pure solvent. That case corresponds to the so-called asymmetric convention or Henry convention. With this definition the Henry constant is needed for the definition of the ideal fugacity.

The reference fugacity stays for the Henry constant limit defined as:

$$f_i^{\text{ref}} = H_i^* = \lim_{x_i \rightarrow 0} \left(\frac{f_i}{x_i} \right) \quad (2.2.19)$$

The ideal fugacity in that case is defined as:

$$f_i^{\text{ideal}} = x_i \cdot H_i^* \quad (2.2.20)$$

The final definition of the fugacity based on the infinite dilution remains:

$$f_i = x_i \cdot H_i^* \cdot \gamma_i^* \quad (2.2.21)$$

A relation can be defined between the Lewis and Henry convention, defined with the relation of the activity coefficients:

$$f_i = x_i \cdot f_i^* \cdot \gamma_i = x_i \cdot H_i^* \cdot \gamma_i^* \quad (2.2.22)$$

With the value of the Henry constant equal to:

$$H_i = \lim_{x_i \rightarrow 0} \left(\frac{f_i}{x_i} \right) = f_i^* \cdot \gamma_i^\infty \quad (2.2.23)$$

Hence the relation between the two conventions is simplified to:

$$\gamma_i^* = \frac{\gamma_i}{\gamma_i^\infty} \quad (2.2.24)$$

The infinite dilution activity coefficient of a component in water varies depending on the operating pressure and temperature. From the last equation it can be deduced that γ_i^* is equal to 1 at infinite dilution. γ_i^* is the rational, unsymmetrical, activity coefficient. That parameter refers to the fact that this activity coefficient has a value of unity at infinite dilution rather than the value of the pure component state [2]. Standard state properties for the reference state based on the unsymmetrical activity coefficient are calculated easier. That is the reason why unsymmetrical activity coefficient is widely used for ions. On the opposite side, the corresponding values for the pure component standard state with symmetric activity coefficients cannot be measured for ions [27].

In case of electrolyte systems, another reference state can be defined based on molality units. The new reference state varies slightly from the ideal behavior and it is often defined as fugacity that is proportional to molality

$$f_i^{\text{ideal (m)}} = \frac{m_i}{m_i^0} \cdot f_i^{\text{ref}} \quad (2.2.25)$$

Where $m_i^0 = 1 \text{ mol/kg}$ and is used so as to have a dimensionless concentration unit. The reference state is then always taken at infinite dilution. The final equation for the fugacity with molality concentration stays for:

$$f_i = m_i \cdot H_i^m \cdot \gamma_i^m \quad (2.2.26)$$

The figure 9 illustrates the ways to define the ideal behavior, and therefore deviation from this ideal behavior.

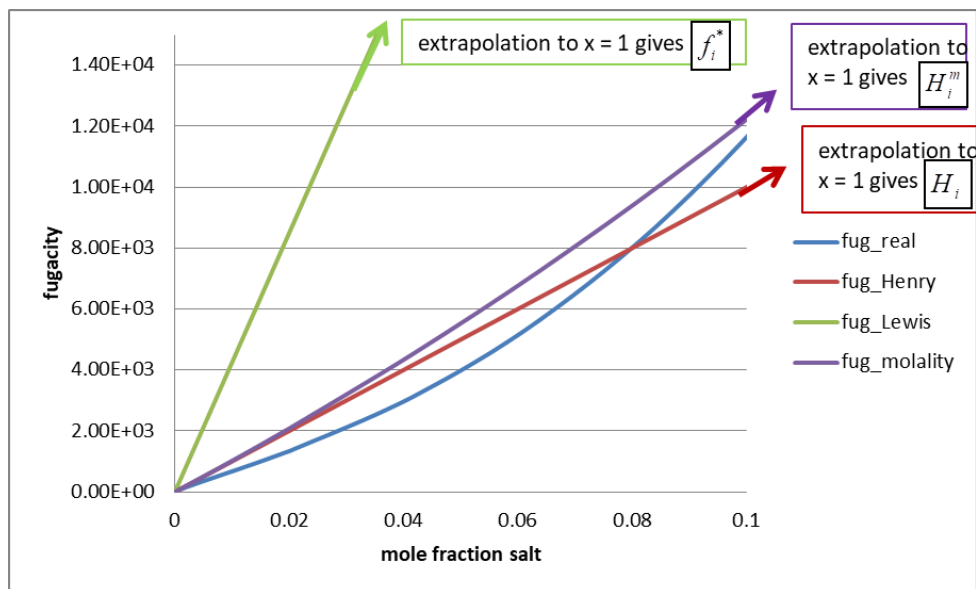


Figure 9. Example of the fugacity of a salt as a function of its mole fraction

The blue line shows the actual fugacity as a function of the mole fraction of salt. The other lines show the different definitions of 'ideal behavior' that may be used to define activity coefficients. The green line represents the symmetric convention and the red line stands for the asymmetric convention (reference state = infinite dilution). In case of electrolyte systems, the ideal behavior is defined as fugacity that is proportional to molality (represented by the violet line in the figure). In contrast to the red and green lines, this line is not straight when plotted as a function of mole fraction. At the origin, it has an identical slope as the red line, but because of the non-linearity between molality and mole fraction, it deviates at higher concentrations. This is why the activity coefficients that correspond to these two reference states are not equal.

The transformation between activity coefficients is made using the relation between the molality and the mole fraction of salt and water as solvent defined in the equation (2.1.11) and the fact that $\lim_{m_i \rightarrow 0} x_{\text{water}} = 1$:

$$H_i^{(m)} = \lim_{m_i \rightarrow 0} \frac{f_i}{m_i} = \lim_{m_i \rightarrow 0} \frac{f_i \cdot x_w \cdot M_w}{x_i} = M_s \cdot \lim_{m_i \rightarrow 0} \frac{f_i}{x_i} = M_w \cdot H_i \quad (2.2.27)$$

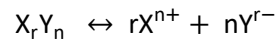
Therefore:

$$f_i = m_i \cdot H_i^{(m)} \cdot \gamma_i^{(m)} = \frac{x_i \cdot M_w \cdot H_i}{x_x \cdot M_w} \gamma_i^{(m)} = x_i \cdot H_i \cdot \gamma_i^* \quad (2.2.28)$$

Which simplifies into

$$\frac{\gamma_i^{(m)}}{x_w} = \gamma_i^* \quad (2.2.29)$$

Generally speaking, the activity coefficient of ionic solutes can never be measured independently from each other. In practice, a mean ionic activity coefficient (MIAC) is defined. Considering one general salt XY that dissociates into X^+ cation and Y^- :



In the equation, r and n are the stoichiometric coefficients of the cation and the anion respectively. With the combination of chemical potential in molality base defined in equation (2.2.13) and the activity coefficients, it can be demonstrated that [27]:

$$\mu_i^{(m)} = r \cdot \mu_c^{(m)} + n \cdot \mu_a^{(m)} + RT \cdot \ln \left(m_c^r \cdot m_a^n \cdot \gamma_c^{(m)r} \cdot \gamma_a^{(m)n} \right) \quad (2.2.30)$$

The mean activity coefficient (MIAC) can be defined as:

$$\gamma^{\text{MIAC}} = (\gamma_{\text{cation}}^r \cdot \gamma_{\text{anion}}^n)^{1/\nu} \quad (2.2.31)$$

Where:

$$\nu = r + n$$

In the same way, the mean molality is defined as:

$$m^{\text{MIAC}} = (m_c^r \cdot m_a^n)^{1/\nu} \quad (2.2.32)$$

If the standard state chemical potential of the salt in solution is:

$$\mu_s^{(m)} = r \cdot \mu_c^{(m)} + n \cdot \mu_a^{(m)} \quad (2.2.33)$$

And we combine the last definitions, the equation (2.60) can be written as:

$$\mu_i^{(m)} = \mu_s^{(m)} + \nu \cdot RT \cdot \ln(m^{\text{MIAC}} \cdot \gamma^{\text{MIAC}}) \quad (2.2.34)$$

2.2.4 Osmotic coefficient and osmotic pressure

The activity coefficient of solvents (most generally water) is not measured in the same way as that of the ions. As a consequence, another concept has to be introduced. The osmotic pressure is the pressure needed to prevent solvent flow across a semipermeable membrane that separates a solution from a solvent. Solvent flows towards the salt containing solution until the pressure difference balances its fugacity on both sides of the membrane. The figure 10 shows a simple representation of the effect of osmotic pressure for a water and salt mixture.

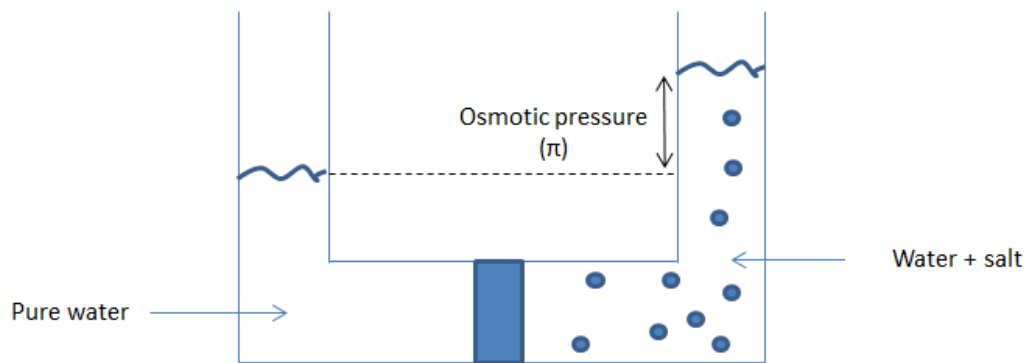


Figure 10. Definition scheme of the osmotic coefficient

The osmotic pressure is defined as:

$$\pi = (P_{\text{salt}} - P_{\text{pure}}) \quad (2.2.35)$$

At equilibrium, the chemical potential of the solvent on both sides of the membrane must be equal. The compartment at the left, has a chemical potential which depends only on the pressure as it contains the pure solvent. On the other side, the compartment on the right, contains the solute. The chemical potential of the solvent depends on the mole fraction of the solvent and on the pressure of the left side. The equilibrium conditions is then defined:

$$\mu_w^*(P_{\text{pure}}) = \mu_w^{\text{mix}}(P_{\text{salt}}) \quad (2.2.36)$$

That equation can also be written with the fugacities relation:

$$f_w^*(P_{\text{pure}}) = f_w^{\text{mix}}(P_{\text{salt}}) \quad (2.2.37)$$

The left hand fugacity (at P_{pure}) can be computed from the pure solvent fugacity at P_{salt} and a Poynting correction:

$$f_w^*(P_{\text{pure}}) = f_w^*(P_{\text{salt}}) \cdot \exp\left(-\frac{\pi \cdot v_w}{R \cdot T}\right) \quad (2.2.38)$$

The right-hand side is computed using activity coefficient:

$$f_w^{\text{mix}}(P_{\text{salt}}) = f_w^*(P_{\text{salt}}) \cdot x_w \cdot \gamma_w \quad (2.2.39)$$

Hence, if the equation (2.2.38) and (2.2.39) are placed in the equation (2.2.37) the fugacity of pure solvent at P_{salt} can be eliminated. The equation remains:

$$\exp\left(\frac{\pi \cdot v_w}{R \cdot T}\right) = x_w \cdot \gamma_w \quad (2.2.40)$$

Taking the logarithm, one finds:

$$\left(\frac{\pi \cdot v_w}{R \cdot T}\right) = -\ln(x_w \cdot \gamma_w) \quad (2.2.41)$$

The osmotic pressure is then found from:

$$\pi = \frac{-R \cdot T \cdot \ln(x_w \cdot \gamma_w)}{v_w} \quad (2.2.42)$$

The osmotic coefficient is related to the osmotic pressure. It quantifies the deviation from a solvent from the ideal behavior. The osmotic coefficient is defined as:

$$\phi = \frac{\pi}{\pi^{\text{ideal}}} \quad (2.2.43)$$

The ideal osmotic pressure is found when the activity coefficient is unity:

$$\pi^{\text{ideal}} = \frac{-R \cdot T \cdot \ln(x_w)}{v} \quad (2.2.44)$$

The mole fraction of water can be expressed in function of the mole fraction of salt:

$$\pi^{\text{ideal}} = \frac{-R \cdot T \cdot \ln(1 - x_s)}{\nu} \quad (2.2.45)$$

In infinite dilution, the mole fraction of salt tends to zero small. When x_s is small the logarithm $\ln(1 - x_s)$ can be approximate to $-x_s$. With that supposition:

$$\pi^{\text{ideal}} = \frac{R \cdot T \cdot x_s}{\nu} \quad (2.2.46)$$

This is not exactly identical to (2.2.44), but in practice, this is the definition used for the ideal osmotic pressure.

The osmotic coefficient (ϕ) represents the activity of solvents within an electrolyte solution. It is a parameter which characterizes the non-ideality of a solvent. For any aqueous solution, the osmotic coefficient is defined as [28]:

$$\phi = \frac{\pi}{\pi^{\text{ideal}}} = \frac{-\ln(x_w \cdot \gamma_w)}{M_w \cdot \nu \cdot m_s} = \frac{-\ln a_{\text{water}}}{M_w \cdot \nu \cdot m_s} \quad (2.2.47)$$

Where:

a_w is the activity coefficient of water; M_w is the molecular weight of the water (kg of water/mol of water); m_s is the molality of the solute (moles of salt/kg of water) and ν is the sum of the stoichiometric coefficients of the electrolytes in the chemical dissociation of the salt.

The Gibbs-Duhem equation can be used to relate the activity coefficients of the previous models with the osmotic coefficient of the solvent. With this equation, it is possible to determine a model for the osmotic coefficient of the solvent thus obtaining the activity coefficient of the water. The Gibbs-Duhem equation at a constant temperature and pressure considers that:

$$\sum n_i \cdot d\mu_i = 0 \quad (2.2.48)$$

Applying the Gibbs-Duhem equation for the system studied of salt and water

$$n_{\text{water}} \cdot d\mu_{\text{water}} + n_{\text{salt}} \cdot d\mu_{\text{salt}} = 0 \quad (2.2.49)$$

The chemical potential of water can be written as:

$$\mu_{\text{water}} = \mu_{\text{water}}^0 + RT \ln(x_w \cdot \gamma_w) \quad (2.2.50)$$

Adding the last equation and equation (2.2.34) to equation (2.2.49), it remains:

$$n_{\text{water}} \cdot d[\mu_{\text{water}}^0 + RT \ln(x_w \cdot \gamma_w)] + n_{\text{salt}} \cdot d[\mu_s^m + \nu \cdot RT \cdot \ln(m^{\text{MIAC}} \cdot \gamma^{\text{MIAC}})] = 0 \quad (2.2.51)$$

As the standard state chemical potentials are constant at constant temperature and pressure, this reduces to:

$$n_{\text{water}} \cdot d \ln a_{\text{water}} + n_{\text{salt}} \cdot \nu \cdot d \ln (m^{\text{MIAC}} \cdot \gamma^{\text{MIAC}}) = 0 \quad (2.2.52)$$

With the definition of molality found in equation (2.1.9), the last equation is written as:

$$d \ln a_{\text{water}} + m_s \cdot M_{\text{Wwater}} \cdot \nu \cdot d \ln (m^{\text{MIAC}} \cdot \gamma^{\text{MIAC}}) = 0 \quad (2.2.53)$$

Integration from $m_s = 0$, where $\phi = 1$ and $\ln \gamma^{\text{MIAC}}$ gives:

$$\ln a_{\text{water}} + M_{\text{Wwater}} \cdot \nu \cdot m_s + m_s \cdot M_{\text{Wwater}} \cdot \nu \cdot \int_0^{m_s} m_s \cdot d \ln (\gamma^{\text{MIAC}}) = 0 \quad (2.2.54)$$

Division with $M_{\text{Wwater}} \cdot \nu \cdot m_s$ and using the definition of the osmotic coefficient in equation (2.2.47) gives:

$$\phi = 1 + \frac{1}{m_s} \int_0^{m_s} m_s \cdot d \ln \gamma^{\text{MIAC}} \quad (2.2.55)$$

Osmotic coefficients can be obtained by integration of equation. The integration can be performed analytically with the application of a thermodynamic model.

2.2.5 Vapor-liquid equilibrium

Another type of property that needs to be calculated is the vapor-pressure. Only the solvent can evaporate, the salts remain in the liquid phase. The equation that is solved is then:

$$P_T = x_{\text{water}} \cdot \gamma_{\text{water}} \cdot P_{\text{water}}^{\sigma}(T) \quad (2.2.56)$$

Where $P_{\text{water}}^{\sigma}(T)$ is the vapor-pressure of the water at the concerned temperature.

The last equation can be expressed in function of the activity of water. The activity coefficient for the water is defined as:

$$a_{\text{water}} = x_{\text{water}} \cdot \gamma_{\text{water}} \quad (2.2.57)$$

So the equation for the vapor-pressure is simplified:

$$P_T = a_{\text{water}} \cdot P_{\text{water}}^{\sigma}(T) \quad (2.2.58)$$

In some cases it is interesting to related the vapor-pressure computation to the osmotic coefficient. The two properties are directly related as they both depend directly on the activity of water. The relation is shown on the next equation:

$$\ln a_{\text{water}} = e^{-\phi \cdot M_w \cdot \nu \cdot m_s} \quad (2.2.59)$$

The parameter ν is the sum of the dissociation coefficients of the salt [2]. In the case of monovalent salts, as the case studied, the value of this parameter is equal to two.

2.2.6 Solid-liquid equilibrium

In electrolyte systems two solid-liquid equilibrium reactions may be encountered. The equilibrium between the liquid and solid for the solvent and the equilibrium of salt saturation. The equilibrium respect to the solvent is more widely studied due to the fact that fundamental properties for the solvent at the temperature and pressure of crystallization are easier to determine than for the salt equilibrium. Considering that the component studied crystallizes as a pure component, the thermodynamic equilibrium condition base on fugacity for solid-liquid equilibrium states that:

$$f_i^{*Solid} = f_i^{*Liquid} \cdot x_i \cdot \gamma_i^{Liquid} \quad (2.2.60)$$

The relation between fugacities can be related by equilibrium properties using the Gibbs-Helmonhltz equation. The equation at any temperature T and pressure P stays for:

$$\ln \left(\frac{f_i^{*Solid}}{f_i^{*Liquid}} \right) = \frac{\Delta H_{F_i}}{R \cdot T_{F_i}} \left(1 - \frac{T_{F_i}}{T} \right) + \frac{\Delta C_{p_{F_i}}}{R} \cdot \left[\frac{T_{F_i}}{T} - 1 - \ln \left(\frac{T_{F_i}}{T} \right) \right] + \frac{\Delta v_{F_i} (P - P_F)}{R \cdot T_{F_i}} \quad (2.2.61)$$

The equation is composed of three terms. The first term corresponds to the effect of temperature on the change in Gibss energy, which is expressed using the enthalpy change upon fusion, the second term refers to the fact that this enthalpy may not be constant, in which case its temperature dependence is taken into account, using cP and the third term of the equation correspond to the correction for the variation on pressure that may affect the system (sort of Poynting effect). The last term can be neglected when the pressure change is low. The equation remains:

$$\ln \left(\frac{f_i^{*Solid}}{f_i^{*Liquid}} \right) = \frac{\Delta H_{F_i}}{R \cdot T_{F_i}} \left(1 - \frac{T_{F_i}}{T} \right) + \frac{\Delta C_{p_{F_i}}}{R} \cdot \left[\frac{T_{F_i}}{T} - 1 - \ln \left(\frac{T_{F_i}}{T} \right) \right] \quad (2.2.62)$$

The physical parameters that form the equation are:

ΔH_{F_i} is the heat of fusion and it is defined as the difference between the enthalpy of the liquid and the enthalpy of the solid. The heat of fusion is positive as the liquid has more energy than the solid.

T_{F_i} is the fusion temperature of the component i

T is the temperature of the study

$\Delta C_{p_{F_i}}$ is the difference in heat capacities. Corresponds to the heat capacity of liquid minus the heat capacity of solid.

2.2.7 Definitions of enthalpies

Experimental values on all energy quantities are defined as differences. They require a process where two containers are mixed to yield a final one. The analysis shown here illustrates the use of enthalpies, but the same definitions apply to Gibbs energies, entropies or heat capacities. Lower case symbols are molar properties, upper case are total properties.

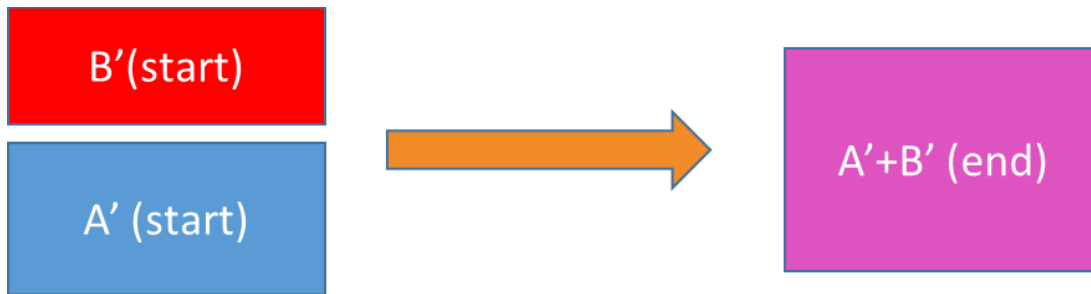


Figure 11. Representation of energy quantities definition

The measurement then yields the difference:

$$\Delta H = (n_{A'} + n_{B'})h_{A'+B'}^{end} - (n_{A'}h_{A'}^{startA'} + n_{B'}h_{B'}^{startB'}) \quad (2.2.63)$$

In that case, the enthalpy difference is a total property measured in J. The molar enthalpy h here has both superscripts and subscripts. The subscripts refers to the composition of the system (A' and B' are often the pure solvent and solute, but one of the two may also be a mixture). The superscript refers to the conditions (pressure, temperature and physical state).

The results are always presented in molar form, which leads to:

$$\Delta h = \frac{(n_{A'} + n_{B'})h_{A'+B'}^{end} - (n_{A'}h_{A'}^{startA'} + n_{B'}h_{B'}^{startB'})}{n} \quad \text{in J/mol} \quad (2.2.64)$$

The enthalpy difference is measured in J/mol and, n may be $n_{A'}$, $n_{B'}$ or $n_{A'} + n_{B'}$.

In some cases it is interesting to distinguish between integral properties, where n is final, and differential properties, which are taken in the limit of n infinitely small: :

$$\Delta h^{\text{inf}} = \lim_{n \rightarrow 0} \frac{(n_{A'} + n_{B'})h_{A'+B'}^{end} - (n_{A'}h_{A'}^{startA'} + n_{B'}h_{B'}^{startB'})}{n} \quad (2.2.65)$$

Table 6 then summarizes the various definitions found for different types of enthalpies

Table 6. Definitions found for different types of enthalpy

	A'		B'		(A+B)'		n	Comment
	Composition	Condition	Composition	Condition	Composition	Condition		
Mixing	pure A	P, T, liquid	pure B	P,T,liquid	always the sum of A' and B'	P,T,Liquid (single phase)	nA + nB	Also called Excess property.
Solution	pure A	P, T, liquid	pure B	P,T,solid		P,T,Liquid (single phase)	nB	---
Solvation	pure A	P, T, liquid	pure B	P,T,solid		P,T,Liquid (single phase)	nB=0	This property is not composition dependent
Dilution	pure A	P, T, liquid	A+B	P,T,liquid		P,T,Liquid (single phase)	nA	Requires two compositions

Let us for convenience also define the partial molar properties which is the heat provided by the system when adding one molecule of type i to the mixture:

$$\bar{h}_i = \left. \frac{\partial H}{\partial n_i} \right|_{T,P,n_{j \neq i}} \quad (2.2.66)$$

Note that this partial molar property is related to the phase equilibrium properties as

$$\bar{h}_A^E = \bar{h}_A - h_A^* = -RT^2 \left. \frac{\partial \ln \gamma_A}{\partial T} \right|_N \quad (2.2.67)$$

Where \bar{h}_i^E is the excess partial molar enthalpy.

The asterisk indicates the pure component property in the same (liquid) phase, at the same pressure and temperature as the mixture.

When an asymmetric activity coefficient is considered (which is the case for electrolyte systems, the excess partial molar enthalpy is in fact:

$$\bar{h}_B^E = \bar{h}_B - h_B^{*\infty} = -RT^2 \left. \frac{\partial \ln \gamma'_B}{\partial T} \right|_N \quad (2.2.68)$$

Where the 'infinite' sign shows that the value is taken at infinite dilution in the solvent.

Since this is a difference between two enthalpies, it is fully defined as such: it doesn't require a reference state. The enthalpy of the liquid mixture is then written as:

$$H = n_A \bar{h}_A + n_B \bar{h}_B = n_A (h_A^* + \bar{h}_A^E) + n_B (h_B^{*\infty} + \bar{h}_B^E) \quad (2.2.69)$$

Or

$$h = x_A (h_A^* + \bar{h}_A^E) + x_B (h_B^{*\infty} + \bar{h}_B^E) \quad (2.2.70)$$

The mixing property is most common in solution thermodynamics, but can often not be measured correctly when the solute is not liquid at the given pressure and temperature.

$$h^M = \frac{(n_A + n_B)h_{A+B} - (n_A h_A^* + n_B h_B^*)}{n_A + n_B} \quad (2.2.71)$$

Which can then be written as:

$$h^M = \frac{(n_A (h_A^* + \bar{h}_A^E) + n_B (h_B^\infty + \bar{h}_B^E)) - (n_A h_A^* + n_B h_B^\infty)}{n_A + n_B} \quad (2.2.72)$$

Or

$$h^M = x_A \bar{h}_A^E + x_B \bar{h}_B^E \quad (2.2.73)$$

The enthalpy of solution is obtained by slowly adding a salt to the solution that is initially pure. Hence the difference in enthalpy is measured between the mixture that contain solvent (A) and solute (B) from the difference between as follows:

$$h^{Sol} = \frac{(n_A (h_A^* + \bar{h}_A^E) + n_B (h_B^\infty + \bar{h}_B^E)) - (n_A h_A^* + n_B h_B^{*,S})}{n_B} \quad (2.2.74)$$

In contrast with the mixing enthalpy, the reference state for the solute, B, is now the solid phase, and the measure ratio is taken over the number of moles of B.

$$\begin{aligned} h^{Sol} &= \frac{n_A \bar{h}_A^E + n_B (h_B^\infty - h_B^{*,S} + \bar{h}_B^E)}{n_B} = \frac{n_A \bar{h}_A^E + n_B \bar{h}_B^E}{n_B} + (h_B^\infty - h_B^{*,S}) \\ &= \frac{(n_A + n_B) h^M}{n_B} + (h_B^\infty - h_B^{*,S}) = \frac{h^M}{x_B} + (h_B^\infty - h_B^{*,S}) \end{aligned} \quad (2.2.75)$$

The zero value is often called Φ_L the relative apparent molar enthalpy of the solute B :

$$\lim_{x_B \rightarrow 0} h^{Sol} = \Phi_L \quad (2.2.76)$$

The enthalpy of dilution is obtained by slowly adding pure solvent A to a solvent + salt mixture. Hence the difference in enthalpy is measured as follows:

$$h^{Dil} = \frac{(n_A^{II} \bar{h}_A^{II} + n_B \bar{h}_B^{II}) - (n_A^I \bar{h}_A^I + n_B \bar{h}_B^I) - n_A^0 h_A^*}{n_A^0} \quad (2.2.77)$$

Where

$$n_A^{II} - n_A^I = n_A^0 \quad (2.2.78)$$

The data often provide two compositions, I and II. As such, they are difficult to use. Yet, differential measurements are interesting since when n_A^0 is very small, we may state $\bar{h}_A^{II} = \bar{h}_A^I = \bar{h}_A$ and $\bar{h}_B^{II} = \bar{h}_B^I = \bar{h}_B$ such that

$$\lim_{n_A^0 \rightarrow 0} h^{Dil} = \frac{(n_A^{II} - n_A^I) \bar{h}_A}{n_A^0} - h_A^* = \bar{h}_A - h_A^* = \bar{h}_A^E \quad \text{which is also noted as } L_A \quad (2.2.79)$$

3. THERMODYNAMIC MODELS FOR ELECTROLYTE SYSTEMS

In order to relate mathematically the fundamental properties of systems and to describe properly the phase behavior of solutions, a thermodynamic model is required [29]. This chapter describes the most important models developed accounting for electrolytes interactions.

3.1 TYPES OF INTERACTIONS IN ELECTROLYTE SYSTEMS

The interactions are classified into long range interactions, intermediate range interactions and short range interactions depending on the effect of the potential energy of the interactions with the distance. An advanced thermodynamic model must be able to represent each of these correctly. Nevertheless, the majority of the models are structured with terms representing only long and intermediate range interactions. Ion-ion interactions are electrostatic interactions considered as long range interactions because they have an effect over a long distance. Ion-dipole interactions, that take place between ions and polar molecules such as water are intermediate range interactions. Those interactions are not as strong as the long range interactions but the potential energy of ion-dipole interactions is proportional to $1/r^2$ and the potential energy of dipole-dipole interactions is proportional to $1/r^3$. Finally, the short range interactions are mainly caused by intermolecular forces such as hydrogen bonds. The potential energy caused by short range interactions is proportional to the sixth power of the inverse separation distance.

The figure 12 represents a scheme of the different interactions existing in electrolyte systems and their classification.

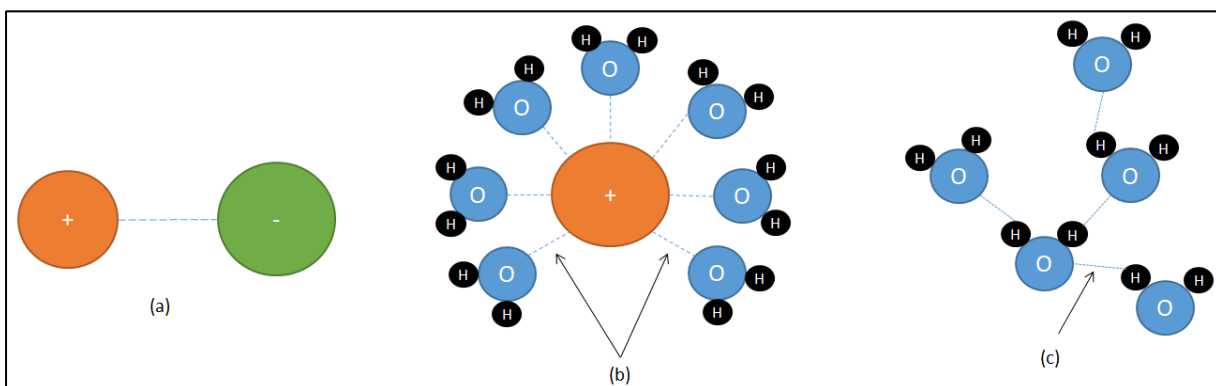


Figure 12. Different interactions in electrolyte systems. (a) Ion-Ion or long range interactions. (b) and (c) represent the short range interactions

3.2 MODELS FOR LONG RANGE INTERACTIONS

The first electrolyte models created, focused only on the electrostatic interactions. The models were based on Debye-Hückel studies [30].

3.2.1 The Debye-Hückel theory

One of the first theoretical works on electrolytes was developed by P. Debye and E. Hückel in 1923 [30]. This theory is one of the oldest models which is capable of describing long-range electrostatic interactions between ions. The Debye-Hückel model explains the deviation of electrolyte solutions from the ideal behavior (activity coefficient model). It uses the Poisson equation to express the energy resulting from the presence of a point charge in a cloud of charges. The final mathematical expression in terms of Helmholtz energy is obtained by solving Poisson's equation and Boltzmann distribution function for volumetric charge density around a central ion. The Debye-Hückel is based on a continuum model that takes into account some assumptions and considerations. These assumptions are summarized in the figure 13

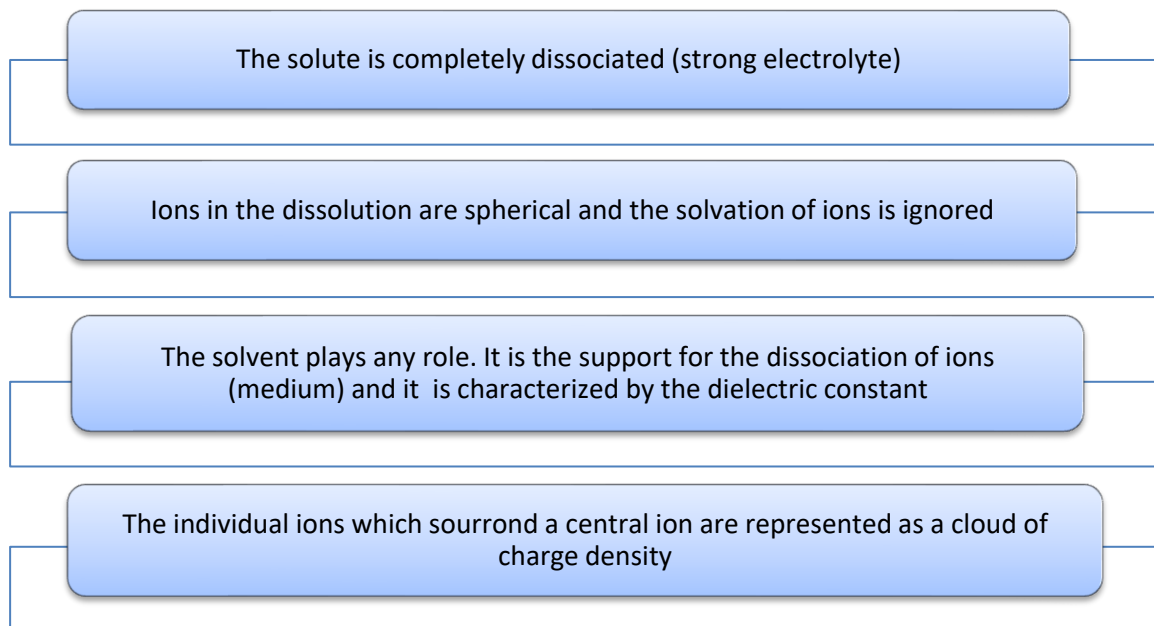


Figure 13. Assumptions for the Debye-Hückel model.

One of these assumptions considers that the solvent does not play any role in the interactions. In fact, in the Debye-Hückel model, the solvent is regarded as a dielectric continuum. The solvent only provides a medium for the ions and it is characterized by the dielectric constant (also known as permittivity). The dielectric constant of a solvent has an effect on the range of Coulombic reactions. It has a value closer to 1 for non-polar solvents and it increases with polar molecules. It is also dependent of the temperature, the solvent and the concentration of solute in the systems. ϵ_0 is the permittivity of vacuum and ϵ_r is the relative permittivity or the dielectric constant. The dielectric constant is reduced as the concentration of salt increases in the mixture [2].

According to Coulomb's law, the forces of interaction between two electric charges, separated by a distance r is given by the following equation:

$$F_C = \frac{Z_1 \cdot Z_2 \cdot e^2}{4 \cdot \pi \cdot \epsilon_r \cdot \epsilon_0 \cdot r^2} \quad (3.2.1)$$

One of the most important property that the electrolyte models takes into account is the Debye screening length ($1/\kappa$). This property represents the approximate radius of the ionic atmosphere created by the ions and it has units of distance. Overall, the Debye screening length, determines the range of ionic interactions and beyond this range the Coulombic interactions are very small or null and can be neglected. The screening distance, κa , is calculated as the product of the distance of closest approach, a and a parameter κ that is expressed as:

$$\kappa = \sqrt{\left(\frac{2 \cdot e^2 \cdot N_A \cdot \rho \cdot I}{\epsilon_0 \cdot \epsilon_r \cdot K_b \cdot T} \right)} \quad (3.2.2)$$

Models based on the Debye-Hückel theory depend of physical parameters that characterize the system and the solvent. The different parameters shown in equations (3.2.1) and (3.2.2) are listed on the table 7.

Table 7. Parameters of the Debye-Hückel model

Parameters	Description of the parameter	Units
κ	Kappa	m^{-1}
Z_1	Charge of cation	Unitless
Z_2	Charge of anion	Unitless
e	Electronic charge	$1,6 \cdot 10^{-19} C$
ϵ_r	Dielectric constant of the solvent	Unitless
ϵ_0	Dielectric constant of vacuum	$8.8542 \cdot 10^{-12} C^2 \cdot J^{-1} \cdot mol^{-1}$
r	Distance between electric charges	m
N_A	Avogrado number	$6.023 \cdot 10^{23} \cdot mol^{-1}$
ρ	Density	$Kg \cdot m^{-3}$
K_b	Boltzmann Constant	$J \cdot K^{-1}$
T	Temperature	K

The ionic strength is a parameter that describes the concentration of ions in the solution. Salts are ionic compounds that dissociate into cations and anions in presence of a solvent. The ionic strength is a function of the concentration of all the ions in the presence of the solution. The ionic strength is calculated with the molality as:

$$I = \frac{1}{2} \sum m_i \cdot z_i^2 \quad (3.2.3)$$

Where:

m_i : Is the molality in moles/kg of ion and z_i correspond to the ionic charge of the ion

3.2.2 Debye Hückel limiting law

The Debye-Hückel limiting law is the basis of all the electrolyte models and its main objective is to represent a model for electrostatic interactions. Applying the Poisson's equation, taking into consideration the electrostatic interactions the following equation can be demonstrated :

$$\ln \gamma = \frac{-/q^+ \cdot q^- / \cdot \kappa}{8 \cdot \pi \cdot \epsilon_0 \cdot \epsilon_r \cdot K_B \cdot T} \quad (3.2.4)$$

If we substitute the Debye screening length equation in the previous formula, we arrive to the following equation:

$$\ln \gamma = \frac{-/q^+ \cdot q^- /}{8 \cdot \pi \cdot \epsilon_0 \cdot \epsilon_r \cdot K_B \cdot T} \cdot \sqrt{\frac{2 \cdot e^2 \cdot N_A \cdot \rho \cdot I}{\epsilon_0 \cdot \epsilon_r \cdot K_B \cdot T}} \quad (3.2.5)$$

The charge of the cation and the anion can be written as: $q = Z \cdot e$, so the equation becomes

$$\ln \gamma = \frac{-/Z^+ \cdot Z^- / \cdot e^2}{8 \cdot \pi \cdot \epsilon_0 \cdot \epsilon_r \cdot K_B \cdot T} \cdot \sqrt{\frac{2 \cdot e^2 \cdot N_A \cdot \rho}{\epsilon_0 \cdot \epsilon_r \cdot K_B \cdot T}} \cdot \sqrt{I} \quad (3.2.6)$$

The equation can be grouped as:

$$\ln \gamma = \frac{-e^2}{8 \cdot \pi \cdot \epsilon_0 \cdot \epsilon_r \cdot K_B \cdot T} \cdot \sqrt{\frac{2 \cdot e^2 \cdot N_A \cdot \rho}{\epsilon_0 \cdot \epsilon_r \cdot K_B \cdot T}} \cdot /Z^+ \cdot Z^- / \cdot \sqrt{I} \quad (3.2.7)$$

The equation can be re-written, and is better known in following form:

$$\ln \gamma = -A_{DH} \cdot z_j^2 \cdot \sqrt{I} \quad (3.2.8)$$

$$A_{DH} = \sqrt{2 \cdot \pi \cdot N_A \cdot \rho} \cdot \left(\frac{e}{\sqrt{4 \cdot \pi \cdot \epsilon_0 \cdot \epsilon_r \cdot K_B \cdot T}} \right)^3 \quad (3.2.9)$$

Where the terms that form the equation are defined as:

- Debye-Hückel parameter: A_{DH}
- Product of the ionic charge of the anion and the cation: $z_j^2 = /Z^+ \cdot Z^- /$
- Ionic strength: $I = \frac{1}{2} \sum m_i \cdot z_i^2$

This model is not valid at high concentration of salt. It is normally applicable up to a concentration of 0.002 molal, otherwise the behavior of the model becomes very distant from the real behavior of the parameters. This model, is known to be good representation of the experimental data only when the concentration is lower than 0.002 molal [27].

3.2.3 Extended Debye-Hückel

The Debye-Hückel model cannot stand alone as a model for electrolyte solutions as it does not consider the short range interactions. It should be combined with another term in order to fully describe the properties of concentrated electrolyte solutions [27]. In extended Debye-Hückel, another constant is added. This constant takes into account the distance of the closest approach (α). The distance is the closest distance that any other ion can approach the central ion. It is close to the hydrated ion diameter. The typical values for the distance of the closest approach are between $3.5 \cdot 10^{-10}$ m and $6.2 \cdot 10^{-10}$ m.

$$\ln \gamma = -A_{DH} \cdot \frac{z_c z_A / \sqrt{I}}{1 + B_{DH} \cdot \sqrt{I}} \quad (3.2.10)$$

The Debye-Hückel constant A remains the same and depends mainly on the solvent and on the temperature.

$$A_{DH} = \sqrt{2 \cdot \pi \cdot N_A \cdot \rho} \cdot \left(\frac{e}{\sqrt{4 \cdot \pi \cdot \epsilon_0 \cdot \epsilon_s \cdot k \cdot T}} \right)^3 \quad (3.2.11)$$

The parameter B stands for:

$$B_{DH} = B \cdot \alpha \quad (3.2.12)$$

$$B = \sqrt{\frac{2 \cdot e^2 \cdot N_A \cdot \rho}{\epsilon_0 \cdot D \cdot k \cdot T}} \quad (3.2.13)$$

The representation of the model versus de experimental data for the NaCl at 298.15 K is represent in the figure 14.

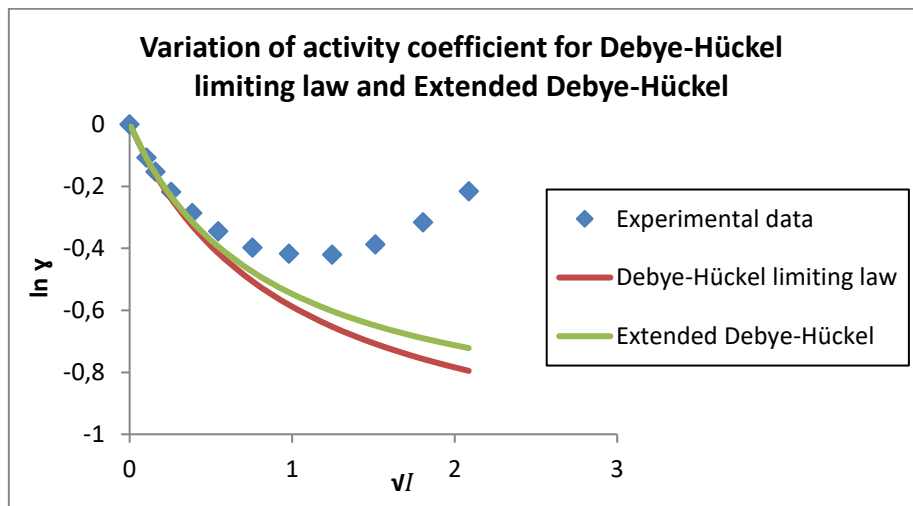


Figure 14. Model of Extended Debye-Hückel for activity coefficient at 298.15 K compared to data [31]

It can be observed that the model is improved and slightly better than the simplified Debye-Hückel thanks to the addition of the parameter B

3.3 EMPIRICAL MODELS FOR SHORT RANGE INTERACTIONS

The Hückel model and the Bromley are described in this chapter. Both models are compared with more detail in the section 6.1

3.3.1 Hückel model description

The Hückel model improves the Debye-Hückel model by the addition of a parameter [32]. It adds a second parameter, proportional to the ionic strength, so as to make it possible to extend the application range of the model and to found a more accurate parameterization. The addition of the parameter allows to calculate activity coefficients up to higher concentrations with good accuracy. The equation of model proposed is as follows:

$$\ln \gamma^* = -A_{DH} \cdot \frac{z_c \cdot z_A / \sqrt{I}}{1 + B_{DH} \cdot \sqrt{I}} + C \cdot I \quad (3.3.1)$$

In this equation, no theoretical development is proposed for the parameter C. It is therefore necessarily adjusted. E. Hückel justified the addition of the C parameter by showing that according to theory, a term proportional to the ionic strength would take the variation of the dielectric constant with the composition into account [32].

3.3.2 Bromley model description

The Bromley equation was developed in 1973 [3]. The objective of the model was to calculate the activity coefficients for aqueous electrolyte solutions with a high concentration range, exceeding the validity limits of the Debye-Hückel model. The model and the parameters of the model will be described as well as the main properties of the equation.

The Bromley model is an electrolyte model that calculates the mean ionic coefficient of aqueous salt solution based on a single adjustable parameter B. The model is based on the Debye-Hückel equation and two additional terms both function of the ionic strength. It is written as:

$$\ln \gamma^m = -A_{DH} \cdot \frac{z_c z_A / \sqrt{I}}{1 + \sqrt{I}} + C \cdot I \quad (3.3.2)$$

$$C / \ln 10 = \frac{(0,06 + 0,6B_{CA}) \cdot z_c z_c /}{(1 + \frac{1,5}{z_c z_A} I)^2} + B \quad (3.3.3)$$

Note that, Bromley replaced the activity coefficient γ^* by the molality based activity coefficient γ^m without any attempt to perform a correct conversion between the two types of activity coefficients. However, at high concentration of salts the approximation is more accurate as the Debye-Hückel contribution has less importance.

An approximation of the optimized B parameter can be calculated with the parameters of Bromley of the cations and anions. Bromley deduced a tendency that was described by the next equation. The values of the Bromley parameters of cations and anions are found in Bromley study [3].

$$B = B_+ + B_- + (\delta_+ \cdot \delta_-) \quad (3.3.4)$$

3.3.3 Pitzer Debye-Hückel

Another empirical model for electrolyte system is the Pitzer model. In 1973, K.S. Pitzer et al. developed their first paper concerning the description of aqueous electrolyte solutions [33]. The model is an activity model developed from the extended Debye-Hückel model [34]. The expression of the excess free energy is:

$$\frac{G^{ex}}{w_w RT} = f(I) + \sum_i \sum_j \lambda_{ij}(I) m_i m_j + \sum_i \sum_j \sum_k \mu_{ijk} m_i m_j m_k \quad (3.3.5)$$

In the last equation, the sub index i, j and k stay for the solutes (ions and neutral species dissociated). The water solvent is implicit. The definition of the other terms is:

I is the Ionic strength

w_w is the solvent mass (kg)

m_i is the molality of the component i (mol/kg d'eau)

λ_{ij} is the interaction binary interaction coefficient for short distance between the component i and j

μ_{ijk} is the interaction ternary coefficient short distance between the component i, j, k

The first function $f(I)$ correspond to Pitzer's empirical modification of the Debye-Hückel Gibbs excess function [35]. It depends on the ionic strength. The second virial coefficient $\lambda_{ij}(I)$, is the binary interaction coefficient for short interactions between pairs of ions. it depends also on the ionic strength. The third virial coefficient is represented by the term μ_{ijk} , it is a ternary interaction coefficient also for short distance between the components i, j, k. The dependence of the μ_{ijk} respect to the ionic strength is neglected. This parameter is used for cation-anion-anion and cation-cation-anion interactions. Cation-cation-cation interactions and anion-anion-anion interactions are also neglected.

$$f(I) = -\frac{4 \cdot A_{DH} \cdot I}{b} \cdot \ln(1 + bI^{1/2}) \quad (3.3.6)$$

The parameter $b = 1.2$ [34].

Pitzer defines also the equation for the mean molal activity coefficient. It is written as:

$$\ln \gamma^m = /z_c \cdot z_A / \cdot f^{\gamma} + m_s \left(\frac{2v_C v_A}{v} \right) B_{\pm}^{\gamma} + m_s^2 \left(\frac{2 \cdot (v_C v_A)^{1.5}}{v} \right) C_{\pm}^{\gamma} \quad (3.3.7)$$

In that equation:

$$f^{\gamma} = -\frac{A_{DH}}{3} \left[\frac{\sqrt{I}}{1 + b\sqrt{I}} + \frac{2}{b} \cdot \ln(1 + b\sqrt{I}) \right] \quad (3.3.8)$$

A_{DH} is the Debye-Hückel parameter and v_C, v_A the stoichiometric coefficients of the dissociated cation and anion. v stands for the sum of both dissociation coefficients.

Moreover, the term B_{\pm}^{γ} stands for:

$$B_{\pm}^{\gamma} = 2\beta_0 + \frac{2\beta_1}{\alpha^2 I} (1 - (1 + \alpha\sqrt{I} - 0.5\alpha^2 I) \exp(-\alpha\sqrt{I})) \quad (3.3.9)$$

In this equation, $\alpha = 2.0$. The two parameters β_0 and β_1 are adjustable parameters in the model.

The term C_{\pm}^{γ} corresponds to:

$$C_{\pm}^{\gamma} = \frac{3}{2} C_{\pm}^{\phi} \quad (3.3.10)$$

Where C_{\pm}^{ϕ} is an adjustable parameter in the model.

3.4 LOCAL COMPOSITION MODELS

Local composition models assume that the composition of a molecule i is affected by its neighboring molecules j , and is therefore different from its overall composition in the liquid [36]. The models based on local composition define that some molecules have a preference to surround specific molecules depending on their sizes, shapes, and interaction energies. Extended UNIQUAC and Electrolyte Nonrandom Two-Liquid (eNRTL) are models for based on local composition.

3.4.1 Extended UNIQUAC

The extended UNIQUAC model is an extension of UNIQUAC. The Debye-Hückel model was added to UNIQUAC model in order to represent electrolyte mixtures. The model has proved its applicability for calculations of vapor-liquid-liquid-solid equilibria and of thermal properties in aqueous solutions containing electrolytes and non-electrolytes. The model is shown in its current form here as it is presented by Thomsen [37].

The extended UNIQUAC model consists of three terms: a combinatorial or entropic term, a residual or enthalpic term and an electrostatic term

$$G^{\text{ex}} = G_{\text{Combinatorial}}^{\text{ex}} + G_{\text{Residual}}^{\text{ex}} + G_{\text{Extended Debye-Hückel}}^{\text{ex}} \quad (3.4.1)$$

The combinatorial and the residual terms are identical to the terms used in the traditional UNIQUAC equation [38].

3.4.2 Electrolyte Nonrandom two-liquid (eNRTL)

The electrolyte NRTL model uses a local composition concept adapted to electrolyte solutions. It is a combination of the NRTL model and the Pitzer-Debye-Hückel term [39]. The local composition concept is modified for ions and the model parameters are salt specific. The electrolyte NRTL model uses a local composition concept adapted to electrolyte solutions [40]. The use of a Pitzer-Debye-Hückel term instead of the Extended Debye-Hückel term does not make much difference.

The NRTL local composition model only has an enthalpic term, it uses no volume and surface area fractions and has no entropic term.

The use of salt specific parameters rather than ion specific parameters requires that a suitable mixing rule is applied. Otherwise calculations of solution properties would depend on how the composition of the solution is defined. A solution of equal amounts of CaCl_2 and MgNO_3 could as well be defined as a solution of $\text{Ca}(\text{NO}_3)_2$ and MgCl_2 . The electrolyte NRTL model is widely used as it is the model implemented in the commercial simulator ASPEN.

3.5 ADVANCED EQUATIONS OF STATE

Equations of state have also been used to describe electrolyte mixtures. They are well summarized in the book by Kontogeorgis [2] or in the thesis by Maribo-Mogensen [41]. Instead of using the Lewis-Randall (PT) framework, equations of state are developed based on the T-V framework. The most well-known ones are cubic, but more recently SAFT-type equations of state are also used.

In all cases, a specific term accounting for long-range interactions needs to be added. Some authors use directly the Debye Hückel term, others use the Mean Spherical Approximation (MSA). Maribo-Mogensen [42] has shown that both terms behave similarly.

Recently, many developments concerning electrolytes systems use the Statistical Associating Fluid Theory (SAFT). SAFT is an advanced thermodynamic equation of state where perturbation terms are used to correct the Helmholtz energy of a reference system. It is based on a statistical perturbation theory. Perturbation theory is a mathematical theory which provides an approximate solution to a problem. The solution is obtained by adding corrections (perturbations) to a reference behavior, as a Taylor series expansion [43] [44]. The mathematical expression describing the residual Helmholtz energy is given as in the following equation:

$$A_{\text{res}} = A_{\text{ref}} + A_{\text{perturbation}} \quad (3.4.2)$$

Where A_{ref} is the Helmholtz energy of reference state, often the hard sphere fluid. The perturbation term ($A_{\text{perturbation}}$), accounts for various interactions such as hard sphere, chain, dispersion, association, polar. No equation of state is used on this work

4. EXISTING DATA

The objective of this chapter is to describe and summarize the data available for electrolyte systems. The general existing data articles for mixtures of water and monovalent salts with water as solvent and with mixed solvents is summarized.

4.1 GLOBAL VIEW OF ALL DATA

Before the analysis of data consistency, data have to be classified. A strategy to classify data is by a representation of different properties for a specific system. In this chapter the properties of monovalent salts with pure water have been summarized. The different phase equilibrium properties studied in this work are represented by a color code as defined in the figure 15.

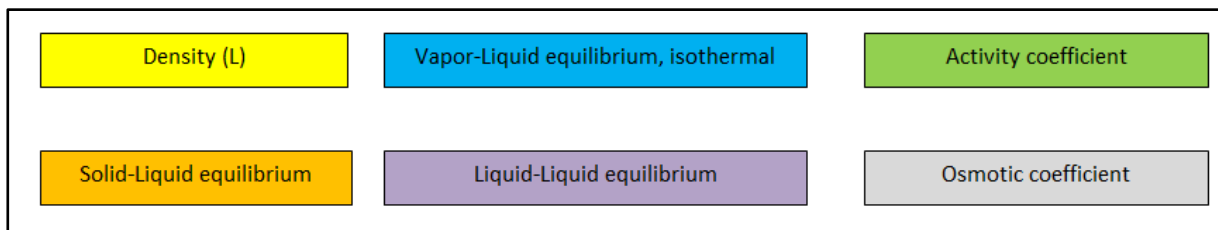


Figure 15. Color legend for the experimental data in phase equilibrium found for different salts type

The following tables represent the number of articles found in Detherm data base (2018 issue). The data series include experimental data for the properties studied for pure water as solvent and for the mixed solvents. In addition to the properties classification, the tables include also the number of articles found and studied in internal consistency and the data series of activity coefficient which have data at different temperature.

The table 8 represent a summary of data series for the pure water as solvent.

Table 8. Classification of experimental data properties for different monovalent salts with pure water as solvent

	Li	Na	K	Rb	Cs
F	7 articles	31 articles	28 articles	7 articles	6 articles
	1 article	11 articles. Only at 298 K	5 articles. Only at 298 K	6 articles. Only at 298 K	6 articles. Only at 298 K
	14 articles	2 articles	3 articles	1 articles	1 articles
		41 articles	21 articles	11 articles	10 articles
	4 articles	6 articles	4 articles	4 articles	
Cl	31 articles	323 articles	266 articles	42 articles	53 articles
	21 articles. Different T	60 articles. Different T	42 articles. Different T	13 articles. Only at 298 K	17 articles. Different T
	25 articles	43 articles	27 articles	6 articles	5 articles
	128 articles	390 articles	374 articles	74 articles	73 articles
	26 articles	47 articles	35 articles	7 articles	18 articles
Br	47 articles	94 articles	112 articles	9 articles	21 articles
	4 articles. Only at 298 K	26 articles. Different T	10 articles. Only at 298 K	4 articles. Only at 298 K	6 articles. Only at 298 K
	11 articles	11 articles	9 articles	1 articles	3 articles
	44 articles	79 articles	113 articles	20 articles	29 articles
	7 articles	13 articles	11 articles	3 articles	5 articles
I	24 articles	70 articles	74 articles	7 articles	7 articles
	4 articles. Only at 298 K	7 articles. Only at 298 K	7 articles. Only at 298 K	4 articles. Only at 298 K	4 articles. Only at 298 K
	4 articles	7 articles	8 articles	1 articles	1 articles
	20 articles	52 articles	77 articles	9 articles	9 articles
	4 articles	6 articles	6 articles	3 articles	3 articles

In this representation it can be shown that data for salts and water as solvent is available for a wide range of properties. Every property studied are found for all the salts. Lithium fluoride (LiF) is the only salt without any data related to activity coefficients. This salt is very insoluble in water. The maximum molality of LiF into water is 0.05 M. It can be also conclude that the majority of the data found was study at 298.15 K. In addition, the majority of articles about density and solid-Liquid equilibrium.

The table 9 represent a summary of data series for different salts and pure water and methanol as solvent.

Table 9. Classification of experimental data properties for different monovalent salts with pure water and methanol as solvent

	Li	Na	K	Rb	Cs
F	NO DATA	3 articles. Only at 298 K Low molality (up to 0,5 M maximum)	1 article	NO DATA	1 article
		2 articles			
Cl	5 articles	11 articles	2 articles	3 articles. Only at 298 K	3 articles
	4 articles. Only at 298 K	7 articles. Only at 298 K (One with 308 and 318 K)	2 articles. Only at 298 K		4 articles. Only at 298 K
	3 articles	5 articles	2 articles		1 article
	2 articles	17 articles	15 articles		
Br	1 articles	2 articles	3 articles	1 articles	3 articles
		1 article. Only at 298 K			2 articles. At 298 K. Low molality (up to 0,7 M maximum)
	2 articles	3 articles	2 articles		1 articles
	1 article	3 articles	5 articles		
I	NO DATA	4 articles	2 articles	NO DATA	3 article
		2 articles	4 articles		1 articles. At 298 K. Low molality (up to 0,7 M maximum)

The summary of data series for the salts combined with water and methanol solvents show that for mixed solvents less properties are available. Some salts present data series only accounting for one specific property whereas other salts such as RbF or LiI do not have experimental data studies. That lack of data may be in some cases due to low solubility of salts in the solvent. Temperature analysis shows that the data for the system studied is available only at 298.15. Only NaCl presents some data at different temperature than the room temperature. In other cases, the data found are only given at low molality. As an example, it is the case for the CsBr, the activity coefficients data series are studied for a maximum molality of 0.7 molal even if its saturation molality with a small concentration of methanol can reach 5 molal of maximum salt concentration. That factor is a limitation for thermodynamics studies as the data does not represent the extend behavior of the salts. These conditions are important and must be analyzed in the internal consistency. Another conclusion of the summary is that the majority of data is related to activity coefficient and solid-liquid equilibrium. Vapour-liquid equilibrium data including vapour phase composition are key to determine the activity of the individual solvents.

The same analysis of available data for the other mixed solvents (ethanol,1-propanol and 1-butanol) are shown in Appendix 1.

4.2 ACTIVITY COEFFICIENTS DATA

The table 10 represents an example of the data available for the LiCl and the activity coefficient property. The table represents the reference of the article, the year and the author. Related to the data the table show the temperature range included in the data, the maximum molality and the number of points of activity coefficients found in the respective article.

Table 10. Data available for LiCl and water for activity coefficient property

LiCl Activity coefficient					
Reference*	Year	Author	Temperature range (K)	Maximum molality (moles/kg)	Number of points
DDB-ELE:2008-JAN/173	1972	Hamer,W.J.;Wu,Y.C.	298.15	19.22	43
DDB-ELE:2015/10145	1920	Noyes,A.A.;MacInnes,D.A.	298.15	3	13
DDB-ELE:2011-DEC/8173	1929	Harned,H.S.	298.15	4	12
DDB-ELE:2015-Mar/9909	1993	Wang,R.L.;Yan,Y.;Zhang,Z.;Wu,G.L.	298.15	6	10
DDB-ELE:2008-JAN/1906	1993	Wang,R.;Yao,Y.;Wu,G.	298.15	6	8
DDB-ELE:2017/11949	1979	Campbell,A.N.;Bhatnagar,O.N.	323.15 ... 423.15	3.2	6
DDB-ELE:2010-DEC/7609	1964	Lebed,V.I.;Aleksandrov,V.V.	298.15 ... 363.15	0.1	5
DDB-ELE:2008-JAN/6189	1966	Shkodin,A.M.;Shapovalov,L.Ya.	298.15	0.006	8
DDB-ELE:2015/10320	1992	Yao,Y.;Sun,B.;Song,P.; Zhang,Z.;Wang,R.;Chen,J.	298.15	19.85	22
DDB-ELE:2008-JAN/5892	1934	Robinson,R.A.;Sinclair,D.A.	298.15	3	10
DDB-ELE:2017/12018	1981	Holmes,H.F.;Mesmer,R.E.	383.15 ... 473.15	6	7
DDB-ELE:2008-JAN/3801	1932	Pearce,J.N.;Nelson,A.F.	298.15	11.1	21
DDB-ELE:2017/12103	1963	Caramazza,R.	273.15 ... 323.15	6	13
DDB-ELE:2017/12631	1960	Lengyel,S.;Giber,J.;Tamas,J.	288.15 ... 308.15	17.73	9
DDB-ELE:2017/12259	1920	MacInnes,D.A.;Beattie,J.A.	298.15	3	8
DDB-ELE:2015/10246	1945	Robinson,R.A.	298.15	20	51
DDB-ELE:2008-JAN/5814	1930	Akerloef,G.	298.15	1	5
DDB-ELE:2015/10722	2014	Zhao,X.;Li,S.;Zhai,Q.;Jiang,Y.;Hu,M.	298.15	1.55	113
DDB-ELE:2011-DEC/8397	2010	Morales,J.W.;Galleguillos,H.R.; Graber,T.A.;Hernandez-Luis,F.	288.15 ... 308.15	4.05	12
DDB-ELE:2008-JAN/1080	1949	Robinson,R.A.;Stokes,R.H.	298.15	20	37
DDB-ELE:2009-AUG/6923	2008	Hu,M.;Tang,J.;Li,S.;Xia,S.;Jiang,Y.	298.15	0.44	9

* The references are coded according to the Detherm conventions: the actual literature references can be extracted from these codes if needed.

The table 11 gives information selecting the maximum temperature range and the maximum molality found for each salt with pure water as solvent. The data is synthesized including the salt, the different properties studied, the number of articles found for each property, the maximum temperature range found and the minimum and maximum molality. The table gives idea about the data existing but a more accurate study implies a more detailed analysis. Note that in some cases the maximum molality is higher than the saturation molality at 298.15 K. In this study, the maximum molality correspond to the article at higher temperature.

The tables concerning the other properties are joined in appendix 2

Table 11. Summary of the salts for activity coefficient

Salts	Activity coefficient		
	Number of articles	Temperature range (K)	Maximum molality data at 298.15 (moles/kg)
LiF	0	---	---
LiCl	21	273.15 - 473.15	19.85
LiBr	4	298.15	20
LiI	4	298.15	12.05
NaF	11	288.15 - 308.15	1
NaCl	57	273.15 - 363.15	6.14
NaBr	26	273.15 - 333.15	9.2
NaI	7	298.15 - 363.15	12
KF	5	298.15 - 473.15	17.5
KCl	38	273,15 - 363,15	5
KBr	10	298.15	5.5
KI	6	298.15	4.5
RbF	6	298.15	3.5
RbCl	12	283.15 - 363.15	7.8
RbBr	4	298.15	5
RbI	4	298.15	5
CsF	6	298.15	3.5
CsCl	17	273.15 - 773.15	35
CsBr	6	298.15	5
CsI	4	298.15	3

4.3 ANALYSIS OF DATA VERSUS SOLUBILITY

The limit of solubility of the salts NaCl and LiCl in function of the temperature are shown in figure 16 and 17 respectively. In both graphs the maximum molality found in experimental data analysis for activity coefficient and osmotic coefficient is also represented. With the representation it is possible to identify how much data is available at a range close to the maximum solubility. It allow also to identify unavailable data at a specific temperature range.

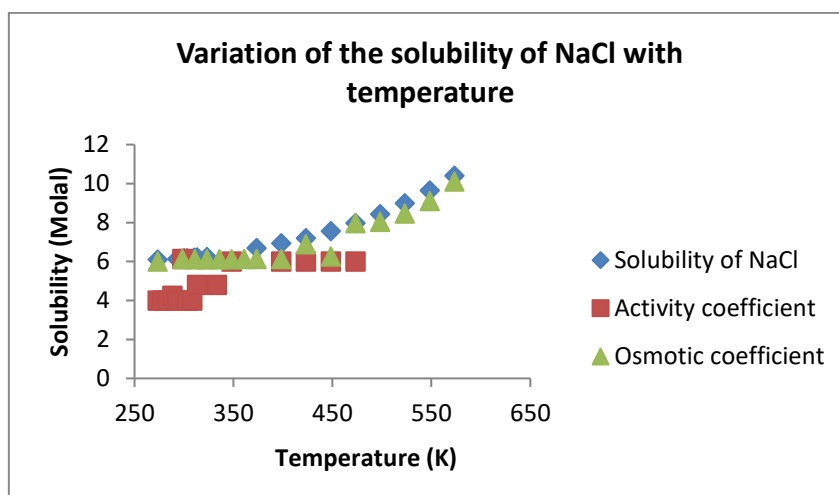


Figure 16. Solubility of NaCl in function of temperature.

For NaCl, it exist a wide variety of data. Specially concerning osmotic coefficient, the number of data involve a large temperature domain close to the saturation of the salt in water. Respect to activity coefficient, data is available until 470 K, after that temperature no data was found concerning activity coefficient of NaCl

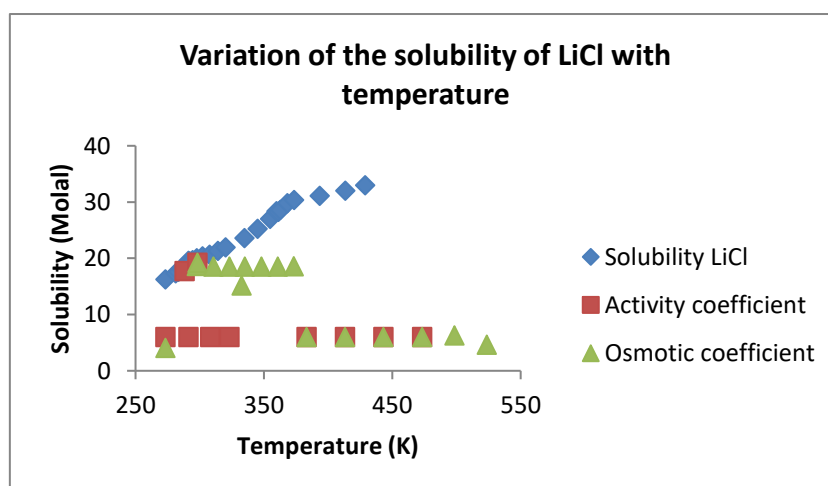


Figure 17. Solubility of LiCl in function of temperature.

In the case of LiCl only data is available until the saturation molality at 298.15 K for activity and osmotic coefficient. At other temperatures, the available data is studied until 5 molal.

The figure 18 presents the solubility in function of the temperature for the salts studied. The x axis refers to the temperature in K and the y axis to the molality. It can be observed that some salts have a wide range of data close to the maximum solubility for activity and osmotic coefficients (NaCl, KCl, NaF). The x axis refer to the temperature in K and the y axis to the molality. Other salts have a lack of data available and the range of molality study is far from the saturation molality (LiBr, KBr, CsCl, NaI).

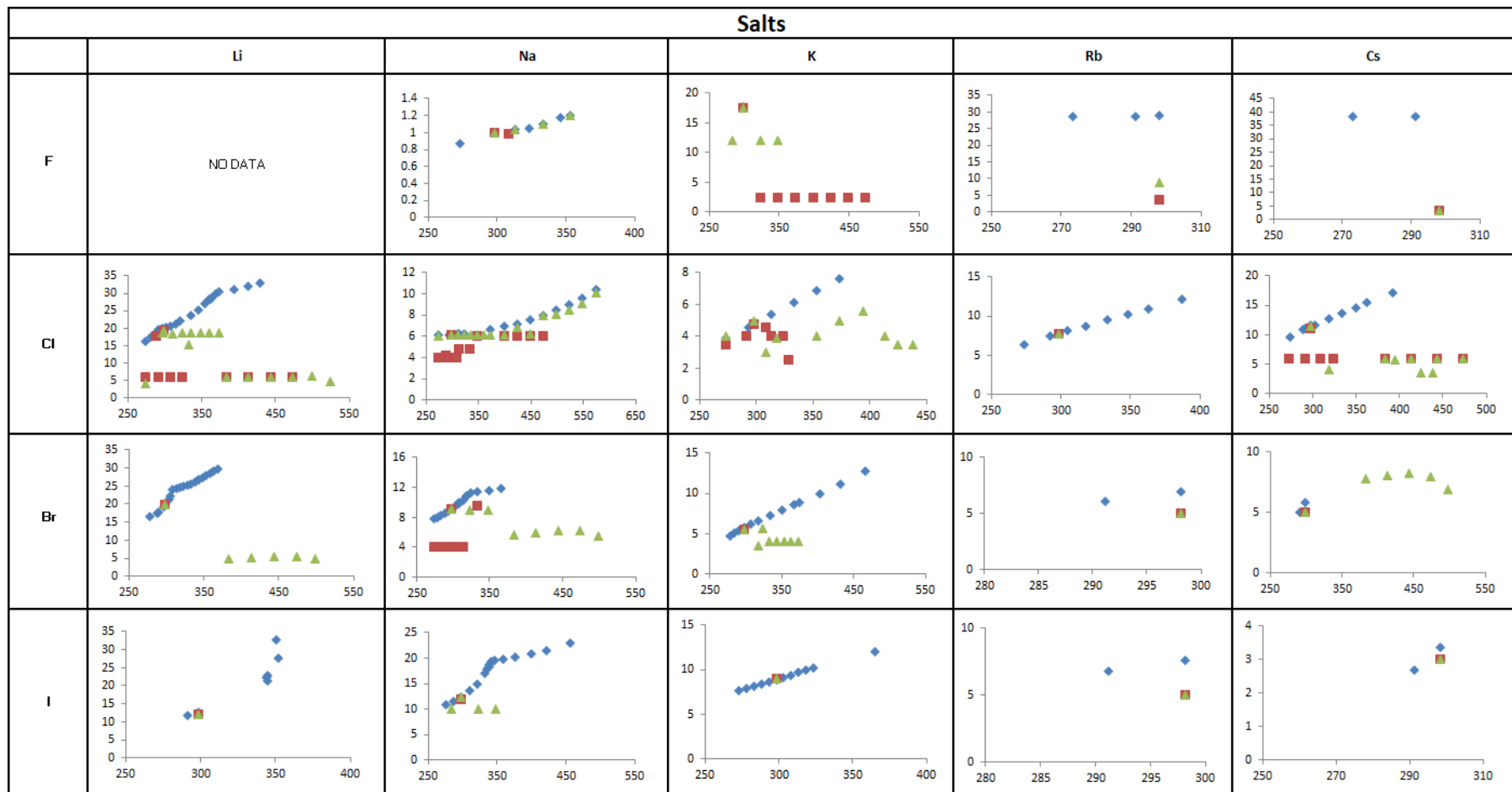


Figure 18. Variation of the solubility with temperature for different salts. The blue diamonds are maximum solubility of the salts in water, the red squares represents the maximum molality found in experimental data of activity coefficient and the green triangles the maximum molality found in experimental data of osmotic coefficient

5. ANALYSIS OF RESULTS FOR INTERNAL CONSISTENCY

5.1 PROCEDURE FOR INTERNAL CONSISTENCY ANALYSIS

The objective of the internal consistency analysis [45] is to evaluate whether the data satisfy thermodynamic consistency. We know that relationships exist among the properties:

- Gibbs-Duhem relates activity coefficients of various compound (solutes and solvents) (equation 2.2.55)
- The modified Raoult law can be used to test consistency of vapor pressures and solvent activity coefficient
- Gibbs-Helmholtz relates the derivatives of the activity coefficients with the enthalpies, or heat of solution

These relationships may not be obvious when looking at the data themselves. A thermodynamic model contains these relationships by construction. This is why it is proposed to use a model to test them. The consistency analysis consists in computing the deviations between the experimental data and the experimental values for a large number of properties. The relative deviations are computed as follows:

$$\text{Relative deviation (\%)} = \frac{X_{\text{calculated}} - X_{\text{experimental}}}{X_{\text{experimental}}} \cdot 100 \quad (5.1.1)$$

Where X is the property studied, in this work, salt activity coefficient (MIAC), osmotic coefficient and solution enthalpy.

Ideally, this model should be as accurate as possible. The relative deviations have been calculated for different properties and systems concerned by this study. In order to analyze the calculations, the deviations are represented as a function of the molality and the temperature. That representation gives information about the molality and temperature effect as it allows to compare the deviations at different concentration and temperature range for all the data series. In a second part of the analysis, the results of the deviations are represented in function of the mean temperature and the mean molality. The last representations does not allow to identify the data series inconsistent as they are based on the mean of temperature and concentration independently of the reference. However, it may give interesting information about the model limits and the specific condition that creates more scatter. For the analysis of results it is important to take into account that the relative deviations calculated can be negative or positive, depending on the values obtained by the model. A negative deviations means that the calculated points are below the experimental points, whereas a positive deviation indicates that the calculated points are greater than the experimental and the model is above the experimental point.

5.2 SELECTION OF THE MODEL FOR INTERNAL CONSISTENCY ANALYSIS

The model selected for internal consistency analysis is the eNRTL model. This model is widely used for industrial applications, and specifically in simulations tools such as ASPEN. The eNRTL contains three adjustable binary parameters for each pair of species. In this study the non-randomness parameter is fixed to 0.2. For a system made of a salt and a solvent the remaining binary parameters are two ($\tau_{\text{water-salt}}$ and $\tau_{\text{salt-water}}$). Two binary parameters are equal for monovalent salt and stay for the interaction between water and cation and the water and the anion, and two other equal parameters for interactions between cation and water and anion and water. The temperature dependence of the parameters is provided in ASPEN with following rule:

$$\tau_{\text{water-salt}} = C_{w-s} + \frac{D_{w-s}}{T} + E_{w-s} \cdot \left(\frac{(T^{\text{ref}} - T)}{T} + \ln \left(\frac{T}{T^{\text{ref}}} \right) \right) \quad (5.2.1)$$

The binary parameters depend on the constants C,D and E that can be found from ASPEN database.

The salts selected for internal consistency study were the LiCl, NaCl, KCl, CsCl with water as pure solvent. The parameters of used in ASPEN for the salts mentioned are specified in the Table 12

Table 12. Parameters used in ASPEN to calculate τ (water-ion) for NaCl

	Parameters from ASPEN: Water-salt		
	C	D	E
Water - LiCl	7.94709	605.785	-2.13858
LiCl - water	-4.30847	-247.351	1.82945
Water - NaCl	5.9802	841.518	7.4335
NaCl - Water	-3.78917	-216.365	-1.10042
Water - KCl	6.84954	402.982	0.206522
KCl - Water	-4.06009	-30.9353	1.42956
Water - CsCl	7.66143	252.948	-1.21597
CsCl - Water	-4.37244	51.2273	1.81383

In the IFPEN (Carnot) code, the temperature dependence is expressed using a simplified equation :

$$\tau_{\text{water-salt}} = C_{w-s} + D_{w-s} \cdot \left(\frac{1}{T} + \frac{1}{T^{\text{ref}}} \right) \quad (5.2.2)$$

This equation only depends on 2 parameters that have a relevant importance for the variation of the temperature. Hence, equivalent parameters need to be determined, Table 13 shows the equivalent parameters that have been fitted in the temperature range of 298.15 K-350.15 K.

Table 13. Parameters used in IFPEN to calculate T (water-ion) for NaCl

	Parameters from IFPEN: Water-cation-anion	
	C	D
Water - LiCl	9.9835	658.988
LiCl - Water	-5.142	-292.931
Water - NaCl	8.7889	669.732
NaCl – Water	-4.5128	-191.012
Water - KCl	8.2007	397.756
KCl - Water	-4.1669	-66.457
Water - CsCl	8.5124	283.114
CsCl - Water	-4.20448	6.1977

Figure 19 compare the two functions for the parameter of water-NaCl as an example.

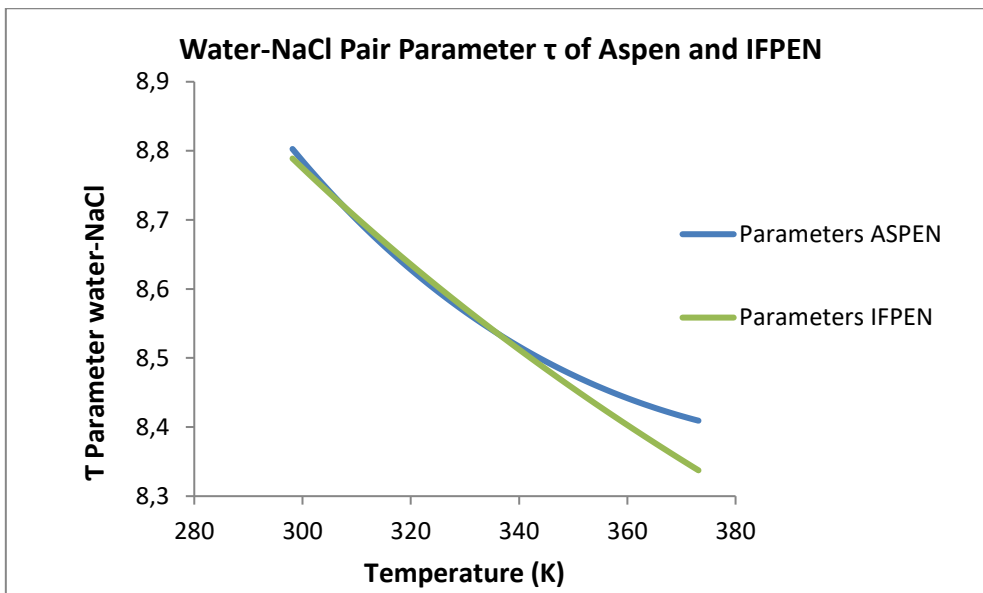


Figure 19. Comparison of parameters T(Water-Ion) of ASPEN and IFPEN

The representation of the parameter Tau for interactions between water with cation or anion is very representative until 340 K. This temperature limit was selected because most data are within the 0 – 100°C range (i.e. 273 – 373K). Above this temperature the parameter calculation is slightly different. That variation is important to take it into consideration, the deviation between the ASPEN model and the IFPEN model will increase above 340 K. However, for internal consistency this can be considered irrelevant as we are looking for clear inconsistent data that does not follow the same trend as the other data series.

5.3 RESULTS OF INTERNAL CONSISTENCY

5.3.1 Analysis and interpretation of the deviations with NaCl

The following figures 20 and 21 are complementary. They represent the relative deviations as a function of the molality (figure 20) or as a function of temperature (figure 21) for activity coefficients of NaCl with water as solvent. Each color and symbol represent a different data series. In some cases, the same data reference presents experimental data at different temperature but following the same experimental analysis. These data series are represented with the same color and symbol.

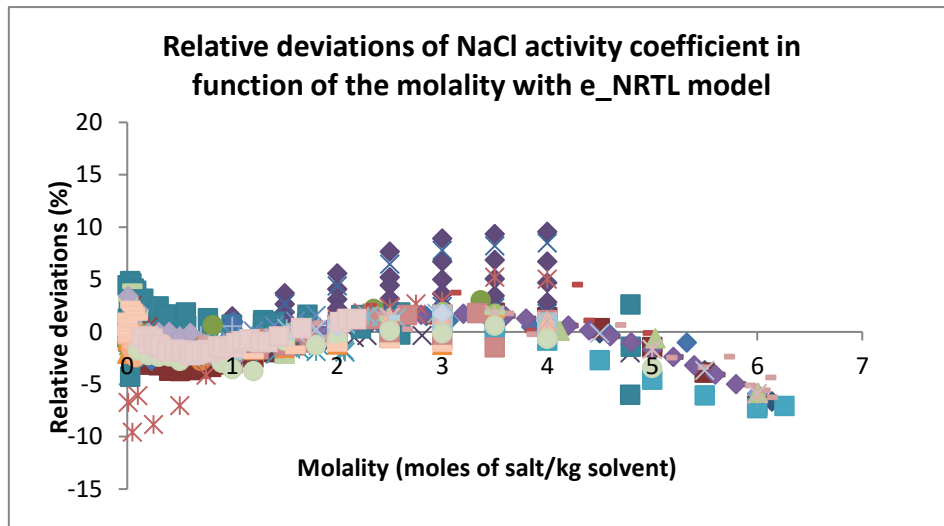


Figure 20. Analysis of the relative deviations in function of the molality for activity coefficients of NaCl with water as solvent

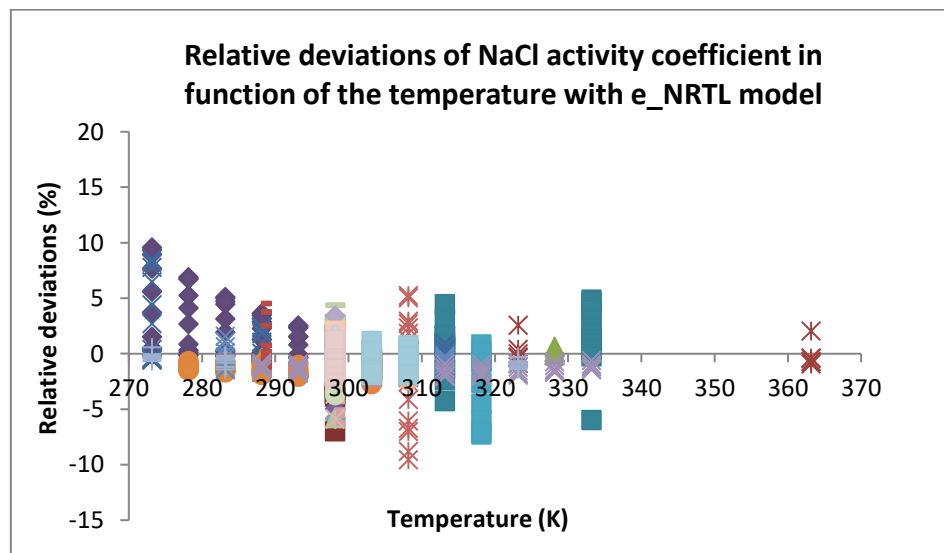


Figure 21. Analysis of the relative deviations in function of the temperature for activity coefficients of NaCl with water as solvent

The Detherm reference of the papers studied in the previous graphs are represented on figure 22

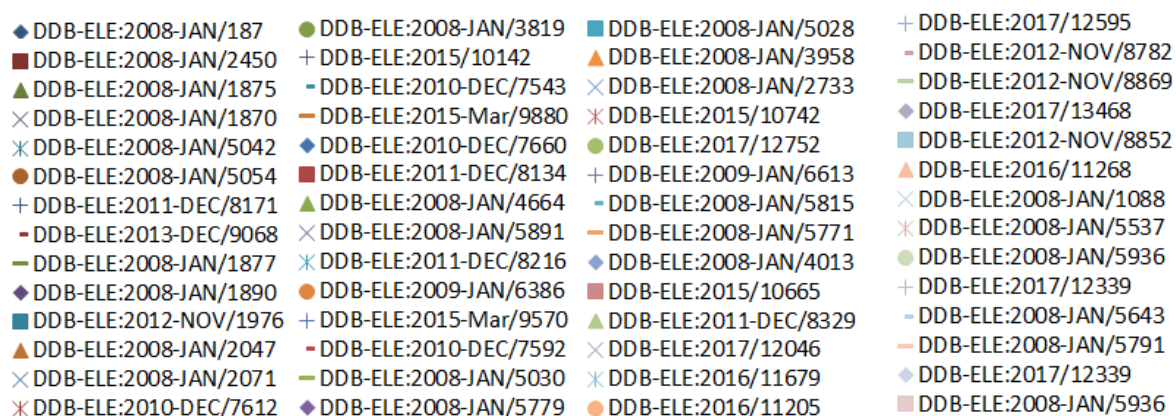


Figure 22. References used for internal consistency of activity coefficient NaCl

If the model and data had been perfect, the deviations should scatter around zero, and the average value of the scatter would provide an indication on the experimental uncertainty. As it is, we in fact see that the points follow a global trend. This is especially visible in figure 20. This global trend illustrates the model imperfections. It is visible that the e-NRTL model is accurate within +/- 5% until a molality of 5, but starts underestimating the activity coefficient beyond that point. Figure 21 shows that e-NRTL as it is coded in the IFP code extrapolates rather well at high temperature, but provides larger deviations at low temperature.

In order to correctly analyze the consistency of specific data series, both graphs have to be analyzed simultaneously. From figure 20, it can be observed that the majority of deviations for different data series are comprised between -5% and +5%. The eNRTL is quite accurate in activity coefficient representation. However, two series have a larger deviations than 5% (DDB-ELE:2008-JAN/1890; DDB-ELE:2008-JAN/2071) and one article reaches the amount -10% of relative deviations (DDB-ELE:2010-DEC/7612). In order to interpret correctly, these deviations have to be located also on figure 21, as a function of temperature. Doing so, it can be found out whether the deviations are caused by a the fact that the model is less accurate at low or high temperature or whether it is due to inconsistent data. It can be seen that for the data series analyzed before, with the highest deviations, both data series have been measured at low temperature, close to 0°C and at high temperature around 333 K for one data series and 363 K for the one with more positive deviations. The trend of the deviations with temperature is consistent among all points and shows that the model extrapolates badly especially at low temperature.

The table 14 represents the references found for activity coefficient of NaCl that have a different trend from the other series of data. That references have been analyzed.

Table 14. Inconsistent data series identified for NaCl activity coefficient

Reference inconsistent	Justification
DDB-ELE:2008-JAN/1890	Article from 1932. Activity coefficient calculated with an amalgam cell. Not accurate technique used for temperatures different from 25°C
DDB-ELE:2008-JAN/2071	Article from 1939. Uses data from the last reference mentioned and they used a specific equation to extropolate the electromotive force data.

Both references are based on the same data measurement. The reference DDB-ELE:2008-JAN/2071 improves slightly the DDB-ELE:2008-JAN/1890 measurements and as it can be seen the deviations are lower. The main problem of both series is that they are the more ancient series studied. The measurement equipment and the extrapolation techniques used to be less precise.

It is interesting also to analyze the deviations found by removing the data series with large deviations, and by zooming on the low molality, so as to eliminate the model imperfections. The representation also allows to analyze the scatter generated. The figure 23 analyzes the relative deviations until a maximum concentration of 2 molal and without the data mentioned before with the highest deviations. It can be seen that the scatter (difference in deviations between series) is approximately 4%.

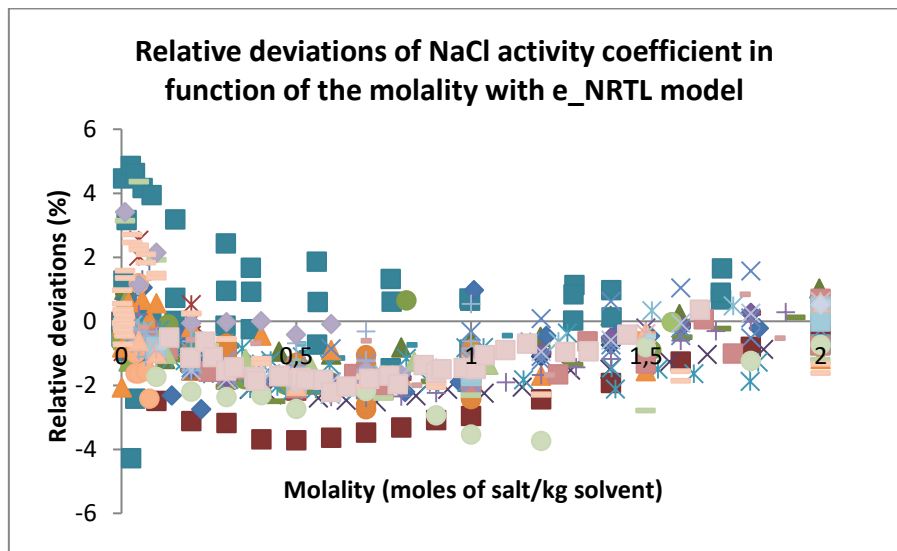


Figure 23. Analysis of the relative deviations in function of the molality for activity coefficients of NaCl with water as solvent without the data series presenting the highest deviations.

It can be concluded that the data series with more deviations (DDB-ELE:2009-NOV/1976) arrive at a maximum of 5% of relative deviations while the rest of data series tend to have less deviations. The temperature related to the experimental data must also be verified. From the representation 18 it can be concluded that the temperature for the mentioned experimental data is 313K and 333 K which is the higher temperature for the represented data. The deviations can also be explained by the model imperfections.

The same study has been done for osmotic coefficient. The figure 24 represents the relative deviations as a function of the molality and the figure 25 as a function of temperature for osmotic coefficients of NaCl with water as solvent.

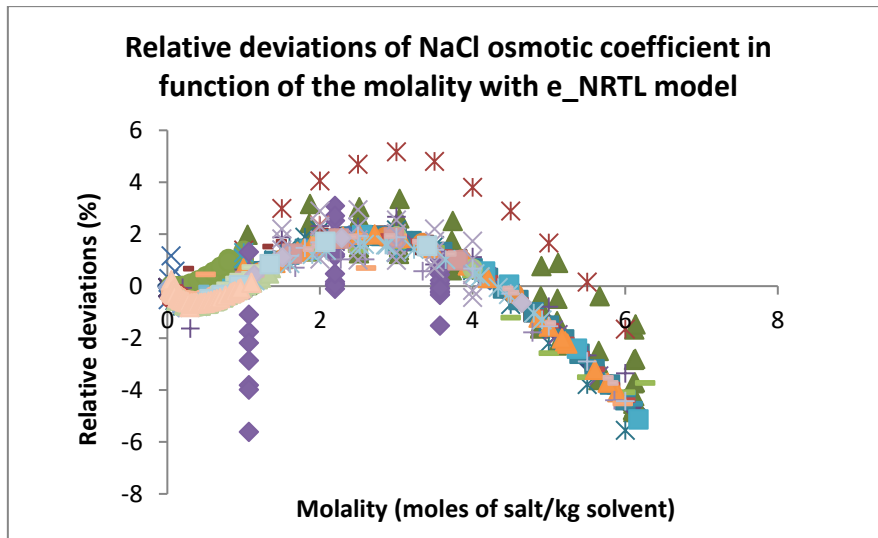


Figure 24. Analysis of the relative deviations in function of the molality for osmotic coefficients of NaCl with water as solvent

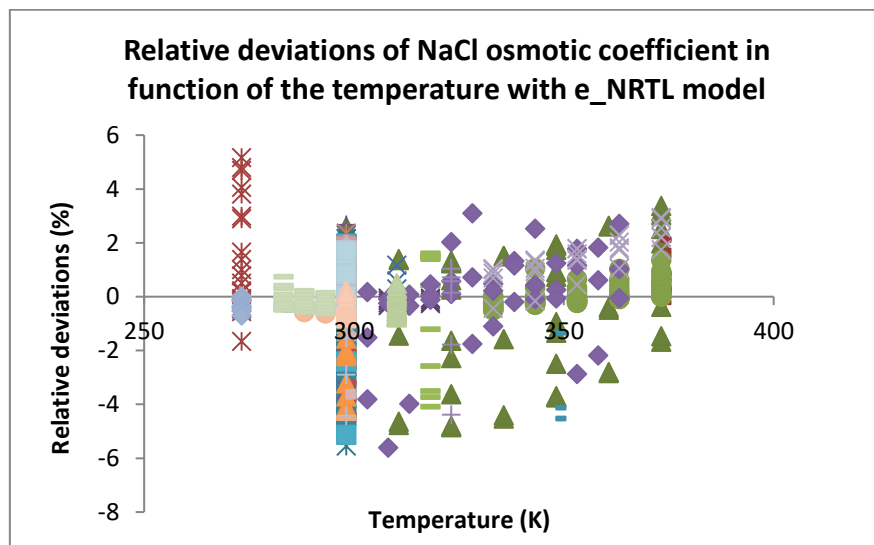


Figure 25. Analysis of the relative deviations in function of the temperature for osmotic coefficients of NaCl with water as solvent

The Detherm references for the osmotic coefficient of NaCl are shown on figure 26.

- ◆ DDB-ELE:2008-JAN/186 ✕ DDB-ELE:2008-JAN/2518
- DDB-ELE:2016/11375 ● DDB-ELE:2008-JAN/76
- ▲ DDB-ELE:2008-JAN/1736 + DDB-ELE:2017/12678
- ✕ DDB-ELE:2008-JAN/5058 ◆ DDB-ELE:2008-JAN/3834
- ✕ DDB-ELE:2008-JAN/6099 - DDB-ELE:2008-JAN/2242
- DDB-ELE:2013-DEC/9067 ■ DDB-ELE:2010-DEC/8045
- + DDB-ELE:2008-JAN/2852 ▲ DDB-ELE:2009-AUG/7495
- DDB-ELE:2008-JAN/480 ✕ DDB-ELE:2008-JAN/4836
- DDB-ELE:2009-AUG/7271 ✕ DDB-ELE:2015/10470
- ◆ DDB-ELE:2015/10412 ● DDB-ELE:2015-Mar/9760
- DDB-ELE:2008-JAN/56 + DDB-ELE:2015/10310
- ✕ DDB-ELE:2008-JAN/3929 - DDB-ELE:2008-JAN/5778
- DDB-ELE:2008-JAN/5027 ▲ DDB-ELE:2017/12842
- ◆ DDB-ELE:2008-JAN/3834 ✕ DDB-ELE:2008-JAN/81
- ▲ DDB-ELE:2008-JAN/6074 ✕ DDB-ELE:2017/13289
- ✕ DDB-ELE:2015/10458 ● DDB-ELE:2017/12976
- DDB-ELE:2015/10645 + DDB-ELE:2008-JAN/1033
- + DDB-ELE:2016/11271 - DDB-ELE:2011-DEC/8207
- DDB-ELE:2012-NOV/8520 - DDB-ELE:2008-JAN/4115
- ◆ DDB-ELE:2008-JAN/5673 ◆ DDB-ELE:2008-JAN/5677
- DDB-ELE:2016/10917 ▲ DDB-ELE:2013-DEC/9026
- ◆ DDB-ELE:2016/11444
- DDB-ELE:2017/12781

Figure 26. Detherm references used for internal consistency of osmotic coefficient NaCl

With the osmotic coefficient it can be seen that the highest deviations are found for the series measured at the lowest temperature (DDB-ELE:2008-JAN/2518). Even with the low temperature, the deviations of the points tend to follow the same trend as the other points of the graph 24. That show again the model imperfections to represent low temperature activity coefficients close to the water freezing point. Concerning high temperatures, the model is also unable to stabilize the deviations. Above 350 K the relative deviations increase significantly but the trend of the deviations in function the trend of the other deviations (DDB-ELE:2015/10412, DDB-ELE:2008-JAN/1736, DDB-ELE:2008-JAN/76). As a consequence, for NaCl osmotic coefficient there is no evidence that any data series study is inconsistent. The model computation at high and low temperatures need to be improved in order to perform a more accurate analysis.

Another study has been performed for the relative deviations of the enthalpy of solution for the NaCl. The figures 27 and 28 represent the study of the deviations for NaCl on the enthalpy of solution in function of the molality and the temperature respectively.

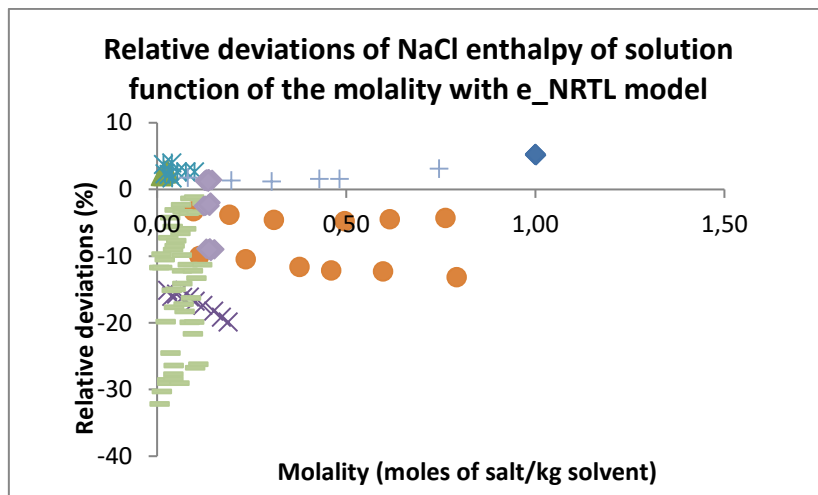


Figure 27. Relative deviations with the molality for enthalpy of dilution of NaCl with water

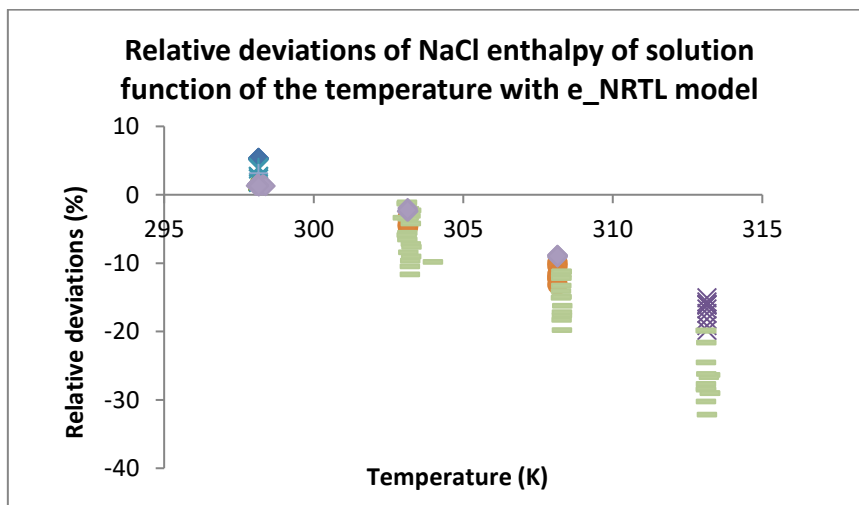


Figure 28. Relative deviations with temperature for enthalpies of solution of NaCl with water

The Detherm references for the enthalpy of solution studied of NaCl are shown on figure 29.

- ◆ 2008-FEB-20-14:50/13349
- ▲ 2008-FEB-20-14:50/16002
- × 2008-FEB-20-14:50/16486
- ✱ 2008-FEB-20-14:50/15875
- 2008-FEB-20-14:50/15282
- + 2008-FEB-20-14:50/15296
- 2008-FEB-20-14:50/16429
- ◆ 2008-JAN-29-13:45/17

Figure 29. Detherm references used for internal consistency of enthalpy of solution LiCl

Both graph show that the data series available for the enthalpy of solutions in NaCl is reduced. It is difficult to evaluate the trend of the relative deviations with low experimental data points. It can be also conclude from the figure 27 the percentage of relative deviations is quite constant as we increase the molality. That effect can be shown mainly in the data series (2008-FEB-20-14:50/15282) and (2008-FEB-20-14:50/15296). On the other hand, the deviations increase significantly as the temperature increases (2008-FEB-20-14:50/16429). As a consequence the model is able to represent the data of enthalpy of solution more accurately as the molality increases but has more difficulty to represent high temperatures.

The internal consistency analysis of the other salts studied (CsCl and KCl) is shown on appendix 3

5.3.2 Analysis and interpretation of the deviations with LiCl

Figures 30 and 31 present the deviations observed with LiCl data. This compound is of specific interest because its solubility is large, and therefore it is a true challenge to the model to reach these high concentration ranges. LiCl saturation molality at 298.15 is around 21.7 molal and the one of NaCl is approximately 6 M. Consequently, the LiCl analysis not only allows to determine the consistency of the data, but also to test the quality of the model at high concentration range. The representation of relative deviations in LiCl salt in function of the molality is represented in figure 30 for activity coefficients and in figure 31 for osmotic coefficient.

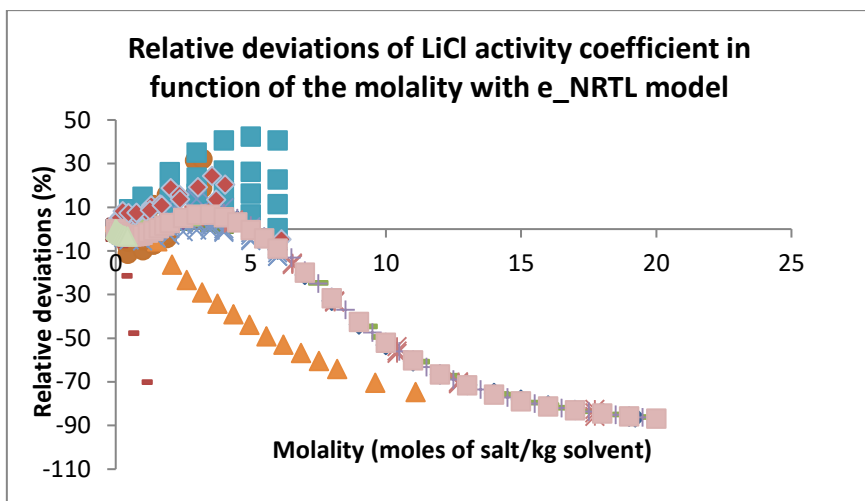


Figure 30. Analysis of the relative deviations in function of the molality for activity coefficients of LiCl

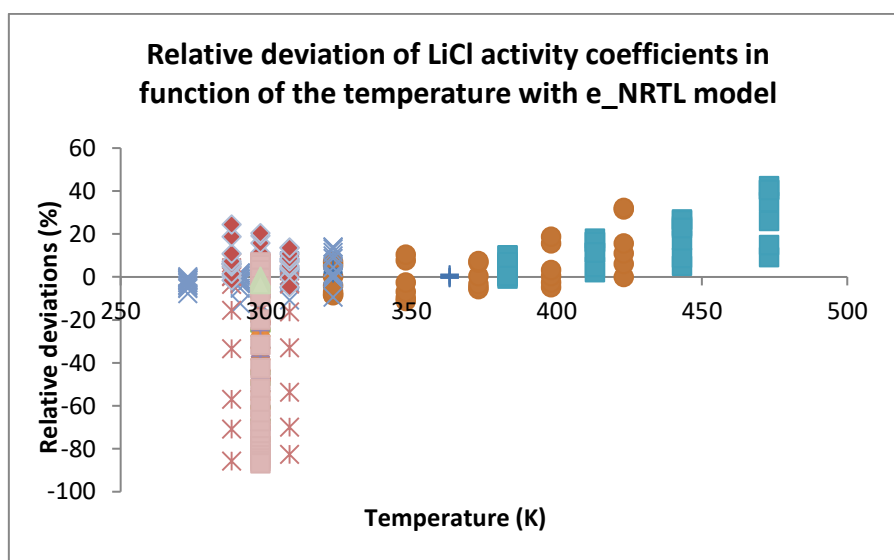


Figure 31. Analysis of the relative deviations in function of temperature for activity coefficients of LiCl

The references from Detherm for the activity coefficient of LiCl are presented on figure 32.

- ◆ DDB-ELE:2008-JAN/173
- DDB-ELE:2015/10145
- ▲ DDB-ELE:2011-DEC/8173
- × DDB-ELE:2015-Mar/9909
- ✱ DDB-ELE:2008-JAN/1906
- DDB-ELE:2017/11949
- + DDB-ELE:2010-DEC/7609
- DDB-ELE:2008-JAN/6189
- DDB-ELE:2015/10320
- ◆ DDB-ELE:2008-JAN/5892
- DDB-ELE:2017/12018
- ▲ DDB-ELE:2008-JAN/3801
- × DDB-ELE:2017/12103
- ✱ DDB-ELE:2017/12631
- DDB-ELE:2017/12259
- + DDB-ELE:2015/10246
- DDB-ELE:2008-JAN/5814
- DDB-ELE:2015/10722
- ◆ DDB-ELE:2011-DEC/8397
- DDB-ELE:2008-JAN/1080
- ▲ DDB-ELE:2009-AUG/6923

Figure 32. Detherm references used for internal consistency of activity coefficient LiCl

Analyzing the last graphs, it can be observed that the highest deviations are found for series with a molality above 6 M (DDB-ELE:2008-JAN/1080, DDB-ELE:2015/10145). However, the majority of the mentioned deviations follow the same trend. It can be concluded that these deviations are caused by model imperfections due to high salt concentrations. On the other hand, model imperfections due to high temperature can also be identified in figure 31. The reference DDB-ELE:2017/12018 show high positive deviations in figure 30. That date series can be identify also in figure 31, the analysis of this data series shows that measurements has been done at a temperature higher than 360K. Moreover, the deviations of the points try to follow the same trend as the rest of the points but with higher deviations due to the temperature. On the other hand, the data series DDB-ELE:2008-JAN/3801 and DDB-ELE:2008-JAN/6189 have very high deviations (-70%) and the data is measured at 298.15 K. Furthermore, these data does not follow the same trend of the other points set by the model. As a consequence, the mentioned data can be classified as inconsistent data.

The table 15 presents the different inconsistent data series found and the explanation of its consistency.

Table 15. Explanation of deviations for data series identified for LiCl activity coefficient

Reference inconsistent	Justification
DDB-ELE:2008-JAN/1080	High molality. Model imperfection
DDB-ELE:2017/12018	High temperature. Model imperfection
DDB-ELE:2008-JAN/3801	Not direct calculation of activity coefficient. Computation from osmotic coefficient with a model
DDB-ELE:2008-JAN/6189	The calculation has not been made by electromotive techniques. Computation from osmotic coefficient with a model

The same study has been done for osmotic coefficient of LiCl. The figure 33 represents the relative deviations as a function of the molality. Following the same logic, the figure 34 represents the relative deviations as a function of temperature for osmotic coefficients.

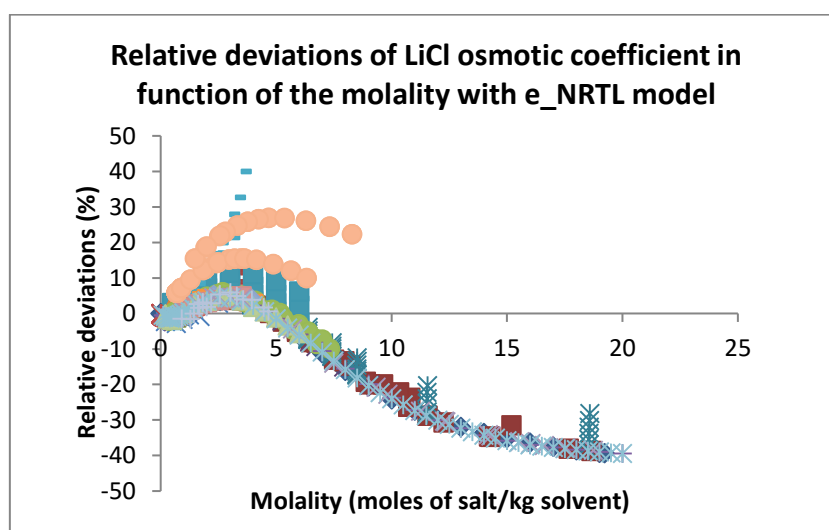


Figure 33. Analysis of the relative deviations in function of the molality for osmotic coefficients of LiCl with water as solvent

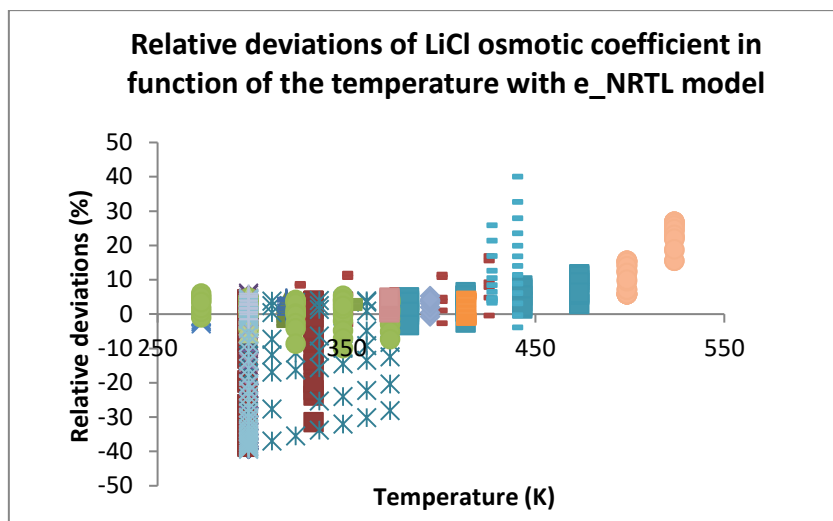


Figure 34. Analysis of the relative deviations in function of the temperature for osmotic coefficients of LiCl with water as solvent

The references from Detherm for the osmotic coefficient of LiCl are presented on figure 35

- ◆ DDB-ELE:2008-JAN/172
- DDB-ELE:2016/11522
- ▲ DDB-ELE:2017/12041
- × DDB-ELE:2008-JAN/2892
- ✱ DDB-ELE:2008-JAN/4133
- DDB-ELE:2008-JAN/2513
- + DDB-ELE:2016/10875
- DDB-ELE:2017/11944
- DDB-ELE:2015/10048
- ◆ DDB-ELE:2016/11352
- DDB-ELE:2008-JAN/3346
- ▲ DDB-ELE:2015/10460
- × DDB-ELE:2012-NOV/8569
- ✱ DDB-ELE:2016/10893
- + DDB-ELE:2008-JAN/1025
- DDB-ELE:2017/12063
- DDB-ELE:2015/10061
- ◆ DDB-ELE:2017/12056
- DDB-ELE:2015/10084
- ▲ DDB-ELE:2017/12677
- × DDB-ELE:2015/10318
- ✱ DDB-ELE:2015/10245
- DDB-ELE:2008-JAN/6145
- + DDB-ELE:2017/13461

Figure 35. Detherm references used for internal consistency of osmotic coefficient LiCl

The same conclusions found in the activity coefficient analysis are found for the osmotic coefficient. Models imperfections due to high molality of LiCl can be found (DDB-ELE:2016/11522; DDB-ELE:2008-JAN/172). That references follow the same trend as all the points, they are measured at 298.15 K but the reach relative deviations around -40% at high molality. The reference DDB-ELE:2008-JAN/6145 is an example of model imperfections caused by high temperatures. The reference is measured at a temperature around 500 K. The figure 33 shows that that the reference try to follow the trend of the other deviations but with higher deviations (more than 20%). By contrast, the reference DDB-ELE:2017/12063 show he highest deviations and the points do not follow the model trend, they just increase without any stabilization as the other points. That data can be consider as inconsistent data.

The representation of the deviations without including the data with the highest deviations is shown in figure 36. It is an strategy to determine the scatter in osmotic coefficient computation for LiCl.

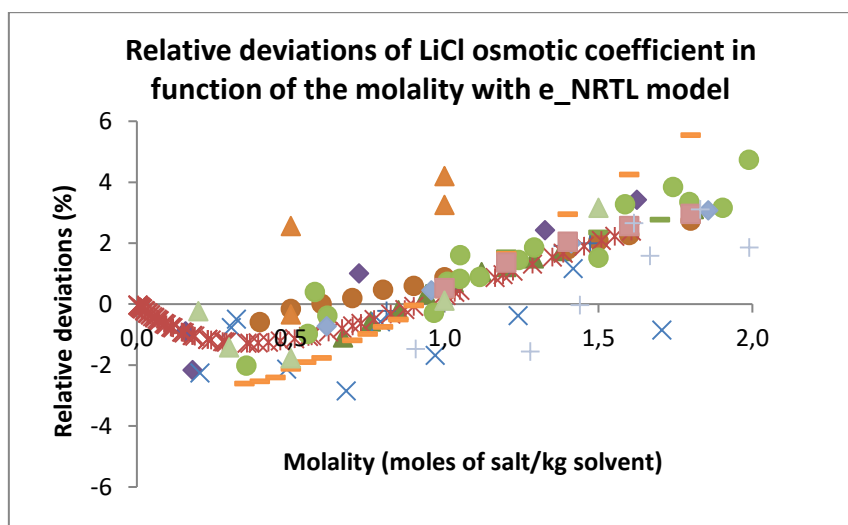


Figure 36. Analysis of the relative deviations in function of the molality for activity coefficients of LiCl with water as solvent until 2M.

In the graph it shown that the scatter around the general trend is lower than that observed for activity coefficients: here, one may state that the experimental uncertainty is close to $\pm 2\%$. In a first part, between 0 and 0.5 molal, the deviations are only negative. That part corresponds to the electrostatic interactions, The osmotic coefficients calculated with the model respect to these interactions are lower than experimental points for all the data series calculated. After 0.5 molal the deviations increase, that become positive deviations after 1 molal.

In Appendix 3 the internal consistency study for the KCl and CsCl is presented.

5.4 CONCLUSION ON INTERNAL CONSISTENCY

The results of internal consistency found for NaCl and LiCl are very different. For NaCl more data is available and the deviations are lower than for the LiCl. Moreover, the deviations found for NaCl are caused by the model imperfections due to high temperature or temperatures lower than 25°C. On the other hand, for LiCl some deviations may be explained by measurements at high temperatures or high molality range. The model used do not represent properly the extreme conditions. However, some data is found inconsistent itself. Different measurement methodologies or extrapolation techniques from other properties are the consequences of stronger deviations in LiCl. As a consequence, the consistency for each salt has to be studied separately. The deviations due to model imperfections have to be identified from the measurement deviations that do not follow the same trend as the other data series.

6. ANALYSIS OF RESULTS FOR EXTERNAL CONSISTENCY

For the external consistency, the data used for parameter adjustment and interpolation has been validated in the internal consistency methodology. Hence, a correct representation and analysis of internal consistency is essential before external consistency determination.

6.1 SELECTION OF THE MODEL FOR EXTERNAL CONSISTENCY ANALYSIS

External consistency requires the selection of a simple model with one adjustable parameter. In that part the selection of the Bromley model for external consistency is justified. The model parameterization consists in minimizing the deviations between consistent data of a specific property and the different models studied are compared. The objective function used is:

$$\text{Standard deviation (\%)} = \frac{1}{n} \cdot \sqrt{\sum_{i=1}^n \left(\frac{X_{\text{calculated}} - X_{\text{experimental}}}{X_{\text{experimental}}} \right)^2} \cdot 100 \quad (6.1.1)$$

Where X is the property studied. In this work, the standard deviation is minimized on activity coefficients, and on osmotic coefficients. It should be noted that when the molality range where data exist is small, the accuracy of the parameter becomes very small (the uncertainty on the parameter is large). This is observed for certain salts with low solubility or with mixed solvents.

The Extended Debye-Hückel model, the Hückel model and the Bromley model have been tested (see section 3.3). In order to select the proper model, the precision on the models regression is compared. The figure 37 presents the comparison of the models for activity coefficient for the MIAC of the NaCl and water mixture at 298.15 K. The parameter of each model have been optimized for consistent experimental data of activity coefficient by the minimization of the standard deviation.

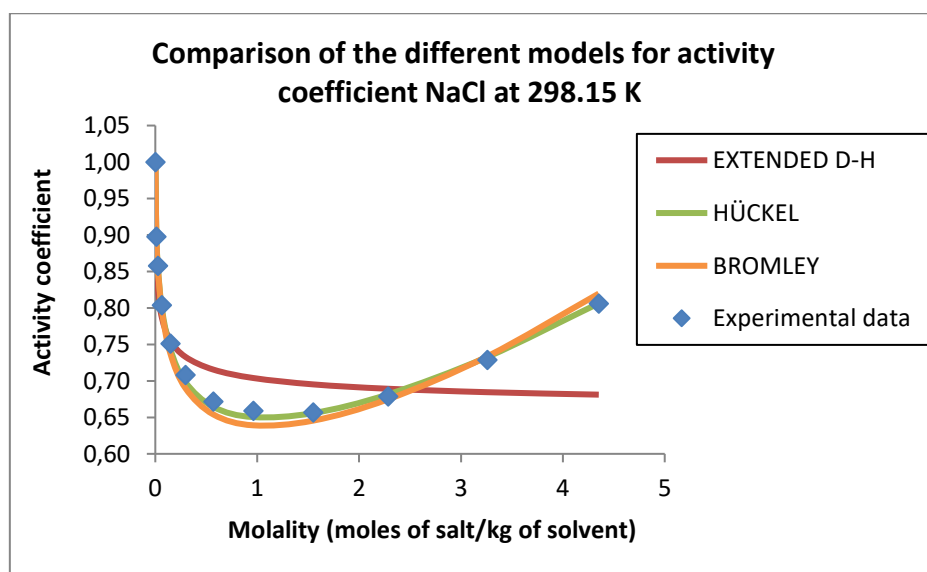


Figure 37. Comparison of the models for activity coefficient at 298.15 K compared to data [31]

The analysis of the deviations and the values of the parameter optimized for each model can be compared in the table 16.

Table 16. Comparison of the parameter adjusted and the standard deviations for the Hückel and the Bromley model in NaCl at 298.15 K

Hückel model		Bromley	
Parameter C of HÜCKEL	Standard Deviation (%)	Parameter B of BROMLEY	Standard Deviation (%)
0.1164	0.24	0.05935	0.532

The model of Extended Debye-Hückel is not a model that represent the tendency of the experimental data up to 0.2 molal approximately. This model only follows the experimental points at low concentration of salt due to the Debye-Hückel limiting law behavior.

Comparing the Hückel model and the Bromley model, it appears that both models represent the experimental data points accurately and there is not a notable difference between them. The model of Hückel present slight less deviations in the regression than the Bromley model. However, a thermodynamic model for external consistency can be selected according to the physical meaning of the adjustable parameter. E. Hückel justified the addition of the C parameter by showing that according to theory, a term proportional to the ionic strength would take the variation of the dielectric constant with the composition into account [46]. As a consequence, the parameter is added to fit the model but a physical sense of the parameter cannot be defined.

On the other hand, the parameter B of Bromley is a predictive parameter that can be calculated as an approximation depending on the electrolytes of the salt, whereas the parameter C in Hückel is an adjustable parameter that gradually modifies the slope of the curve but cannot be predicted. Consequently, the Bromley model is more predictive in terms of parameterization thus meaning an important advantage for extrapolation and parameter estimation. The Bromley model is a more predictive model. However, a drawback of the Bromley model is that the author replaces the rational, unsymmetrical, activity coefficient (γ_i^*) with the molality base activity coefficient (γ_i^m) without any explanation and without any attempt to perform a correct conversion between the two types of activity coefficients. In other words, the model wrongly assumes that the Debye-Hückel term is molality based [27].

Taking the advantages and drawbacks of every model, the Bromley model was selected. It has been shown that the parameter has a consistent trend when comparing different salts [3] [47].

6.2 EVALUATION OF THE BROMLEY MODEL

6.2.1 Analysis and influence of the parameters of the Bromley model

In order to achieve external consistency, it is important to understand the meaning and influence of the parameters of the model. The Bromley equation is:

$$\ln \gamma = -A_{DH} \cdot \frac{z_c z_A / \sqrt{I}}{1 + \sqrt{I}} + C \cdot I \quad (6.2.1)$$

$$C / \ln 10 = \frac{(0,06 + 0,6B_{CA}) \cdot z_c z_c /}{(1 + \frac{1,5}{z_c z_A} I)^2} + B \quad (6.2.2)$$

The parameter A_{DH} of the Bromley equation represents the electrostatic interactions at low concentration of salt. It stands for the decrease of the activity coefficient and represents the slope of first part of the curve. The parameter is dependent mainly in the temperature, density and the dielectric constant of the solvent. The parameter B represents the increase in the activity coefficient at high molality caused by solvation. Consequently, a higher value of the parameter B implies a stronger increase in the activity coefficient. The graph on figure 38 represents the contribution in the Bromley model in the activity coefficient equation.

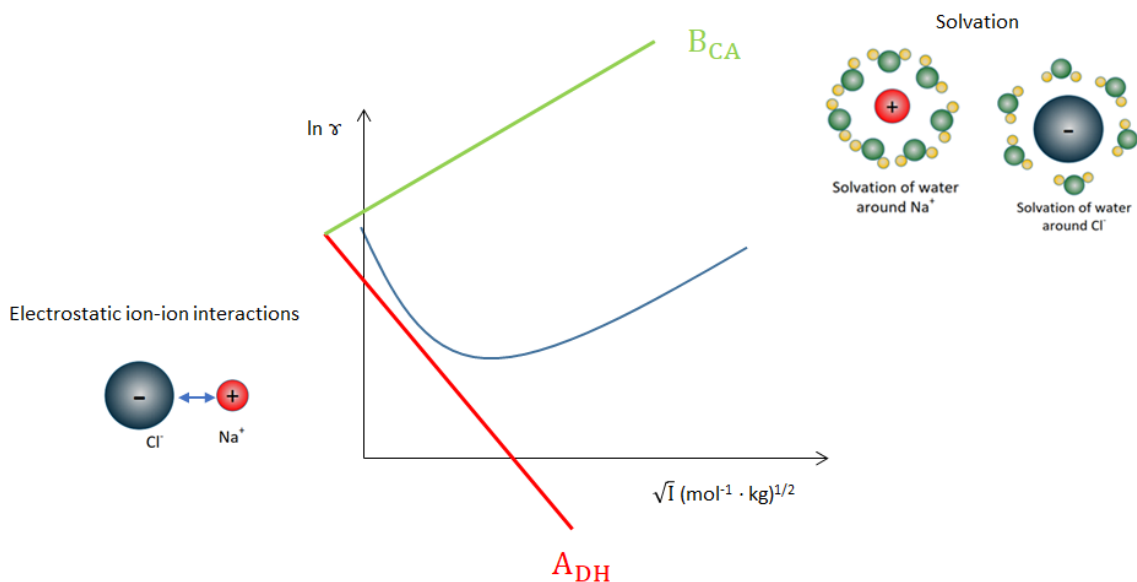


Figure 38. Type of interactions represented by the parameter of the Bromley model and effects on the activity coefficient.

6.2.2 Computation and relation of properties with Bromley model

The parameter B has been optimized for every system from the activity coefficient experimental data. The left columns of Table 17 represents the values of the optimized parameter B of Bromley for different monovalent salts. The right columns collect the standard deviations.

Table 17. Values of the parameters B obtained for Bromley model for different salts at 298.15 K

Ions	Li		Na		K		Rb		Cs	
F	Non data		0.0174	0.438 %	0.0632	0.288 %	0.0749	0.748 %	0.0990	0.598 %
Cl	0.1345	0.345 %	0.0594	0.532 %	0.0264	0.549 %	0.0178	0.087 %	0.0089	0.431 %
Br	0.1542	0.544 %	0.0808	0.527 %	0.0318	0.410 %	0.0132	0.103 %	-0.0018	0.373 %
I	0.1922	0.462 %	0.1014	0.113 %	0.0457	0.613 %	0.0129	0.057 %	-0.0147	0.107 %

Any data was found for the Lithium Fluoride (LiF) activity coefficient due its low solubility in water. For CsBr and CsI salts, the parameter B has a negative value. That negative values correspond to a constant value of the parameter B at high molality. In the results of external consistency the effect of the solvation in the parameter B is tested. Overall, the standard deviations of the salts have a low value.

The consistency of the Bromley model is analyzed for NaCl. The activity coefficient property is related with the osmotic coefficient through the Gibbs-Duhem equation (equation 2.2.55). The analytical calculation found in Bromley paper [3] is compared to numerical calculation of osmotic coefficient.

Figure 39 shows the mentioned comparison. The parameter B used for both representations has been optimized from the activity coefficient.

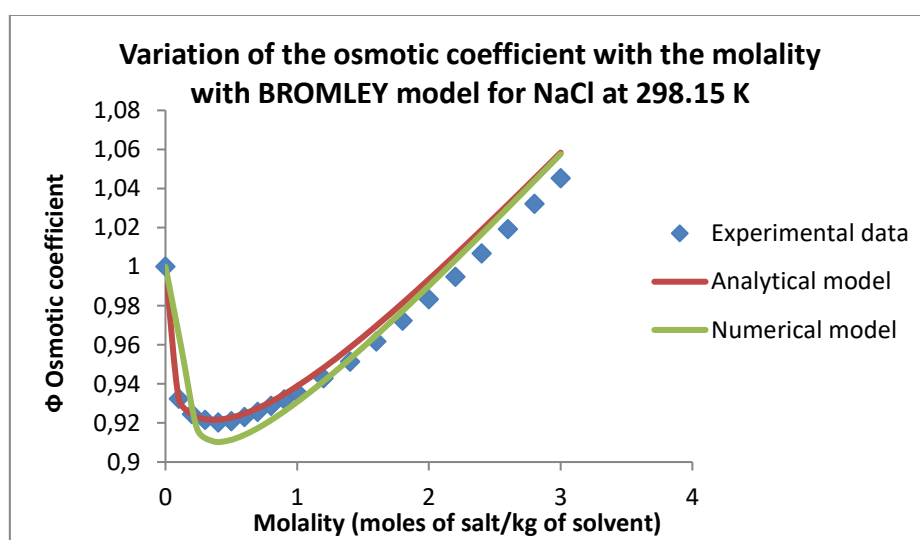


Figure 39. Model of Bromley for osmotic coefficient at 298.15 K compared to data [48]

From the graph it can be concluded that both model follow the tendency of experimental data. The figure determine that the analytical model is more precise than the numerical model as expected. In order to validate the relation of properties with the Bromley model, the vapor-pressure is also computed following equation (2.2.58) in chapter 2.2.5. The calculation of the water activity allows to calculate the vapor-pressure of the system. The representation of vapor pressure for the NaCl at 298.15 K is compute on the figure 40.

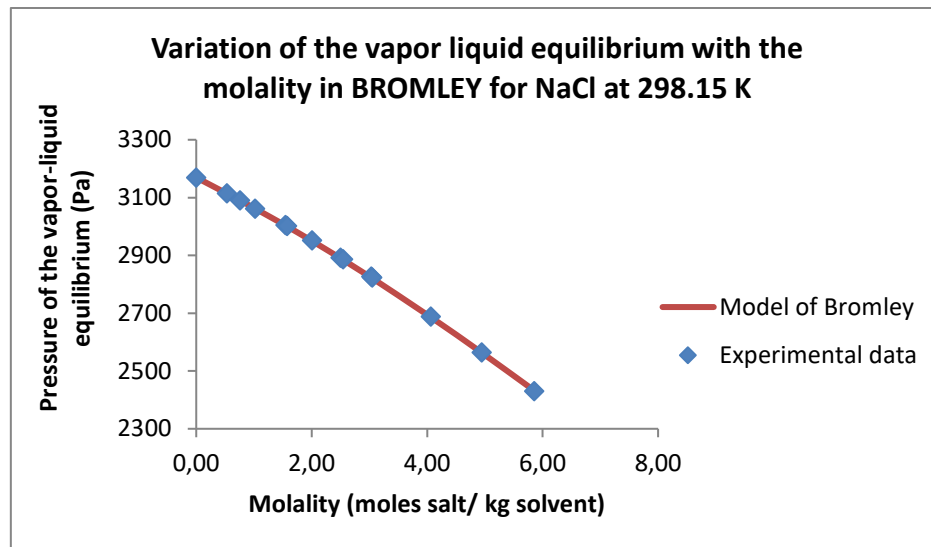


Figure 40. Model of Bromley for Vapor Liquid equilibrium at 298.15 K compared to data [49]

The standard deviation of the representation is 0.0189 %. As it can be with that value also in the graph the regression of the vapor-pressure for the NaCl is quite precise. The Bromley model is as a consequence a consistent model for monovalent salts and the fundamental properties of systems can be related with the selected model.

6.2.3 Different behavior of salts

The behavior in the trend of the variation of the activity coefficient may be different depending on the salt studied. In some cases, the activity coefficient increases highly, whereas, with other salts, the increase is not notorious. The figures 41 and 42 represent the activity coefficient for LiI and the CsCl salts with water at 298.15 K.

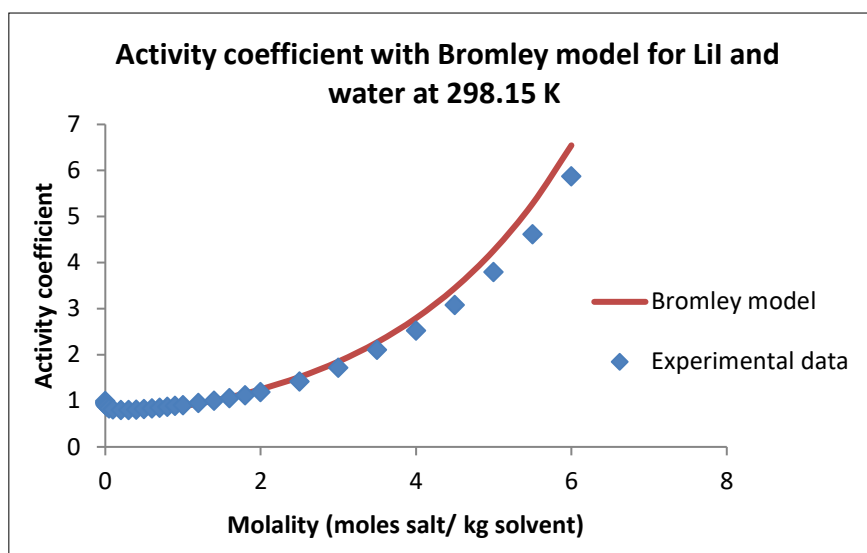


Figure 41. Computation of activity coefficient with Bromley for LiI with water at 298.15 K

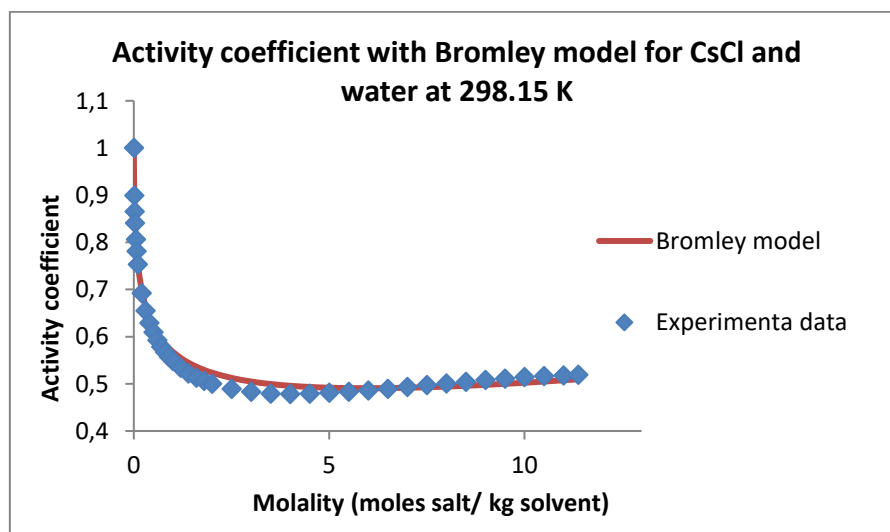


Figure 42. Computation of activity coefficient with Bromley for CsCl with water at 298.15 K

The activity coefficient of the LiBr increases at high concentration of salt. On the other hand, activity coefficient of CsCl remains quite constant after 1 molal. The parameter B represents the increase in the activity coefficient due to the solvation. As a consequence we might think that for that it is possible that for the CsCl the solvation is less than for the other salt or even that there is not solvation. In fact the parameter B of LiBr was 0.1542 and 0.0089 for CsCl. The activity coefficient representation of all the salts studied is represented in the next figure 43.

The x axis refer to the molality and the y axis to the activity coefficient. The blue points correspond to the experimental data and the red line is the Bromley model representation with the optimized parameter B.

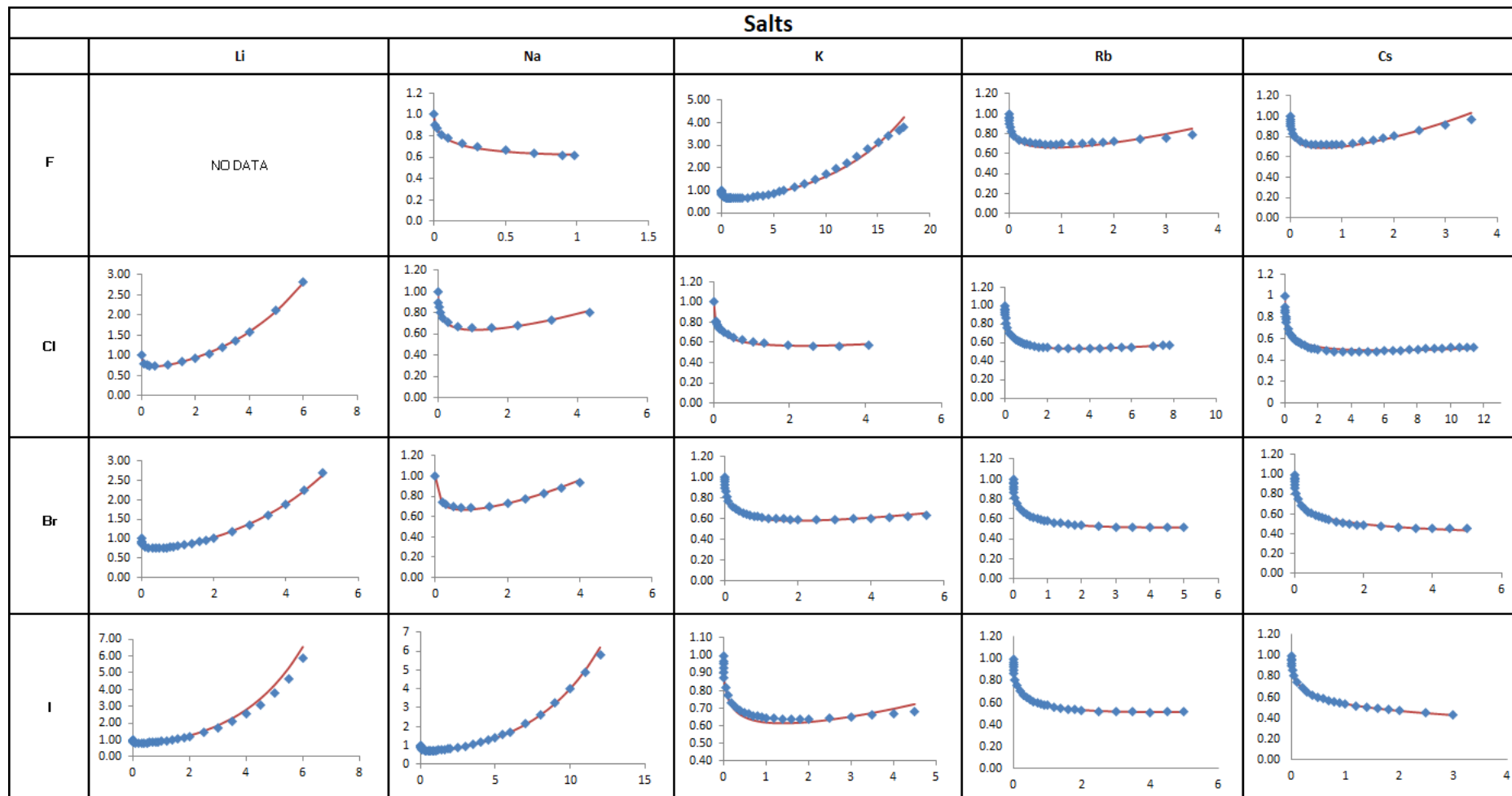


Figure 43. Variation of the activity coefficient with molality for different salts. The blue diamonds are the experimental data, the red line represent the Bromley model computation for the activity coefficient.

Some salt are highly soluble in water and can reach high saturation molality. The saturation molality of LiBr is 21.68 molal [50]. The figure 44 shows the representation of the activity coefficient of LiBr.

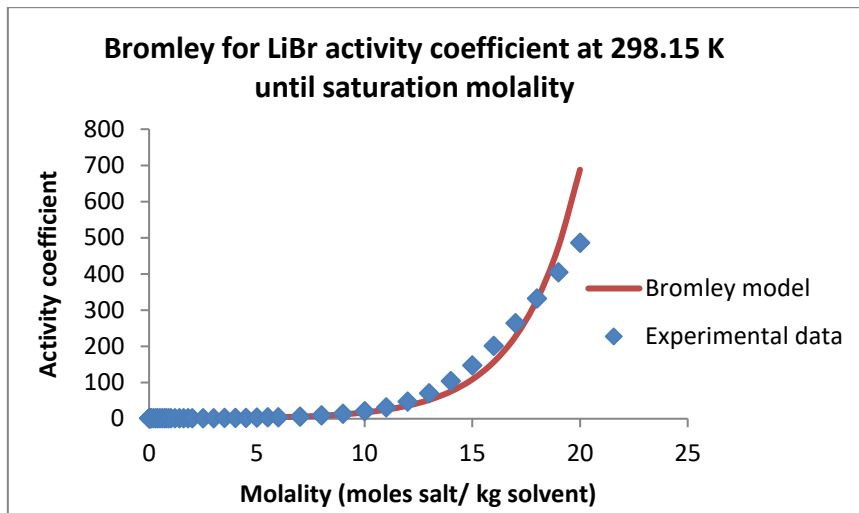


Figure 44. Activity coefficient with Bromley for LiBr with water at 298.15 K

In that representation the imperfections of the model due to the high molality are shown. The Bromley model is able to represent the experimental data behavior until 10 molal approximately. When the increase of the activity coefficient is more severe, the model do not follow the trend of experimental data. In fact, any existing thermodynamic model is able to represent this high molality range [1]. The parameters of the more developed models are optimized considering a limited maximum molality. The figure 45 represents the computation of the same data series but for the osmotic coefficient with the Bromley model.

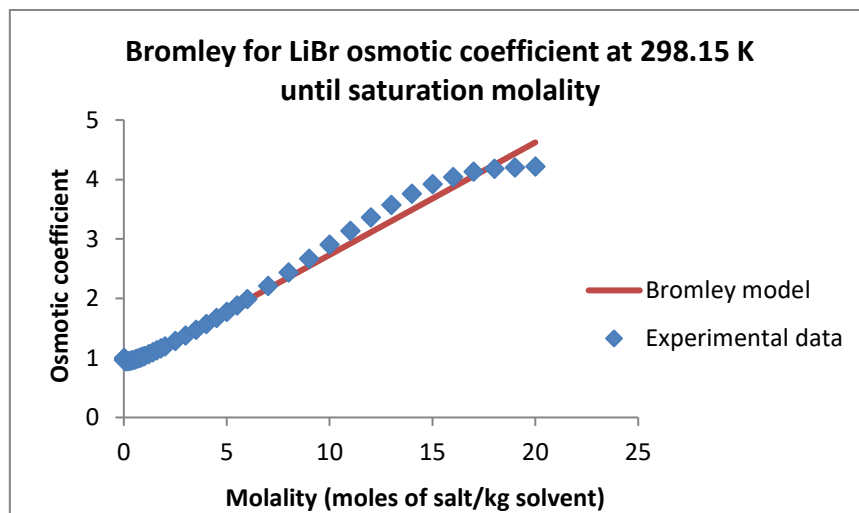


Figure 45. Osmotic coefficient with Bromley for LiBr with water until saturation molality.

In that representation the imperfection of the model at high molality are can also be found. It is interesting to note that at high molality the experimental data trend becomes flat and tends to stabilize at around 4 M. That behavior has been observed for all the salts at high saturation molality in the osmotic coefficient representation.

6.3 EXTERNAL CONSISTENCY FOR PURE WATER SOLVENT

The parameter B seems to have a relation with the different trends shown in the previous chapter. Relations between the parameter B and physical properties of the systems are analyzed. Several tests are proposed below, inspired for a large part by the works of Duignan [51] and Collins [52].

6.3.1 Variation of the parameter B of Bromley with the Free Energy of Solvation

Duignan et al suggests that the parameter B, as it describes the solvation, is related to the Gibbs energy of solvation [51]. The values of cation and anion solvation energies were determined by Tissandier et al [53]. These solvation energy represents the best measure of the ion's affinity for water.

The analysis is repeated here and is represented on figure 46. The values of the parameter B were the optimized parameters found in table 17. It shows the variation of the optimized parameter B against the difference in cation and anion solvation energies.

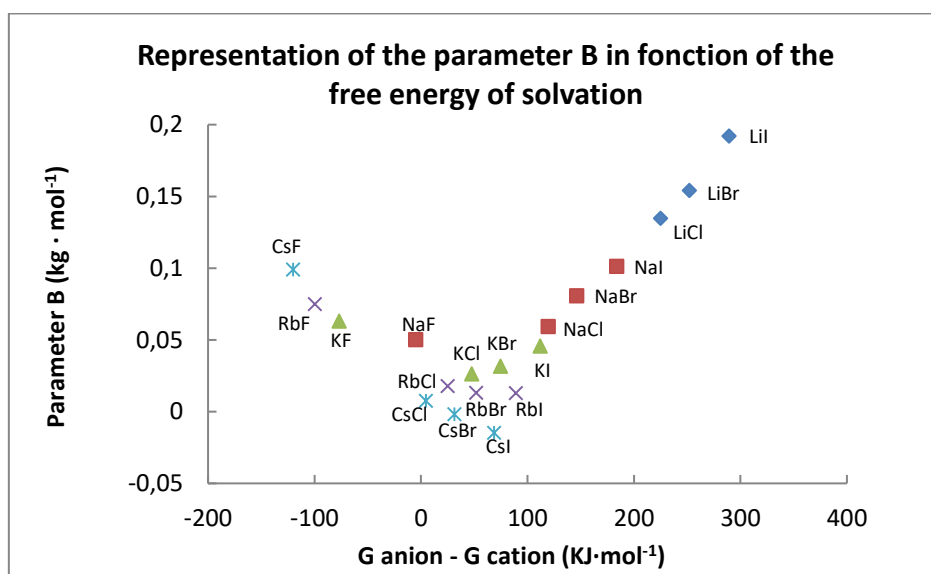


Figure 46. Variation of the optimized parameter B in function of the difference in cation and anion solvation energies

The results obtained were the same as the results of Duignan et al [51]. The salts with higher difference between the solvation of the cation and the anion have a higher value of the parameter B. The ionic solvation energy is related to the ionic size through the Born equation.

The relation may be observed by the representation of the difference between the values of cation and anion solvation energies in function of the difference between the diameter of the anion and the cation. In that representation the influence of the solvation and the ions size can be analyzed.

Pauling diameter values used have been taken from Saifuddin work [43]. The diameters difference are shown in Table 18.

Table 18. Values of the difference of the anion and the cation Pauling diameter (in Armstrong)

Ions	Li	Na	K	Rb	Cs
F	1.52	0.82	0.06	-0.24	-0.66
Cl	2.42	1.72	0.96	0.66	0.24
Br	2.7	2	1.24	0.94	0.52
I	3.12	2.42	1.66	1.36	0.94

The figure 47 represents the difference between the values of cation and anion solvation energies in function of the difference between the diameter of the anion and the cation

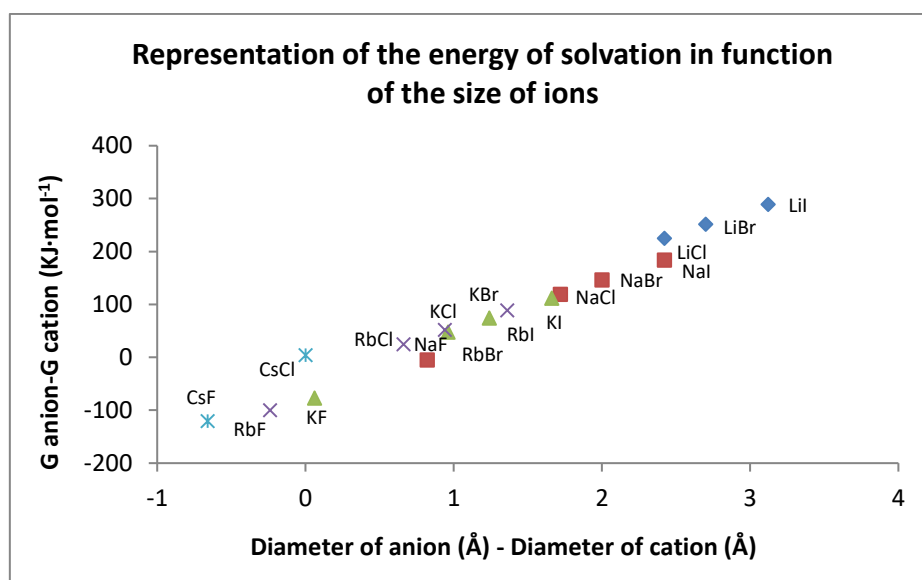


Figure 47. Representation of the energy of solvation in function of the size of difference between the size of ions

From the graph it can be observed that the higher the difference between the diameter of the ions is, the higher the solvation energy. Moreover, the different salts seem to have a linear tendency and they are located in preferential areas according to the anion size. As a consequence, the parameter B and the solvation might also be dependent on the cations and anions diameter. The variation of the parameter B with the size of ions is studied.

6.3.2 Variation of the parameter B of Bromley with the size of ions

The influence of cation and anion size on the parameter B of Bromley model is studied. A strategy is to represent the variation of the parameter with the difference between the diameter of anion of cation calculated on the previous table 18. The values of the optimized parameter B are taken from table 17. The figure 48 gives information about the variation of the optimized parameter B with the size of ions.

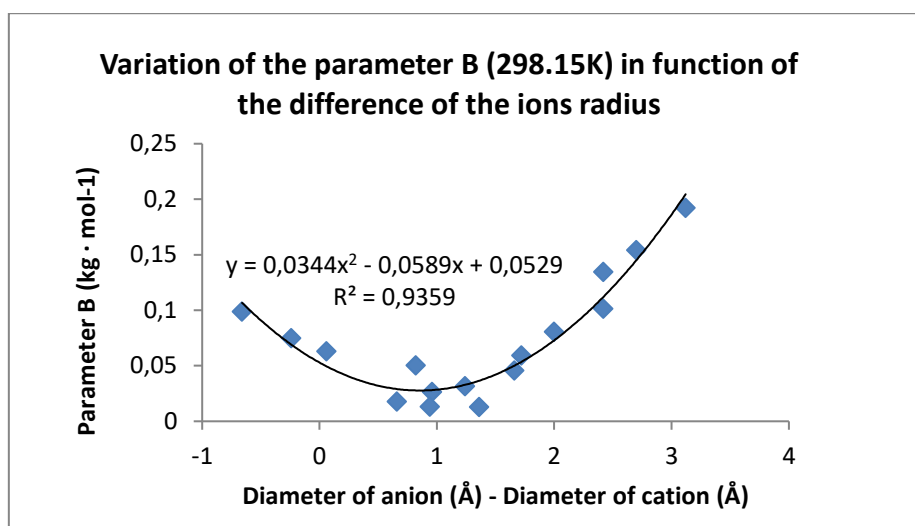


Figure 48. Variation of the parameter B with the diameter of anion and cation difference

A higher difference between the size of the ions means a higher value of the parameter B. It can be also seen that the parameter B seems to have a minimum when the difference between ions is equal to 1. The parameter increases when the diameter of the cation is higher than the anion diameter but it increases more significantly when the anion is bigger than the cation. The parameter B is affected by the cation and anion size in a different manner. As a consequence, the anion size has more importance in the prediction of the parameter B with the size of the ions. A parabolic curve appears, that can be approximated with the correlation:

$$\text{Parameter B (298.15 K)} = 0.0344 \cdot x^2 - 0.0589 \cdot x + 0.0529 \quad (6.3.1)$$

This phenomenon is explained by Collins using the Law of Matching Water Affinities [54]. That law states that there is a different effect on the hydration of ions depending on their charge and their size. According to the author, small ions (with high charge density) are considered kosmotropes, strongly hydrated ions. In opposition, the large monovalent ions (low charge density) are weakly hydrated ions and called chaotropes.

Based on the heat of the solution the affinity with water according to the size of ions can be determined. The combination of small ions or big ions together do not involve strong interactions with water. On the other hand, the combination of ions with different salts involves strong interactions with water. The figure 49 shows the law of matching water affinities for the combination of ions with different size. The figure is based on the representation from [52].

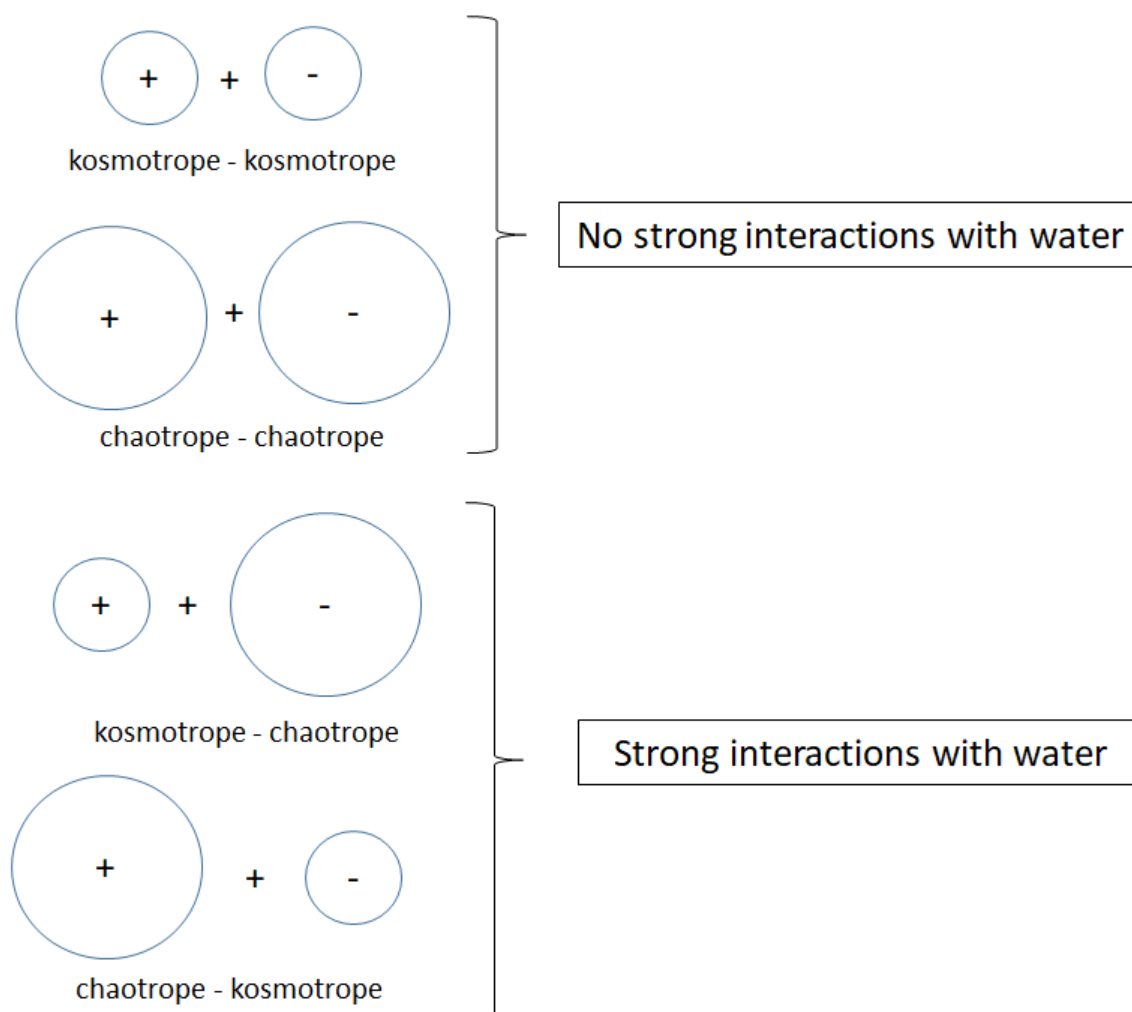


Figure 49. Influence of the size of ions in the interactions with water. The law of matching water affinities.

6.3.3 Variation of the parameter B with the solubility of salts

The parameters B optimized for each monovalent salt are represented in function of the solubility at 298.15 K. The table 19 gives information of the solubility of the monovalent salts at 298.15 measured in molality [55].

Table 19. Solubility for the monovalent at 298.15 K in molality (moles of salt/kg of water)

Ions	Li	Na	K	Rb	Cs
F	0.051	1.00	17.72	28.8	29.88
Cl	19.44	6.31	4.84	7.85	11.59
Br	21.68	9.22	5.72	6.91	5.8
I	12.75	12.31	8.93	7.63	3.35

The figure 50 represents the variation of the parameter B with the solubility.

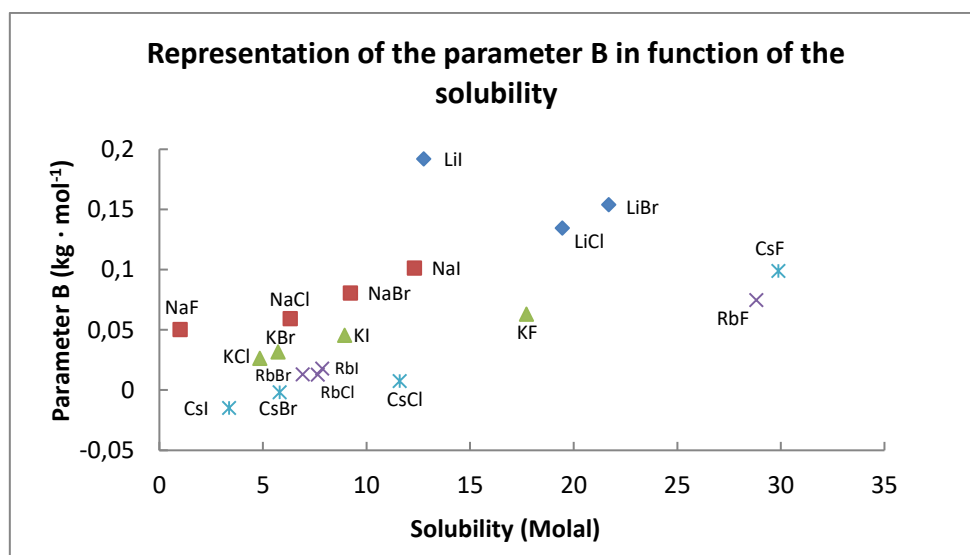


Figure 50. Variation of the optimized parameter B in function of against the solubility of salts in water at 298. 15 K

From the representation it is observed that it is more difficult to find a relation of the parameters with the solubility. In fact, the solubility the saturation of salts in the systems. It is so more difficult to find a relation with the parameter B as it is representing the increase of the activity coefficient due to medium range interactions. However, it can be also concluded that the salts are located in preferential zones according to the cation of the salt. The exception stand for the CsF and RbF and KF. All these salts have in common the presence of fluoride which is a very small atom. It is known that fluorides behaves very differently from the other salts because of very strong hydration: the parameter B increases with increasing cation size [29] [43].

6.3.4 Variation of the parameter B of Bromley with the temperature

6.3.4.1 High temperature behavior

It has been observed by some authors [56] that the temperature behavior of the activity coefficient is not monotonous: Figure 51 shows that the activity coefficient curves first increase and then decrease. The experimental data [57] [58] is presented with smoothed lines in order to have a more clear view and interpretation of the variation.

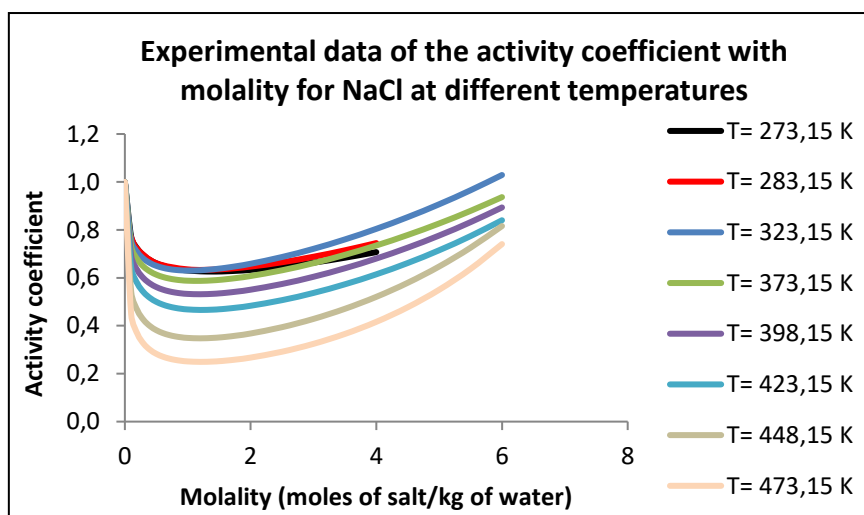


Figure 51. Representation of experimental data for NaCl at different temperatures [57] [58].

The observed behavior can be related to the parameter B. As the parameter represents the increase of the model for the activity coefficient, it is expected that the parameter B may reach a maximum at around 323.15 K. The figure 52 presents the optimized parameter in function of the temperature

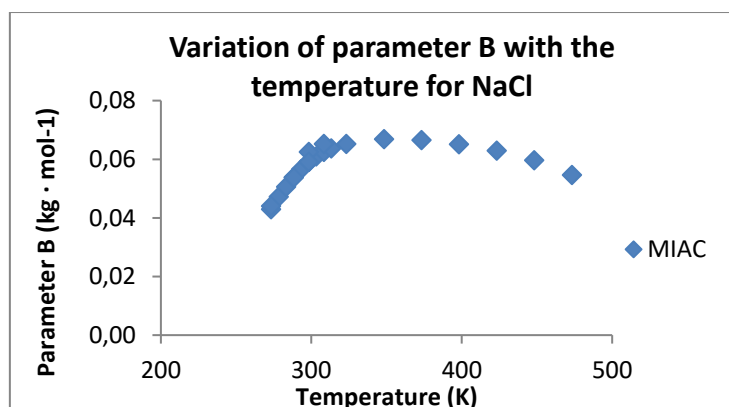


Figure 52. Study of the variation of the parameter B of Bromley with the temperature for the NaCl

From the graph represented it is observed that the parameter B increases until a maximum corresponding to 323.15 K and decreases after this temperature. If it is accepted that B expresses the solvation (ion-water) interactions, it may be concluded that the solvation reaches a maximum close to 323K, and that beyond this temperature, water-ion interactions decrease. In order to verify if this trend is common for the monovalent salts, the same analysis has been done for different salts. The parameter B was regressed also from osmotic coefficients in order to have more temperature data available.

Figure 53 shows the behavior of the B parameter with temperature for all salts. The blue diamonds are obtained from activity coefficient data, and the red squares from osmotic coefficients.

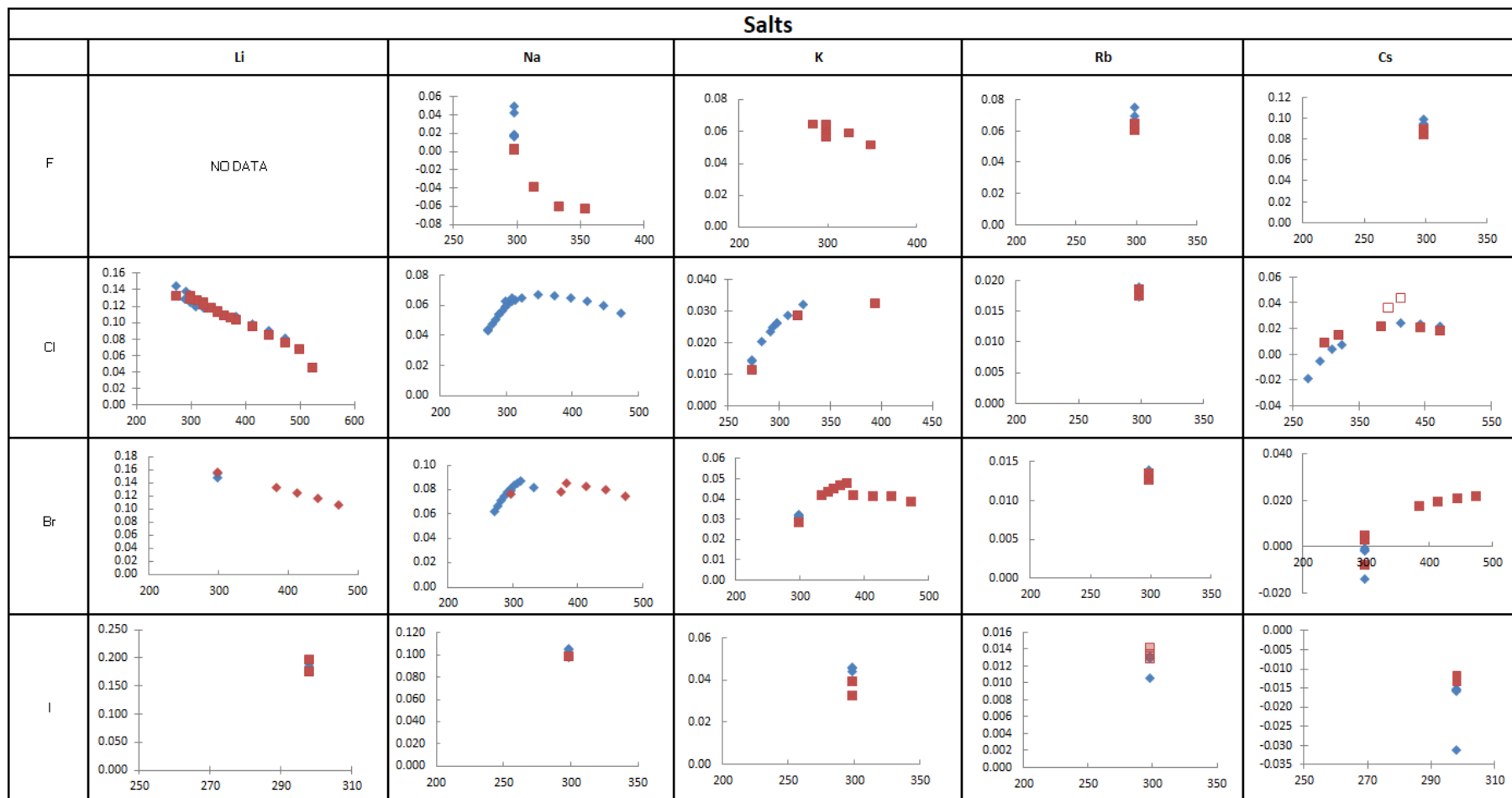


Figure 53. Variation of the parameter B of Bromley adjusted with the activity coefficient and the osmotic coefficient at different temperatures for different salts. The blue diamonds are obtained from the activity coefficients, the red squares from osmotic coefficient.

Several conclusions are obtained from the previous figure 53. The first conclusion obtained concerns the availability of experimental data at different temperatures for the salts studied. Some salt data are available at 298.15 K for the activity and osmotic coefficient data. That is the case of all the iodides, all salt including rubidium and the cesium fluoride. Other salts, even if they cover a wide range of temperature, have some missing data at specific temperatures. That lack of data can be observed in the previous figure and make difficult the interpretation of results. In some cases the lack of data is notorious. For the KCl and the NaBr missing data for activity coefficient and osmotic coefficient can be shown between 300 and 400 K. Furthermore, the data at high temperature is compute only from osmotic coefficient because the temperature cover by the activity coefficient measurements is always lower. The fact of computing the parameter B from to different properties creates more scatter in the model computation and makes more difficult to identify the precise trend of the parameter with temperature.

Following the data analysis, in some cases, some inconsistent points may be found. In the case of CsCl, two points are determined to be inconsistent as they do not follow the sale trend as the other. These point are marked with an empty square in the figure. As it can be observed the incertitude increases with these points. It can also be seen that they may be inconsistent, the calculated parameter B for this points is slightly higher than the normal tendency of the other points.

For the other salts, the variation of the parameter B with the temperature follows different tendencies depending on the salt. It can be observed that the NaCl and NaBr salts have a maximum value of the parameter B at an specific temperature. That inflexion temperature is around 340 K for the NaCl and 320 K for NaBr. On the other hand, other salts do not present a maximum value of the parameter B. That is the case of the LiCl and the LiBr. In these cases, the parameter B always decreases with the increase of temperature. It can be thought that the maximum of these salts has already been achieve as the tendency of the parameter B is to decrease.

A different trend of the parameter B with the temperature is followed by the NaF. For that salt the variation of the parameter B represents a very different trend compared to the other salts. It can be seen that the parameter B drops as the temperature increases and it seems to reach a minimum. More data is needed at higher temperatures than 360 K in order to analyze more precisely the variation of the parameter of the NaF.

6.4 EXTERNAL CONSISTENCY FOR MIXED SOLVENTS

6.4.1 Computation and analysis of properties for mixed solvents

In mixed solvents, the parameters used to characterize the solvent are different. The variation of the mole fraction of alcohol has a direct impact on the dielectric constant and as a consequence on the properties computations. The mixed solvents investigated are composed of water and alcohol. The dielectric constant and the density of the solvent may vary significantly with a variation of the alcohol concentration, thus affecting the value of the Debye-Hückel parameter A_{DH} .

6.4.1.1 Model for density

The calculation of the density in a mixture was calculated by a the mixed rule. As the density is an specific property, the density of the mixture is calculated within the specific volume.

$$\rho_{\text{mix}} = \frac{1}{v_{\text{mix}}} = \frac{1}{\sum_{i=1}^n v_i \cdot x_i} \quad (6.4.1)$$

Figure 54 represents the variation of the density of the mixed solvents in function of the molar fraction of methanol.

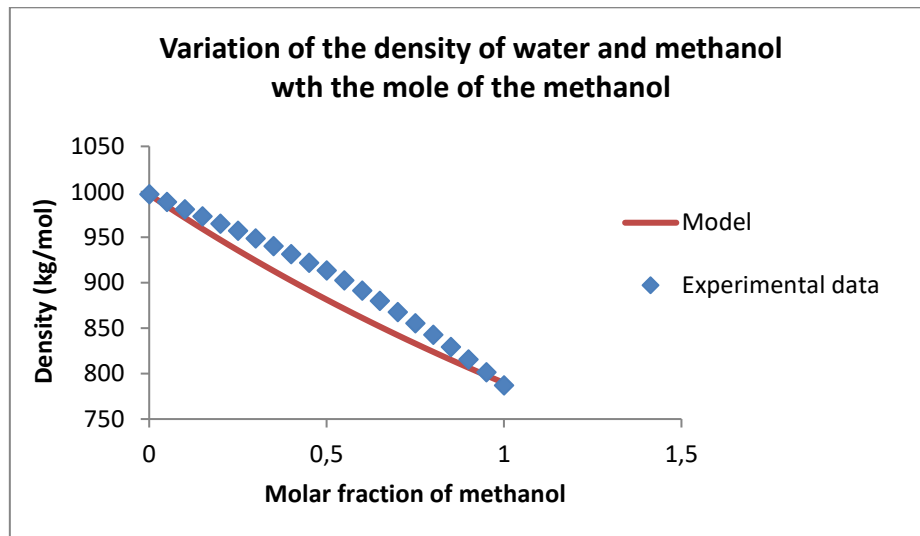


Figure 54. Representation of the experimental data and the model for the density of methanol with water [59]

For the water and methanol as solvent it can be seen that the model represents correctly the variation of the density. The deviations from experimental data are justified by the use of the volumetric fraction. Volumetric fractions suppose a problem in non-ideal mixtures as the excess volume is not calculated in the model. For the solvents used in this work the mixing rule model is consider as valid because is a simple model and with low deviations in the solvents studied.

6.4.1.2 Model for dielectric constant

The dielectric constant represents the factor by which the electric field between the charges is decreased relative to vacuum. The approximation used for the model is calculated as the volume fraction average of the pure dielectric constants for the solvents involved in the process.

$$D = \sum_{i=1}^{\text{solvents}} V_i D_i \quad (6.4.2)$$

The volume fractions are calculated with the molar fractions and the molar densities of the solvents:

$$V_i = \frac{\text{Volume}_i}{\sum_i \text{Volume}_i} = \frac{x_i / \rho_i}{\sum \frac{x_i}{\rho_i}} \quad (6.4.3)$$

The following figure 55 represents the variation of the dielectric constant with the molar fraction of methanol. The graphs show the experimental data representation and the tendency of the model.

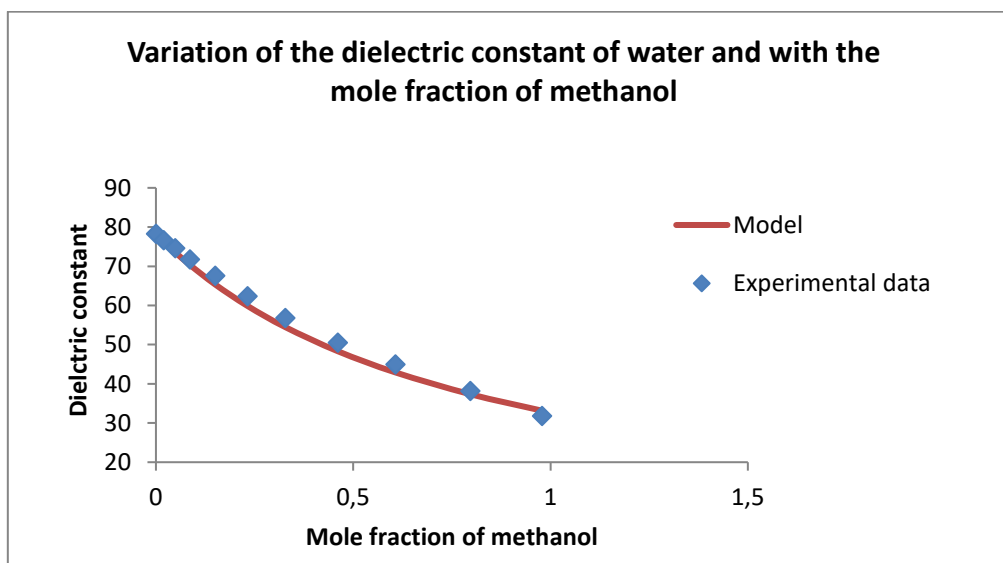


Figure 55. Representation of the experimental data and the model for the dielectric constant of methanol with water [60]

The model based has approximately the same pattern as the experimental data. For other solvents, higher deviations may be done because the model varies with the temperature and with the molar fraction of solvent but it is considered to be independent on the salt concentration. Even the negative aspects, the dielectric constant model is selected. It is a simple model, not difficult to represent and quite precise for the mixed solvents studied. The same mixed rule model has been done apply for the alcohol solvents.

6.4.1.3 Activity coefficient computation

The quality of the Bromley model for mixed solvents is evaluated. In that study the temperature used for every system is 298.15 K as no data have been found for alcoholic mixed solvents systems at different temperatures. In mixed solvents the variation of the parameter B is influenced mainly by the concentration of alcohol in the solvent. The figure 56 represents the model regression and the experimental for the pure water and different concentrations of methanol.

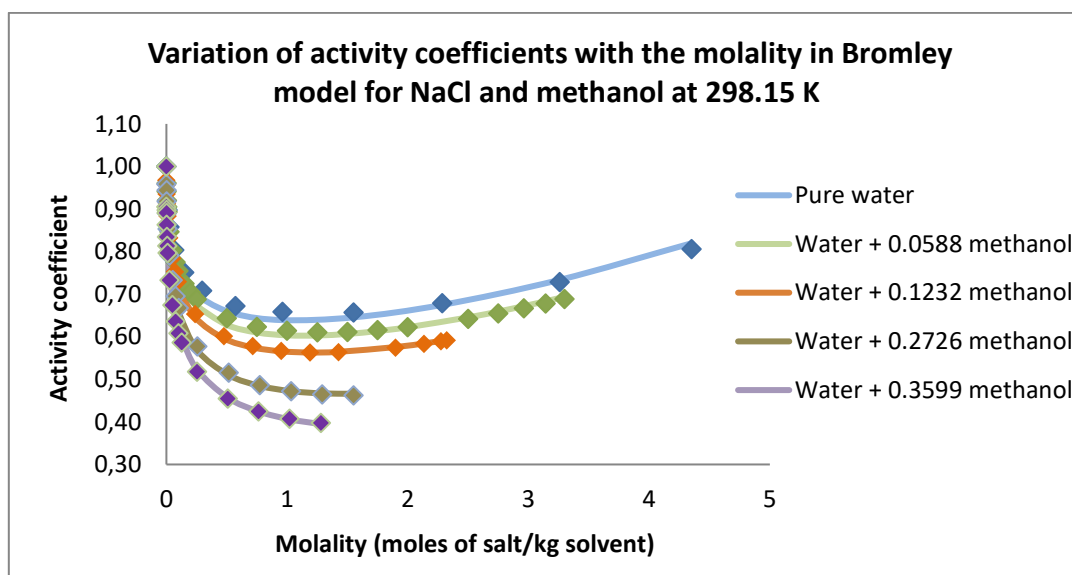


Figure 56. Representation of the experimental data of activity coefficients for the NaCl in function of the molality of the salts at different molar fraction of methanol [31, 61].

The study is completed with the table 20. It collects the results obtained for the parameter of Debye-Hückel, the adjusted Bromley parameter and the standard deviations. The numerical values allow a better analysis of the results.

Table 20. Different results obtained in the regression of NaCl with methanol

Pure water			Water + 0.1232			Water + 0.2726		
Param. A_{DH}	Param. B ($\text{kg}\cdot\text{mol}^{-1}$)	Std dev (%)	Param. A_{DH}	Param. B ($\text{kg}\cdot\text{mol}^{-1}$)	Std dev (%)	Param. A_{DH}	Param. B ($\text{kg}\cdot\text{mol}^{-1}$)	Std dev (%)
1.1728	0.0594	0.532	1.4512	0.0654	0.133	1.8082	0.0662	0.259

It can be observed that as we increase the concentration of methanol in the mixture Debye-Hückel parameter increases (A_{DH}). This is directly related to the decrease on the dielectric constant with the concentration of methanol. The lower polarity of the solvent, so the interactions between anion and cation increase. In addition, it can also be seen that the parameter B of Bromley increases with the alcohol content (with decreasing polarity). The higher the alcohol content, the more difficult it becomes to determine B because the salt saturation strongly decreases.

6.4.2 Variation of the parameter B of Bromley with the concentration of solvent

The variation of the parameter B with the mole fraction of the alcohol is studied for different salt. The results are represented in figure 57.

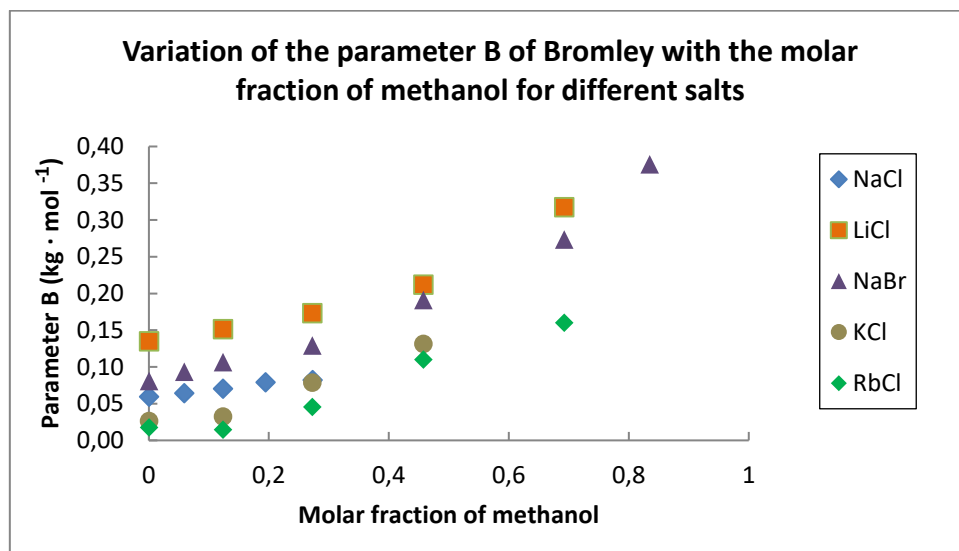


Figure 57. Representation of the B of Bromley in different salts for different molar fractions of methanol.

The parameter B increases as the mole fraction of solvent increases for every salt studied. That behavior was not as expected. With an alcoholic solvent the solvation of water is reduced. Consequently, with an increase in the concentration of solvent and the decrease of the dielectric constant, the parameter B should decrease if it stands for the solvation of water. The increase of the parameter B can be explained by the increase of the parameter of Debye-Hückel (A_{DH}) shown before in Table 19. When the dielectric constant increases, the parameter A_{DH} increases. The parameter A_{DH} increases more than the solvation decreases and the parameter B has a higher value in order to compensate that increase on the slope of the activity coefficient at low concentration. The parameter B is a semi-empirical parameter and cannot represent the mixed solvents interactions due to the non-ideality of the system. As a consequence, the parameter of the model cannot reflect the physical properties relations for mixed alcoholic solvents.

The figure 58 gives the same type of information with a solvent that is even less polar, ethanol.

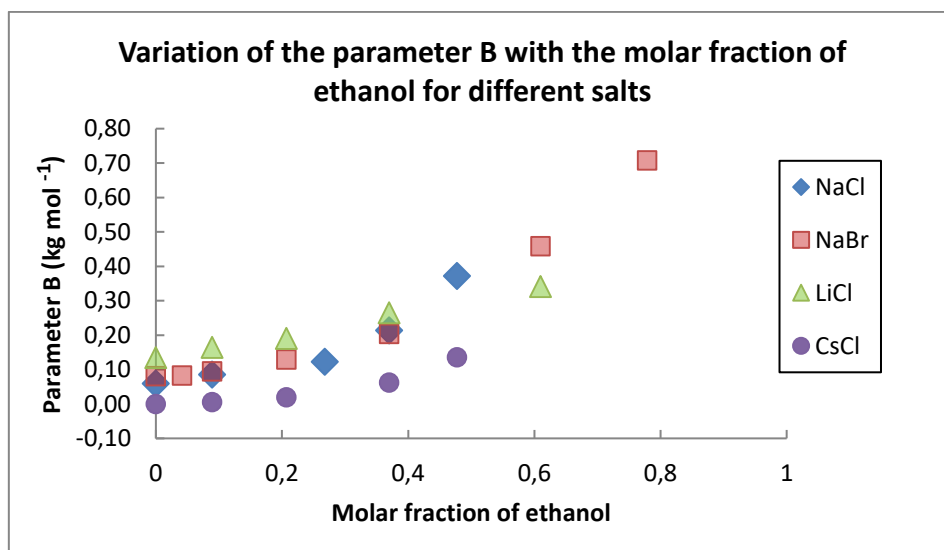


Figure 58. Representation of the B of Bromley in different salts for different molar fractions of ethanol.

The shapes of the curves obtained in the graph are similar to those obtained with methanol. The curves present a more linear behavior at low ethanol concentration and increases more severely with more alcohol concentration. In the case of ethanol the parameters optimized B is larger than with methanol for all the salts. The parameter A_{DH} is higher with a more non polar solvent and as a consequence the parameter B optimized has to be higher. That also accounts for the solubility, the more the molecular weight and the concentration of the alcohol solvent the less soluble the salt is in the system.

6.4.3 Variation of the parameter B of Bromley with the size of ions

The parameter B optimized in mixed solvents has been represented in function of the size of the ions. The figure 59 represents the optimized parameter B in function of the diameter of anion and cation obtained from table 18. The representation includes results for methanol as solvent for different salts a different concentrations of solvent.

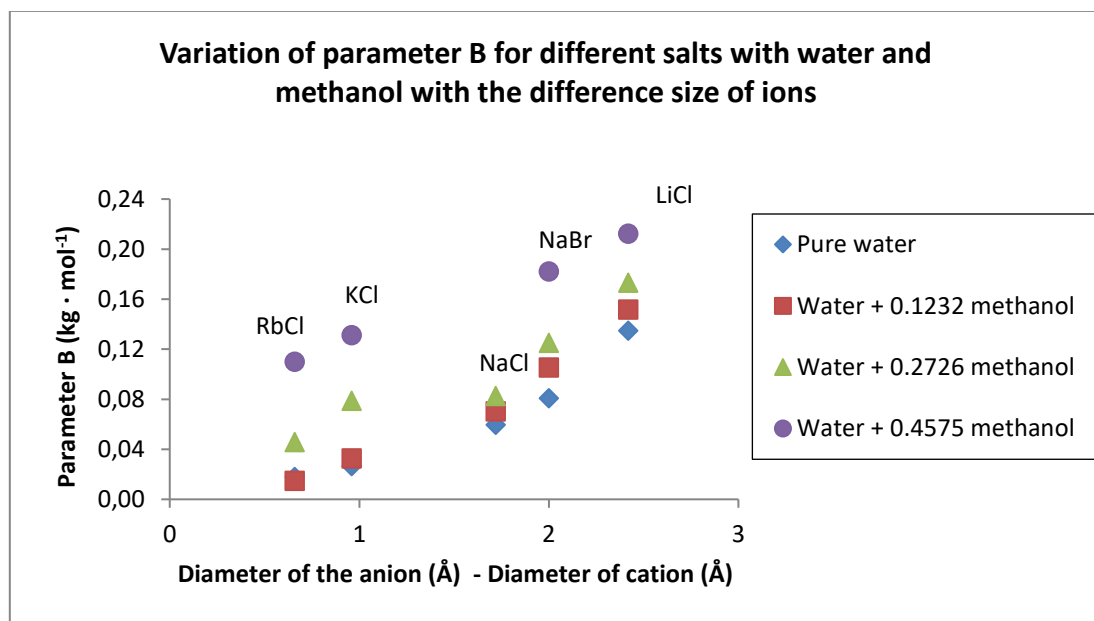


Figure 59. Representation of parameters B of Bromley in function of the difference between the ions diameter for different concentration of water and methanol as solvents

The plot can be compared to that of figure 48 in pure water. Less salts could be investigated so that only the increasing branch of the parabola is visible here (we have only examples where the anion is much larger than the cation). In that case, the parameter B increases when the difference between the diameter of anion and cation increases. The law of matching water affinities justify that behavior. It can be also seen that the parameter B increases as the mole fraction of methanol increases. The more the concentration of methanol, the higher the parameter B. That relation might be useful for the extrapolation of the parameter B for a monovalent salt at a specific alcohol concentration.

6.4.4 Variation of the parameter B of Bromley with the dielectric constant

We have observed that the polarity of the solvent has an important impact on the ionic activity coefficient. The dielectric constant may be used as a convenient measure of the polarity. Consequently, we evaluate here how the parameter B depends on the dielectric constant. The figure 60 represents the ratio of B/B₀ parameter for all the salts. The study takes into account the data at 25°C. The analysis compares the different alcoholic solvents and different concentrations. The parameter B regression for solvents with smaller dielectric constants is prone to very large uncertainties as a consequence of the very low solubility of the salts in these solvents (figure 56). Consequently, the minimum value of the dielectric is limited to 45. Figure 60 presents the parameter B/B₀ in the y axis where B₀ is the parameter optimized at 298.15 K and with pure water. That division has been done in order to have the same starting point for the same salts.

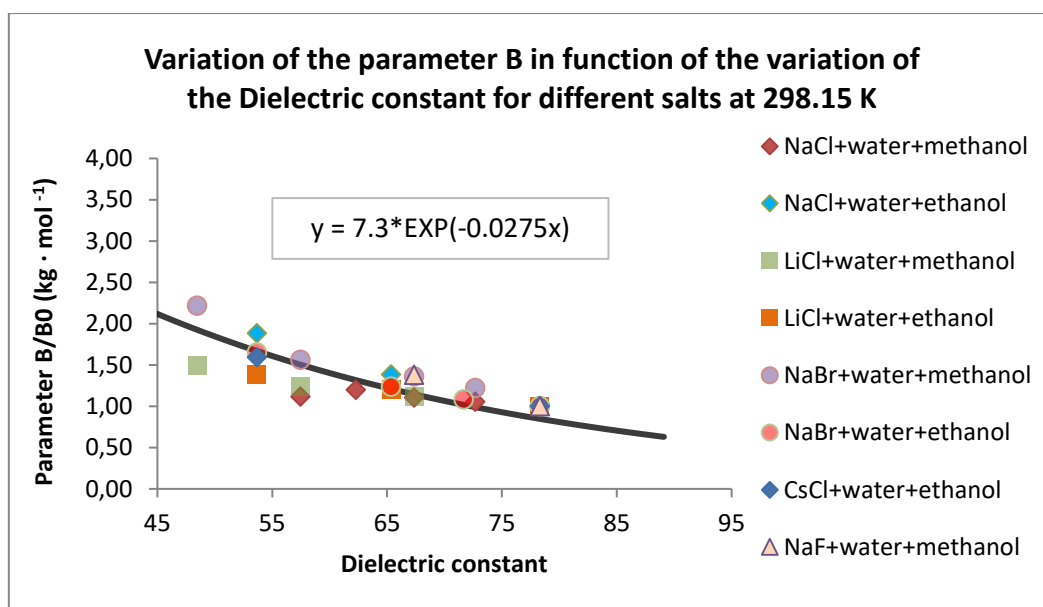


Figure 60. Variation of the parameter B of Bromley with the dielectric constant for different salts and concentration of alcoholics solvents

The points are in general terms in the same area and the increase in a similar manner as the dielectric constant decrease or as the concentration of alcoholic solvent increases. A correlation can be constructed through the points:

$$B/B_0 = 7.3 \cdot e^{(-0.0275 \cdot D)} \quad (6.4.1)$$

7. EXTRAPOLATION CALCULATIONS

7.1 EXTRAPOLATION TO LOW TEMPERATURE

The example described below shows how temperature extrapolation towards the low temperature makes it possible to reconcile two different types of properties (activity coefficients and water freezing point depression).

The relation between the parameter B and the temperature can be used for predicting the parameter at other temperatures. A prediction of this parameter has been done at low temperatures for the computation of the solid-liquid equilibrium of LiCl. The figure 61 presents the variation of the optimized parameter B with temperature for the mentioned salt and the linear equation established for the parameters extrapolation.

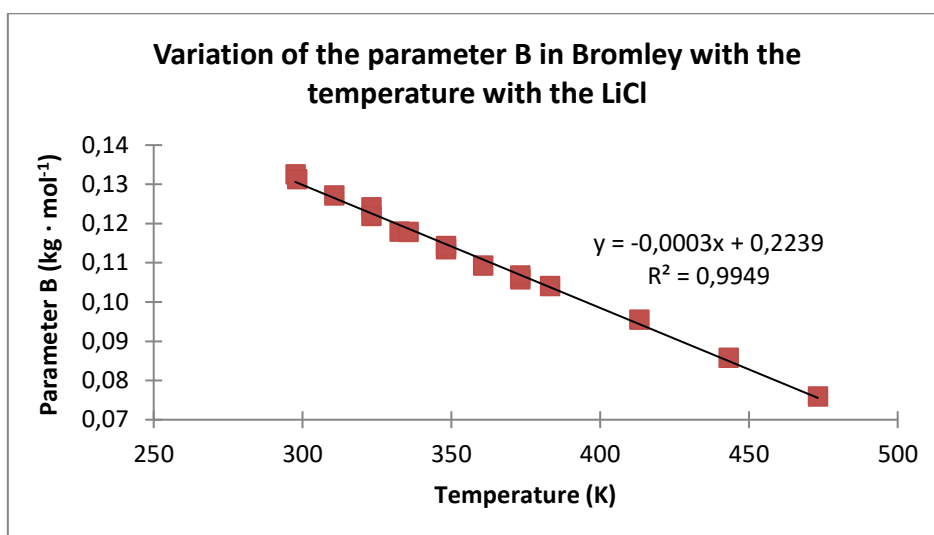


Figure 61. Variation of the optimized parameter B with temperature for LiCl

The equation that represent this regression is as follows:

$$\text{Parameter B for LiCl}(T) = -0.0003 \cdot T + 0.2239 \quad (7.1.1)$$

In solid-liquid equilibrium, the data studied [62] takes into account the crystallization of water between 268.25 K and 273.15 K. The parameter B of systems at the mentioned temperatures is calculated with the regressed equation. With the parameter B the activity of water can be calculated. The activity was calculated from the osmotic coefficient computed using the analytical equation of Bromley [3].

The theoretical values of the activity of water at the studied temperature were also calculated in order to compared with the results with the Bromley model. The theoretical calculations were determined with the equation 2.2.62 in chapter 2.2.6.

Figure 62 shows the results obtained. The graph presents the theoretical calculations of the activity of water and the calculation with the Bromley model and the estimated parameter B.

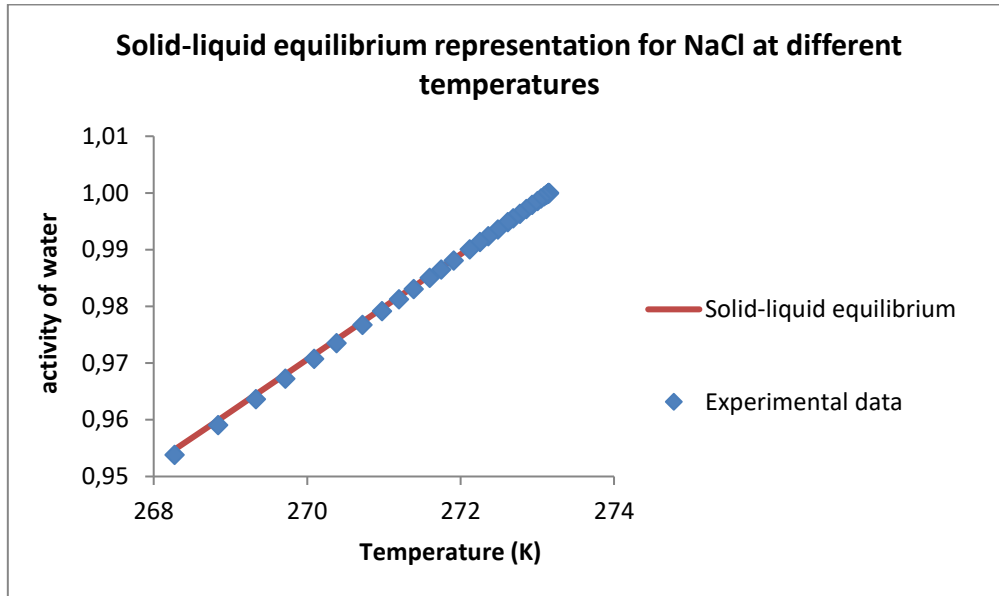


Figure 62. Solid-liquid equilibrium for the LiCl

As it can be shown the results obtained are satisfactory. The Bromley model is able to represent the solid-liquid equilibrium for water as solvent and with the LiCl as solute. It can be said that extrapolation of the parameters B at lower temperatures are satisfactory.

7.2 EXTRAPOLATION FOR MIXED SOLVENTS PREDICTIONS

Using the correlative equations that have been shown for the observed trends, a prediction of the behavior of a salt + solvent system can be estimated. The procedure is as follows:

- Estimate the B_0 parameter from the difference in anion and cation diameters (equation 6.3.1, figure 48)
- Estimate the B/B_0 ratio from the solvent dielectric constant (equation 6.4.1, figure 60)
- Using B , and the properties relations, predict the behavior of the desired property.

A predictivity test is performed for mixed solvents. The parameter B was evaluated for NaCl and 0.1232 mole fraction of methanol. Data have been found for this system, that have not been used in the development of the method [61]. The calculation of the regressed parameter B considering the variation of the dielectric constant, is summarized in Table 21.

Table 21. Prediction of the parameter B for NaCl with 0.1232 mole fraction of methanol

D water and methanol 0.1232 molar (Dimensionless)	67.36
B/B_0 (Dimensionless)	1.184
Diameter of anion (Å) - Diameter cation (Å)	1.72
B_0 predicted for NaCl (298.15 K) ($\text{kg} \cdot \text{mol}^{-1}$)	0.0518
B predicted for NaCl and 0.1232 methanol ($\text{kg} \cdot \text{mol}^{-1}$)	0.06137

Figure 63 shows the activity coefficient of NaCl with 0.1232 mole fraction of methanol at 298.15 K.

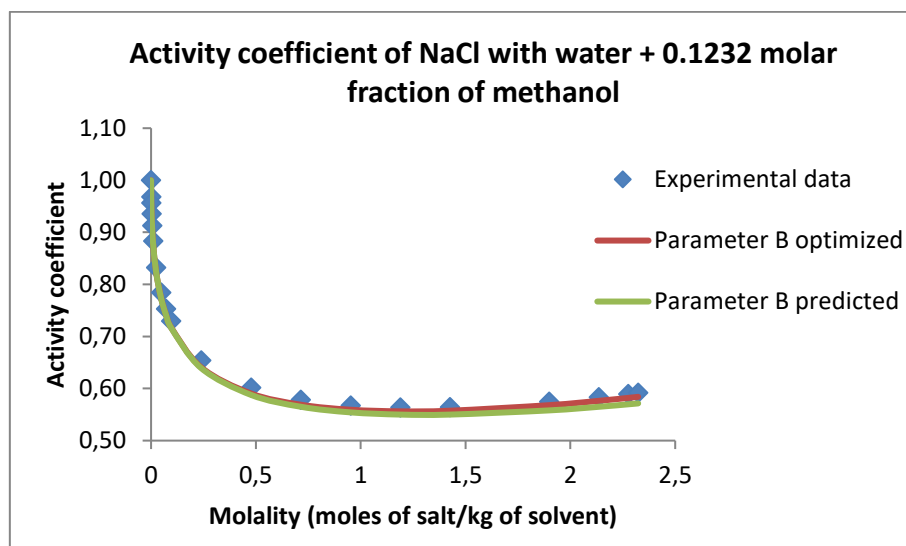


Figure 63. Activity coefficient for NaCl with 0.1232 mole fraction of methanol at 298.15 K

Very good agreement is found. The B parameter can be either regressed on these data ($B = 0.06543 \text{ kg} \cdot \text{mol}^{-1}$) or predicted using the proposed methodology ($B = 0.06137 \text{ kg} \cdot \text{mol}^{-1}$). The difference between the two values is less than 0.41 %

If we assume that the mixed solvent behaves as a unique compound with intermediate properties between those of water and methanol, then it is in principle possible to also predict solvent properties, as for example vapor pressure. Such data do exist [63]: Figure 64 shows the bubble pressure of NaCl + methanol + water at 298.15 K. The prediction is done as represented in Table 22.

Table 22. Prediction of the parameter B for NaCl with 0.1 mole fraction of methanol

D water and methanol 0.1 molar fraction (Dimensionless)	69.19
B/Bo (Dimensionless)	1.089
Diameter of anion - Diameter cation (Å)	1.72
B0 predicted for NaCl (298.15 K) (kg · mol ⁻¹)	0.0518
B predicted for NaCl and 0.1 methanol	0.0564

Raoult's law has been used in the model for the calculation of the pressure of the mixture and the calculated pressure has been modified by the activity of the solvent determined with the Bromley model.

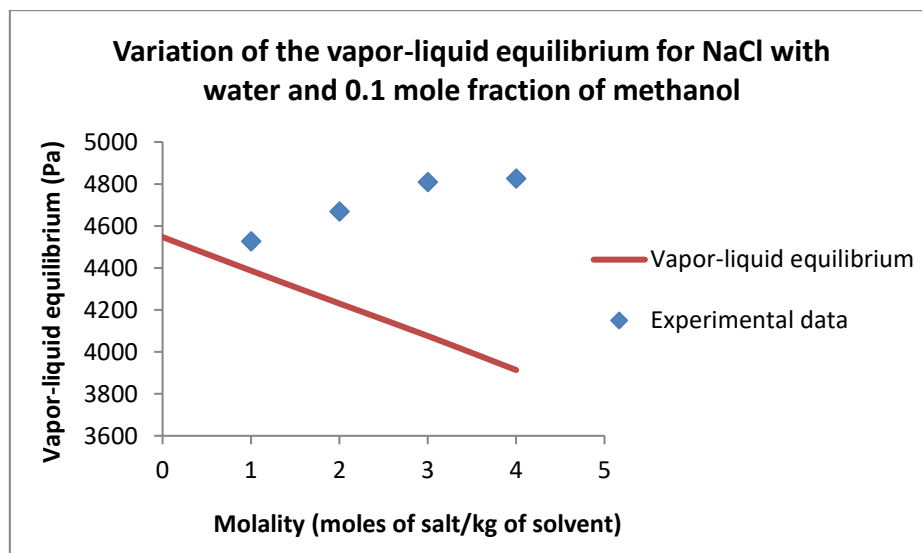


Figure 64. Vapor-liquid equilibrium of NaCl with water and 0.1 mole fraction of methanol at 298.15 K

The predicted vapor pressure decrease with molality while the experimental data increase in mixed solvents. The Bromley model cannot represent properly the experimental data tendency. The reason is related to the fact that the two solvent compounds interact very differently with the salt: the activity coefficients of each compound cannot be replaced by an average one for the solvent. Water is strongly solvated, so that its activity coefficient is smaller than one, while the alcohol doesn't like the presence of the salt, and features consequently a strongly positive activity coefficient. The high bubble pressure shows that the alcohol preferentially vaporizes. The only way to reproduce correctly the mixed solvent VLE data is to use a model where the two solvents are distinguished, as for example e-NRTL.

8. CONCLUSIONS

This work is performed as a part of the EleTher JIP, whose objective is to define best practices for the development of industrial models. The scope of this work is the analysis of non-reactive, monovalent salts in water and mixed solvents. A large number of data exist for these systems. The data have been collected and analyzed following a thermodynamic methodology. Several conclusions can be drawn:

- Pure water solvent: Although the data for these type of salts are numerous, they are limited in number when reaching higher temperatures. Up to 373.15 (100°C), data are generally available until the solubility limit. At higher temperature, data become much scarcer. Rb salts and I salts have not data of activity coefficients at a temperature different from 298.15 K. For Cs, this is the case for CsF and CsI. In addition, KCl has a lack of data between 340 K and 400 K with activity coefficient and osmotic coefficients. LiBr and NaBr have also a lack of data between 300 K and 400 K for the same properties.
- In the case of mixed solvents, the missing data is more notorious. Some monovalent salts have not any type of data when they are combined with water and with an alcohol. As the complexity of the alcohol increases, less data can be found. For water and ethanol as mixed solvents, only data of activity coefficient was found for NaCl, LiCl, CsCl, NaBr. If we focus on water and 1-propanol, only data concerning activity coefficient was found for KCl. Moreover, mixed solvents systems have only data at 298.15 K. The lack of data available makes it difficult to validate the trends that are observed.

The internal consistency results show that the methodology of data analysis by calculation of the deviations with the eNRTL is a technique to identify possible inconsistent data. The methodology contributes also to determine the limitations of the model at different conditions such as high molality and high temperature. From the internal consistency analysis it has been observed that the model eNRTL has high deviations as the molality or temperature range increases. The consistency between three properties have been analyzed : activity coefficient, osmotic coefficient and dilution enthalpy. for LiCl, NaCl, KCl and CsCl. Among these salts, for activity coefficient, the percentage of consistent data has been 85%, 91%, 86%, 64% respectively. Some inconsistent points have also been identified with CsCl and NaF.

External consistency was performed using the Bromley model. It provides a method to identify relations between the physical properties of the electrolyte systems and the parameter B. Those relations can be used for parameter prediction and properties computations. The parameter B shows a logical tendency when it is represented in function of size difference between anion and cation. The parameter can represent the solvation interactions for the systems of salts and water as solvent. That relation can be explained by the law of matching water affinities.

The variation of the parameter B with the temperature could be analyzed for a large number of salts. It often presents a maximum value with temperature. This was clearly visible with several chlorides and bromide salts (except for Li^+ as cation, where the trend is systematically decreasing). This observation is worth to be further analyzed and related to the change in solvation behavior with temperature.

For mixed solvents, the Bromley model is used by assuming a pseudo-solvent having intermediate properties between that of water and alcohol. Here, one can no longer state that the size of the B parameter is indicative of solvation. In fact, this parameter increases with decreasing polarity of the solvent. A relationship of B with the dielectric constant of the mixed solvent could be identified. It allows extrapolating the observed behaviour. This trend could be also further analysed with non-alcoholic mixed solvents.

REFERENCES

- [1] E. Hendriks *et al.*, "Industrial Requirements for Thermodynamics and Transport Properties," *Ind. Eng. Chem. Res.*, vol. 49, no. 22, pp. 11131–11141, 2010.
- [2] G. M. Kontogeorgis and G. K. Folas, *Thermodynamic models for industrial applications: From classical and advanced mixing rules to association theories*. Chichester U.K.: Wiley, 2010.
- [3] Leroy A. and Bromley, "Thermodynamic properties of strong electrolytes in aqueous solutions," *AIChE Journal*, vol. 19, no. 2, pp. 313–330, 1973.
- [4] J. A. Robinson and T. N. Srinivasan, "Chapter 21 Long-term consequences of population growth: Technological change, natural resources, and the environment," in *Handbook of Population and Family Economics*: Elsevier, 1997, pp. 1175–1298.
- [5] B. E. Poling, J. M. Prausnitz, and J. P. O'Connell, *The properties of gases and liquids*, 5th ed. New York: McGraw-Hill, 2001.
- [6] IFPEN, *IFPEN*. [Online]. Available: <https://www.ifpenergiesnouvelles.fr/>
- [7] H. S. Shin and S. M. Lee, "Removal of Nutrients in Wastewater by using Magnesium Salts," *Environmental Technology*, vol. 19, no. 3, pp. 283–290, 1998.
- [8] O. Lefebvre and R. Moletta, "Treatment of organic pollution in industrial saline wastewater: A literature review," *Water Research*, vol. 40, no. 20, pp. 3671–3682, 2006.
- [9] S. Abou-Elala, M. Kamel, and M. E. Fawzy, "Biological treatment of saline wastewater using a salt-tolerant microorganism," *Desalination*, vol. 250, pp. 1–5, 2010.
- [10] M. Bok, Z.-J. Zhao, S. Jeon, J.-H. Jeong, and E. Lim, "Ultrasonically and Iontophoretically Enhanced Drug-Delivery System Based on Dissolving Microneedle Patches," *Scientific Reports*, vol. 10, no. 1, p. 2027, 2020.
- [11] R. Latham, R. Linford, and W. Schlindwein, "Pharmaceutical and medical applications of polymer electrolytes," *Ionics*, vol. 9, pp. 41–46, 2003.
- [12] B. Li and D. Xia, "Anionic Redox in Rechargeable Lithium Batteries," *Advanced materials (Deerfield Beach, Fla.)*, vol. 29, no. 48, 2017.
- [13] F. Croce, G. B. Appetecchi, L. Persi, and B. Scrosati, "Nanocomposite polymer electrolytes for lithium batteries," *Nature*, vol. 394, no. 6692, pp. 456–458, 1998.
- [14] A. Manuel Stephan and K. S. Nahm, "Review on composite polymer electrolytes for lithium batteries," *Polymer*, vol. 47, no. 16, pp. 5952–5964, 2006.
- [15] R. C. Agrawal and G. P. Pandey, "Solid polymer electrolytes: Materials designing and all-solid-state battery applications: an overview," *J. Phys. D: Appl. Phys.*, vol. 41, no. 22, pp. 1–18, 2008.
- [16] Heat Transfer Solutions, *Fouling*. [Online]. Available: <http://www.hcheattransfer.com/fouling1.html>
- [17] R. Sheikholeslami and A.P. Watkinson, "Scaling of Plain and Externally Finned Heat Exchanger Tubes," *Journal of Heat Transfer*, vol. 108, pp. 147–152, 1986.
- [18] A. P. Watkinson, L. Louis, and R. Brent, "Scaling of enhanced heat exchanger tubes," vol. 52, no. 5, pp. 558–562, 1974.
- [19] Heat Transfer Solutions, *Fouling*.
- [20] A. Eslamimanesh, A. H. Mohammadi, D. Richon, P. Naidoo, and D. Ramjugernath, "Application of gas hydrate formation in separation processes: A review of experimental studies," *The Journal of Chemical Thermodynamics*, vol. 46, pp. 62–71, 2012.
- [21] H. Haghghi, A. Chapoy, and B. Tohidi, "Methane and Water Phase Equilibria in the Presence of Single and Mixed Electrolyte Solutions Using the Cubic-Plus-Association Equation of State," *Oil & Gas Science and Technology - Rev. IFP*, vol. 64, no. 2, pp. 141–154, 2009.

- [22] M.-K. Hsieh, Y.-T. Yeh, Y.-P. Chen, P.-C. Chen, S.-T. Lin, and L.-J. Chen, "Predictive Method for the Change in Equilibrium Conditions of Gas Hydrates with Addition of Inhibitors and Electrolytes," *Ind. Eng. Chem. Res.*, vol. 51, no. 5, pp. 2456–2469, 2012.
- [23] V. L. Jozian S., "Mathematical Modeling of the Gas Hydrate Formation in a 90° Elbow Utilizing CFD Technique," *Chemical Engineering Transactions*, vol. 70, pp. 2167–2172, 2018.
- [24] J. Gibbins and H. Chalmers, "Carbon capture and storage," *Energy Policy*, vol. 36, no. 12, pp. 4317–4322, 2008.
- [25] L. Faramarzi, "Post-combustion capture of CO₂ from Fossil Fueled Power Plants," Technical University of Denmark, 2010.
- [26] V. Darde, K. Thomsen, W. J.M. van Well, D. Bonalumi, G. Valenti, and E. Macchi, "Comparison of two electrolyte models for the carbon capture with aqueous ammonia," *International Journal of Greenhouse Gas Control*, vol. 8, pp. 61–72, 2012.
- [27] K. Thomsen, "Electrolyte Solutions: Thermodynamics, Crystallization, Separation Methods," pp. 1–61, 2009.
- [28] W. R. Smith, F. Moučka, and I. Nezbeda, "Osmotic pressure of aqueous electrolyte solutions via molecular simulations of chemical potentials: Application to NaCl," *Fluid Phase Equilibria*, vol. 407, pp. 76–83, 2016.
- [29] R. A. Robinson and R. H. Stokes, *Electrolyte Solutions: Second Revised Edition*: Dover Publications, Incorporated, 2012.
- [30] H. E. Debye P., "Zur Theorie der Elektrolyte. I. "Gefrierpunktserniedrigung und verwandte Erscheinungen", *Physikalische Zeitschrift*," vol. 24, pp. 185–206, 1923.
- [31] J. W. Morales, H. R. Galleguillos, M. E. Taboada, and F. Hernández-Luis, "Activity coefficients of NaCl in PEG 4000+water mixtures at 288.15, 298.15 and 308.15K," *Fluid Phase Equilibria*, vol. 281, no. 2, pp. 120–126, 2009.
- [32] Hückel E., "Zur Theorie konzentrierterer wässriger Lösungen starker Elektrolyte," *Physikalische Zeitschrift*, no. 26, pp. 93–147, 1925.
- [33] T. Z. Fahidy, "Activity coefficients in electrolyte solutions (second edition), edited by Kenneth S. Pitzer" *Can. J. Chem. Eng.*, vol. 71, no. 3, p. 494, 1993.
- [34] K. S. Pitzer, "Thermodynamics of electrolytes. I. Theoretical basis and general equations,"
- [35] K. S. Pitzer, "Electrolytes. From dilute solutions to fused salts," *Journal of the American Chemical Society*, vol. 102, no. 9, pp. 2902–2906, 1980.
- [36] G. M. Wilson, "Vapor-Liquid Equilibrium. XI. A New Expression for the Excess Free Energy of Mixing," *Journal of the American Chemical Society*, vol. 86, no. 2, pp. 127–130, 1964.
- [37] K. Thomsen, "Aqueous Electrolytes Model Parameters and Process Simulation," Technical University of Denmark, 1997.
- [38] D. S. Abrams and J. M. Prausnitz, "Statistical thermodynamics of liquid mixtures: A new expression for the excess Gibbs energy of partly or completely miscible systems," *AIChE J.*, vol. 21, no. 1, pp. 116–128, 1975.
- [39] Chaun-Chyun Chen, H. I. Britt, J. F. Boston, and L. B. Evans, "Local composition model for excess Gibbs energy of electrolyte systems. Part I: Single solvent, single completely dissociated electrolyte systems," *AIChE Journal*, vol. 28, no. 4, pp. 588–596, 1982.
- [40] Chaun-Chyun Chen and L. B. Evans, "A local composition model for the excess Gibbs energy of aqueous electrolyte systems," *AIChE Journal*, vol. 32, no. 3, pp. 444–456, 1986.
- [41] B. Maribo-Mogensen, "Development of an Electrolyte CPA Equation of state for Applications in the Petroleum and Chemical Industries,"

- [42] B. Maribo-Mogensen, G. M. Kontogeorgis, and K. Thomsen, "Comparison of the Debye–Hückel and the Mean Spherical Approximation Theories for Electrolyte Solutions," *Ind. Eng. Chem. Res.*, vol. 51, no. 14, pp. 5353–5363, 2012.
- [43] S. Ahmed, "Modélisation thermodynamique des mélanges électrolytiques multi-solvants pour les simulateurs de procédés," 2018.
- [44] G. Maurer and J. M. Prausnitz, "On the derivation and extension of the uniquac equation," *Fluid Phase Equilibria*, vol. 2, no. 2, pp. 91–99, 1978.
- [45] J. I. Carrero-Mantilla, D. d. J. Ramírez-Ramírez, and J. F. Suárez-Cifuentes, "Thermodynamic and statistical consistency of vapor–liquid equilibrium data," *Fluid Phase Equilibria*, vol. 412, pp. 158–167, 2016.
- [46] Hückel E., "Zur Theorie konzentrierterer wässriger Lösungen starker Elektrolyte," *Physikalische Zeitschrift*, 1925, pp. 93–147, 1925.
- [47] Joseph F. Zemaitis Jr, Diane M. Clark, Marshall Rafal, and Noel C. Scrivner, *Activity Coefficients of Single Strong Electrolytes*, 1986.
- [48] R. F. Platford, "Osmotic coefficients of aqueous solutions of seven compounds at 0.deg.,"
- [49] J. I. Partanen and A. K. Covington, "Re-Evaluation of the Thermodynamic Activity Quantities in Aqueous Sodium and Potassium Chloride Solutions at 25 °C †," *J. Chem. Eng. Data*, vol. 54, no. 2, pp. 208–219, 2009.
- [50] J. P. Simmons, H. Freimuth, and H. Russell, "The Systems Lithium Chloride–Water–Ethyl Alcohol and Lithium Bromide–Water–Ethyl Alcohol^{1,2}," *Journal of the American Chemical Society*, vol. 58, no. 9, pp. 1692–1695, 1936.
- [51] T. T. Duignan, D. F. Parsons, and B. W. Ninham, "Collins's rule, Hofmeister effects and ionic dispersion interactions," *Chemical Physics Letters*, vol. 608, pp. 55–59, 2014.
- [52] K. D. Collins, "Ions from the Hofmeister series and osmolytes: Effects on proteins in solution and in the crystallization process," *Methods (San Diego, Calif.)*, vol. 34, no. 3, pp. 300–311, 2004.
- [53] M. D. Tissandier *et al.*, "The Proton's Absolute Aqueous Enthalpy and Gibbs Free Energy of Solvation from Cluster-Ion Solvation Data," *The Journal of Physical Chemistry A*, vol. 102, no. 40, pp. 7787–7794, 1998.
- [54] K. D. Collins, "Charge density-dependent strength of hydration and biological structure,"
- [55] David Lide, "CRC Handbook of Chemistry and Physics, 91th Edition: Aqueous Solubility of Inorganic Compounds at Various Temperatures,"
- [56] M. A. Selam, I. G. Economou, and M. Castier, "A thermodynamic model for strong aqueous electrolytes based on the eSAFT-VR Mie equation of state," *Fluid Phase Equilibria*, vol. 464, pp. 47–63, 2018.
- [57] H. S. Harned and L. F. Nims, "The thermodynamic properties of aqueous sodium chloride solutions from 0 to 40°," *Journal of the American Chemical Society*, vol. 54, no. 2, pp. 423–432, 1932.
- [58] H. F. Gibbard, G. Scatchard, R. A. Rousseau, and J. L. Creek, "Liquid-vapor equilibrium of aqueous sodium chloride, from 298 to 373.deg.K and from 1 to 6 mol kg⁻¹, and related properties," *J. Chem. Eng. Data*, vol. 19, no. 3, pp. 281–288, 1974.
- [59] K. Akita and F. Yoshida, "Phase-Equilibria in Methanol–Ethyl Acetate–Water System," *J. Chem. Eng. Data*, vol. 8, no. 4, pp. 484–490, 1963.
- [60] Hülya YILMAZ, "Excess Properties of Alcohol - Water Systems at 298.15 K," *Turk J Phys*, vol. 26, no. 3, 243-246., 2002.

- [61] F. Deyhimi and M. Abedi, "NaCl + CH₃OH + H₂O Mixture: Investigation Using the Pitzer and the Modified Pitzer Approaches To Describe the Binary and Ternary Ion–Nonelectrolyte Interactions," *J. Chem. Eng. Data*, vol. 57, no. 2, pp. 324–329, 2012.
- [62] G. Scatchard and S. S. Prentiss, "The Freezing Points of Aqueous Solutions. IV. Potassium, Sodium and Lithium Chlorides and Bromides," *Journal of the American Chemical Society*, vol. 55, no. 11, pp. 4355–4362, 1933.
- [63] S.-O. Yang and C. S. Lee, "Vapor–Liquid Equilibria of Water + Methanol in the Presence of Mixed Salts," *J. Chem. Eng. Data*, vol. 43, no. 4, pp. 558–561, 1998.

APPENDIX

APPENDIX 1. Existing data summary for different properties

The table 23 represent a summary of data series for different salts and pure water and ethanol as solvent.

Table 23. Classification of experimental data properties for different monovalent salts with pure water and ethanol as solvent

	Li	Na	K	Rb	Cs
F	NO DATA	1 article	2 articles	NO DATA	1 article
		1 article (Isobaric)	2 articles		
		1 article			
		1 article			
Cl	3 articles	4 articles	4 articles	3 articles	2 articles
	2 articles. Only at 298 K	4 articles. Only at 298 K	1 articles. Only at 298 K. The maximum molar fraction of ethanol is very low		2 articles. Only at 298 K
	3 articles	7 articles	4 articles	4 articles	3 articles
	3 articles	29 articles	22 articles		1 article
	1 article			1 article	
Br	2 articles	2 articles. Only at 298 K	1 article	3 articles	1 article. At 298 K. Low molality (up to 0,7 M maximum)
		1 articles	1 article		2 articles
	1 article	2 articles	10 articles		
I	NO DATA	6 articles	4 articles	NO DATA	NO DATA
		1 article	9 articles		
		4 articles			

The system composed by water and ethanol present more salts without any type of data than the previous system. Additionally, there are less variety of data properties for each salt. NaCl, KF, NaF and CsCl salt show some results of experimental data related to liquid-liquid equilibrium. In this system also the solid-liquid equilibrium property is the predominant property. It is also more difficult to find data for activities coefficients.

The table 25 and 26 represent a summary of data series for different salts and pure water with 1-propanol and pure water with 1-butanol respectively.

Table 24. Classification of experimental data properties for different monovalent salts with pure water and 1-propanol as solvent

	Li	Na	K	Rb	Cs
F	NO DATA	NO DATA	4 articles	NO DATA	NO DATA
Cl	7 articles	1 article	1 article	2 articles	1 article
	5 articles (VLE isobaric)	3 articles	2 articles		3 articles
	articles	13 articles	4 articles (VLE isobaric)		
	2 articles	12 articles	4 articles		
Br	NO DATA	1 article (VLE isobaric)	1 article	NO DATA	NO DATA
		2 articles			
I	NO DATA	3 articles	2 articles	NO DATA	3 articles
		2 article	2 article (VLE isobaric)		
			3 articles		

Table 25. Classification of experimental data properties for different monovalent salts with pure water and 1-butanol as solvent

	Li	Na	K	Rb	Cs
F	1 article	1 article	2 articles	NO DATA	NO DATA
Cl	1 article	1 article. At 298 K Low Molality	2 articles	1 article	1 article
		1 article			
		4 articles			
Br	NO DATA	10 articles	6 articles	NO DATA	NO DATA
		1 article	2 articles		
I	NO DATA	3 articles	1 article	NO DATA	NO DATA

The two type of solvents present less data properties available for the properties. In addition, some salts do not present any type of properties data. The Liquid-Liquid equilibrium is the predominant property as we increase the number of carbon of the solvent. The decrease of the solubility of the salt as we increase the number of carbons of the solvent make more the difficult the data measurements.

APPENDIX 2. Summary of available data for monovalent salts

Table 26. Summary of the salts for osmotic coefficient

Salts	Osmotic coefficient		
	Number of articles	Temperature range (K)	Maximum molality (moles/Kg)
LiF	0	---	---
LiCl	25	273.15 - 473.15	20
LiBr	7	298.15 - 498.15	20
LiI	4	298.15	12.05
NaF	4	298.15 - 353.15	1.2
NaCl	47	273.15 - 573.15	6.14
NaBr	13	298.15 - 498.15	10.618
NaI	5	283.15 - 348.15	12.34
KF	6	283.15 - 473.15	17.5
KCl	35	273,15 - 523,15	8.5
KBr	11	298.15 - 498.15	7.43
KI	6	298.15	8.98
RbF	4	298.15	3.5
RbCl	6	298.15	7.8
RbBr	3	298.15	5
RbI	3	298.15	5
CsF	4	298.15	3.5
CsCl	17	298.15 - 523.15	11.4
CsBr	5	298.15 - 498.15	8.27
CsI	3	298.15	3

APPENDIX 3. Internal consistency analysis for the KCl and the CsCl

KCl Analysis:

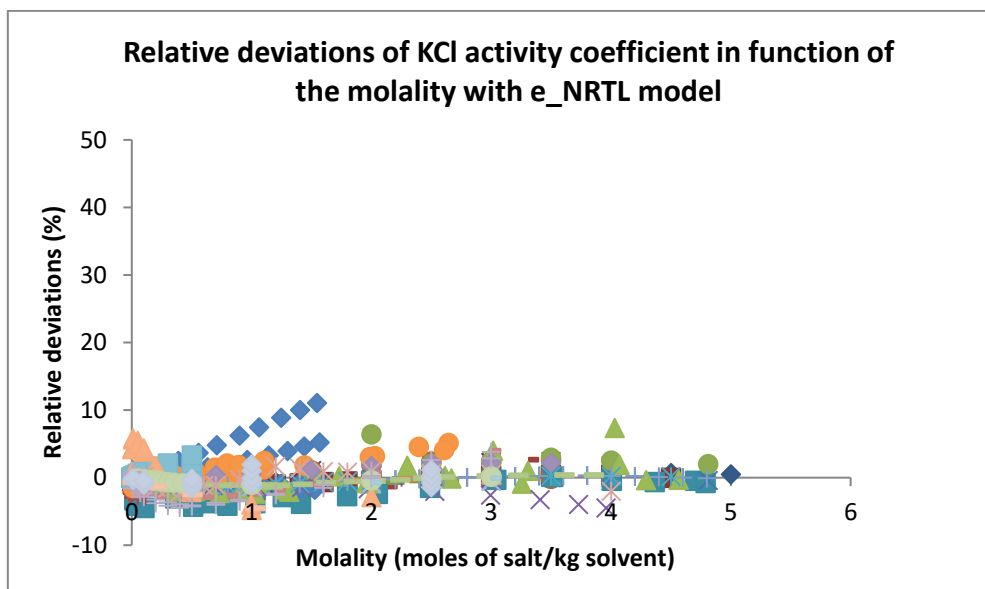


Figure 65. Analysis of the relative deviations in function of the molality for activity coefficient of KCl with water as solvent

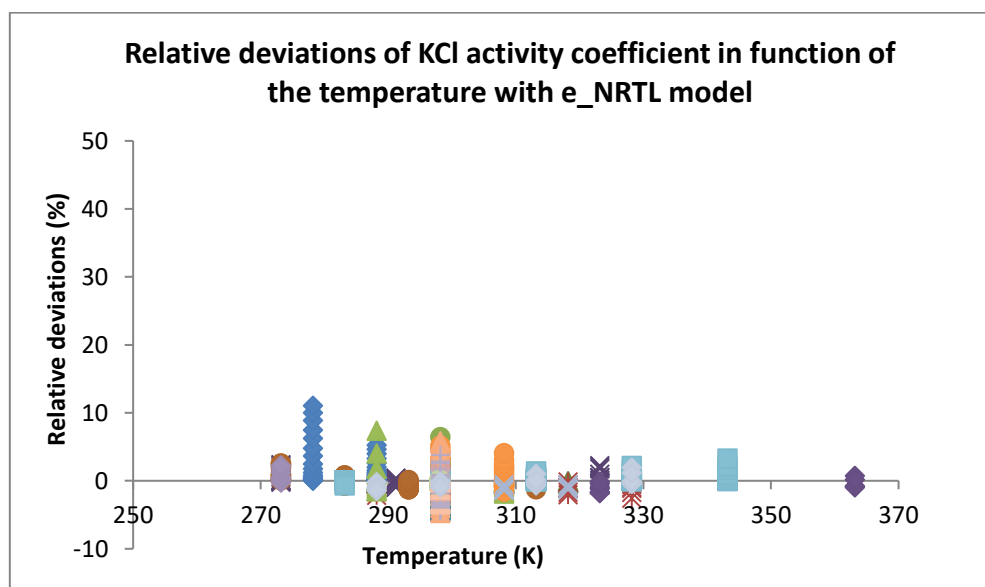


Figure 66. Analysis of the relative deviations in function of the temperature for activity coefficient of KCl with water as solvent

- ◆ DDB-ELE:2008-JAN/2451
- DDB-ELE:2008-JAN/207
- ▲ DDB-ELE:2008-JAN/5043
- × DDB-ELE:2009-JAN/6432
- ✱ DDB-ELE:2011-DEC/8169
- DDB-ELE:2011-DEC/5020
- + DDB-ELE:2013-DEC/9070
- DDB-ELE:2015/10200
- DDB-ELE:2008-JAN/1878
- ◆ DDB-ELE:2010-DEC/7619
- DDB-ELE:2008-JAN/2607
- ▲ DDB-ELE:2015-Mar/9879
- × DDB-ELE:2008-JAN/5890
- ✱ DDB-ELE:2016/11122
- DDB-ELE:2008-JAN/3794
- + DDB-ELE:2015-Mar/9947
- DDB-ELE:2015/10163
- DDB-ELE:2008-JAN/3852
- ◆ DDB-ELE:2011-DEC/8240
- DDB-ELE:2008-JAN/5816
- ▲ DDB-ELE:2011-DEC/8229
- × DDB-ELE:2012-NOV/8727
- ✱ DDB-ELE:2008-JAN/1100
- DDB-ELE:2012-NOV/1979
- + DDB-ELE:2009-AUG/5781
- DDB-ELE:2008-JAN/3959
- DDB-ELE:2017/13341
- ◆ DDB-ELE:2009-JAN/6576
- DDB-ELE:2017/12725
- ▲ DDB-ELE:2016/11706
- × DDB-ELE:2017/13228
- ✱ DDB-ELE:2016/11406
- DDB-ELE:2008-JAN/4408
- + DDB-ELE:2008-JAN/5795
- DDB-ELE:2017/12340
- DDB-ELE:2008-JAN/5062
- ◆ DDB-ELE:2009-AUG/7482

Figure 67. References used for internal consistency of activity coefficient KCl

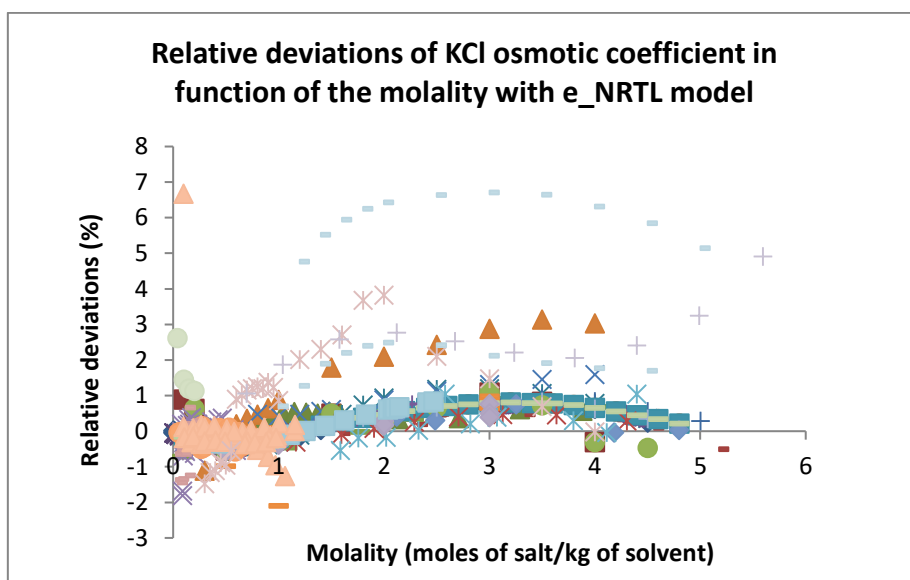


Figure 68. Analysis of the relative deviations in function of the molality for osmotic coefficient of KCl with water as solvent

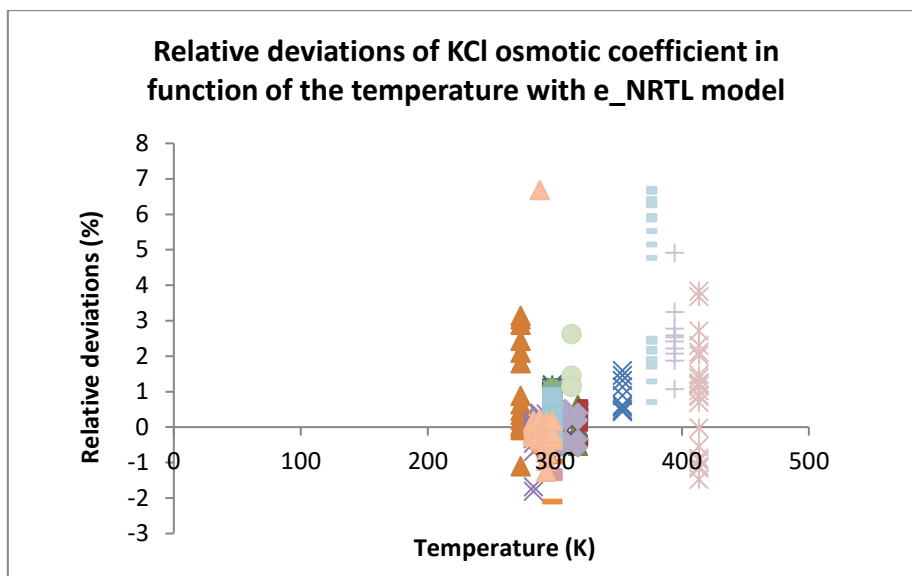


Figure 69. Analysis of the relative deviations in function of the temperature for osmotic coefficient of KCl with water as solvent

- | | | | |
|-------------------------|-------------------------|-------------------------|-------------------------|
| ◆ DDB-ELE:2008-JAN/206 | ◆ DDB-ELE:2015/2097 | | |
| ■ DDB-ELE:2008-JAN/4979 | ■ DDB-ELE:2009-JAN/6358 | ◆ DDB-ELE:2015-Mar/9762 | |
| ▲ DDB-ELE:2017/12042 | ▲ DDB-ELE:2008-JAN/57 | ▲ DDB-ELE:2008-JAN/5780 | ◆ DDB-ELE:2008-JAN/1045 |
| × DDB-ELE:2008-JAN/5047 | × DDB-ELE:2008-JAN/2873 | × DDB-ELE:2008-JAN/3401 | ■ DDB-ELE:2008-JAN/4507 |
| × DDB-ELE:2008-JAN/6100 | × DDB-ELE:2008-JAN/2519 | × DDB-ELE:2008-JAN/6146 | ▲ DDB-ELE:2011-DEC/4119 |
| ● DDB-ELE:2013-DEC/9069 | ● DDB-ELE:2015/10050 | ● DDB-ELE:2016/10908 | × DDB-ELE:2015/10062 |
| + DDB-ELE:2008-JAN/2815 | + DDB-ELE:2016/11277 | + DDB-ELE:2012-NOV/8521 | ● DDB-ELE:2015/10752 |
| - DDB-ELE:2016/10876 | - DDB-ELE:2017/12679 | - DDB-ELE:2012-NOV/8794 | + DDB-ELE:2017/12057 |
| - DDB-ELE:2008-JAN/1911 | - DDB-ELE:2008-JAN/4502 | - DDB-ELE:2017/12979 | - DDB-ELE:2015/10085 |

Figure 70. References used in internal consistency of osmotic coefficient for KCl

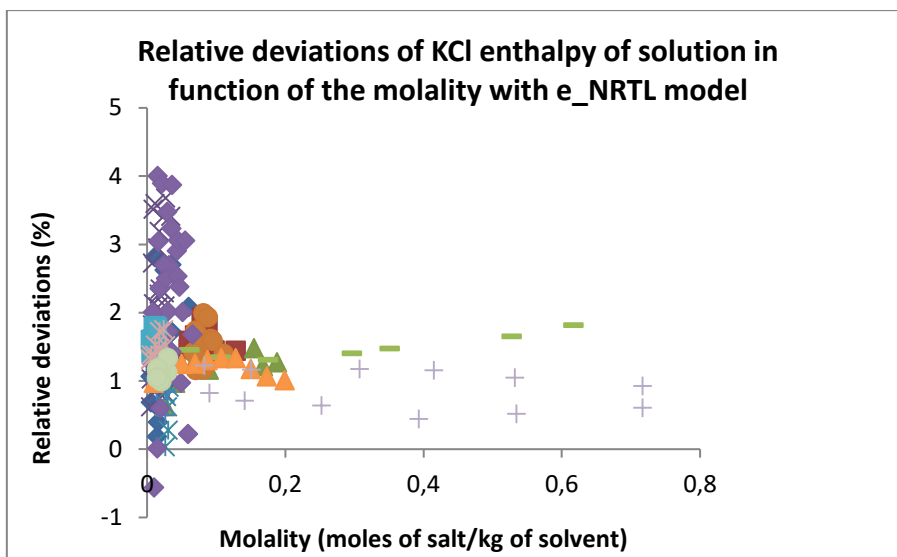


Figure 71. Analysis of the relative deviations in function of the molality for enthalpy of solution of KCl with water as solvent

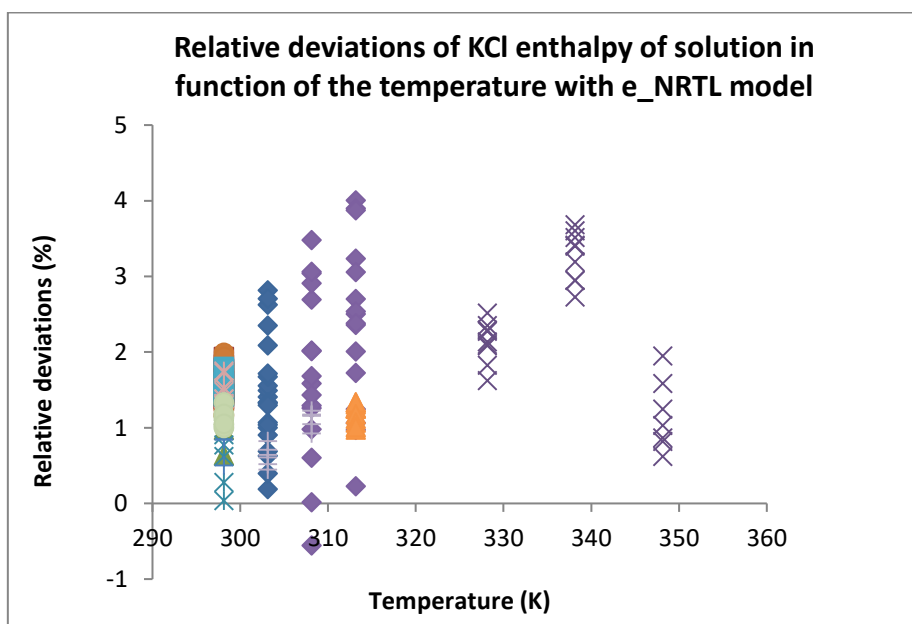


Figure 72. Analysis of the relative deviations in function of the temperature for enthalpy of solution of KCl with water as solvent

- ◆ 2008-FEB-20-14:50/16126
- 2008-FEB-20-14:50/14934
- ▲ 2008-FEB-20-14:50/14482
- × 2008-FEB-20-14:50/15067
- ✱ 2008-FEB-20-14:50/15657
- 2008-FEB-20-14:50/15079
- + 2008-FEB-20-14:50/13357
- 2008-FEB-20-14:50/15297
- ◆ 2008-FEB-20-14:50/15392
- 2008-FEB-20-14:50/16003
- ▲ 2008-FEB-20-14:50/16488
- × 2008-FEB-20-14:50/15876
- 2008-FEB-20-14:50/15896
- + 2008-FEB-20-14:50/15283

Figure 73. References used in internal consistency of enthalpy of solution for KCl

KCl Analysis:

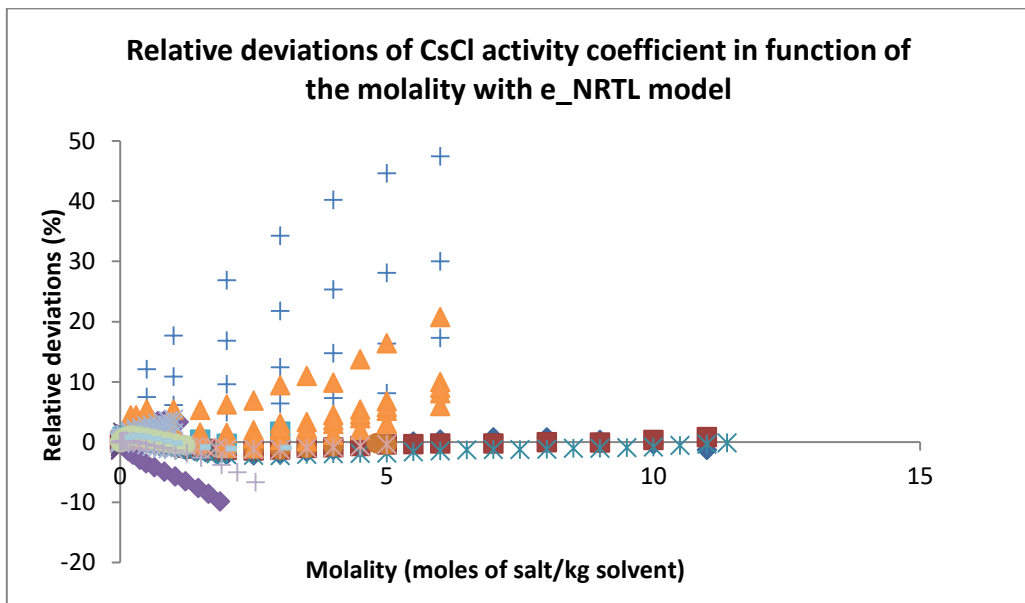


Figure 74. Analysis of the relative deviations in function of the molality for activity coefficient of CsCl with water as solvent

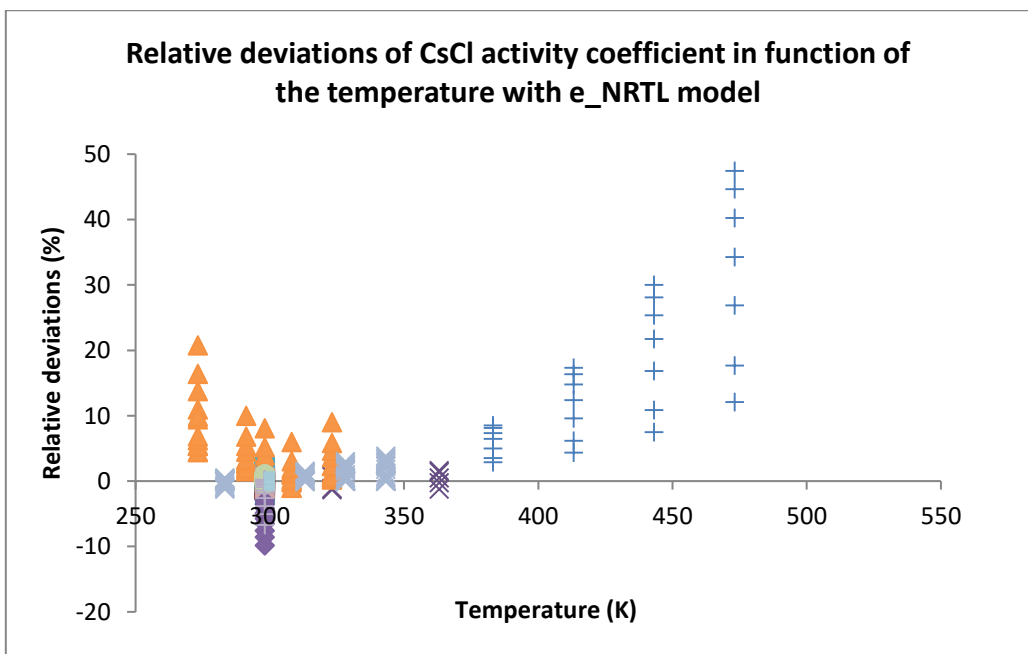


Figure 75. Analysis of the relative deviations in function of the temperature for activity coefficient of CsCl with water as solvent

- ◆ DDB-ELE:2008-JAN/2452
- DDB-ELE:2008-JAN/879
- ▲ DDB-ELE:2008-JAN/2173
- × DDB-ELE:2010-DEC/7625
- ✱ DDB-ELE:2008-JAN/2382
- DDB-ELE:2008-JAN/5894
- + DDB-ELE:2017/12022
- DDB-ELE:2015-Mar/9546
- DDB-ELE:2015-Mar/9601
- ◆ DDB-ELE:2009-JAN/6468
- DDB-ELE:2009-JAN/6580
- ▲ DDB-ELE:2015/10296
- × DDB-ELE:2017/12731
- ✱ DDB-ELE:2008-JAN/1114
- DDB-ELE:2012-NOV/8684
- + DDB-ELE:2017/13271
- DDB-ELE:2008-JAN/2452

Figure 76. References used in internal consistency of activity coefficient for CsCl

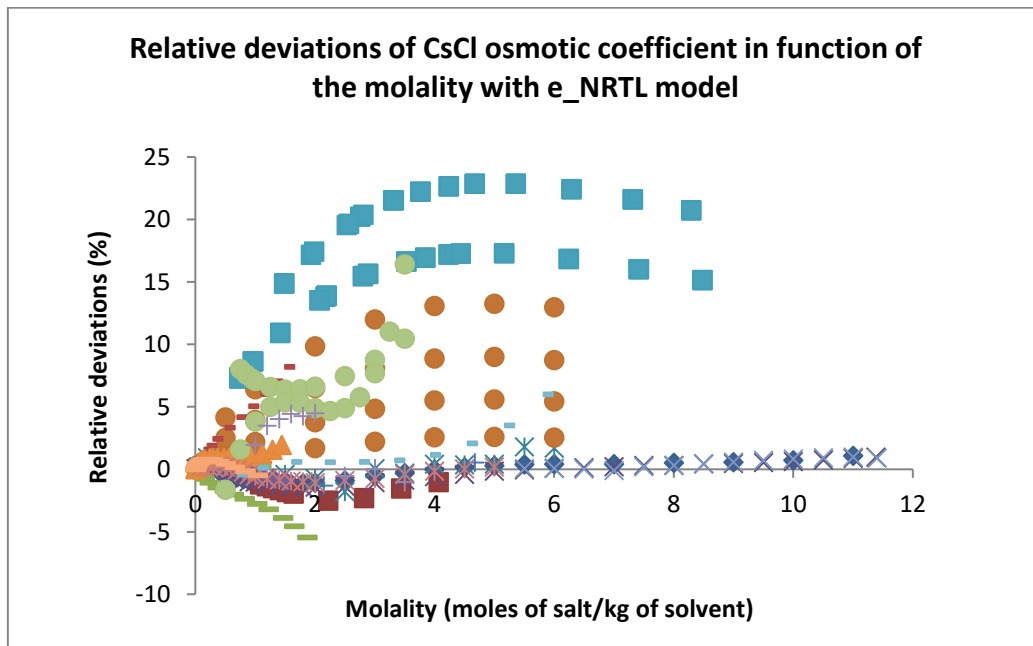


Figure 77. Analysis of the relative deviations in function of the molality for osmotic coefficient of CsCl with water as solvent

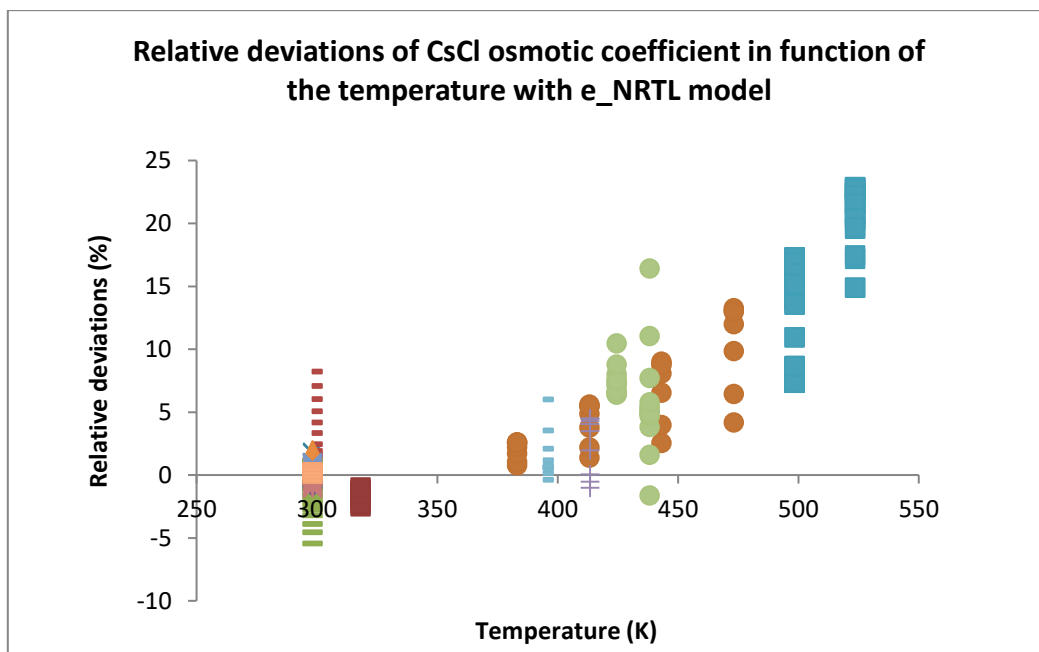


Figure 78. Analysis of the relative deviations in function of the temperature for osmotic coefficient of CsCl with water as solvent

- ◆ DDB-ELE:2008-JAN/878
- DDB-ELE:2017/12043
- × DDB-ELE:2008-JAN/2381
- ✱ DDB-ELE:2017/12681
- DDB-ELE:2008-JAN/3350
- + DDB-ELE:2015/10309
- DDB-ELE:2010-DEC/7711
- DDB-ELE:2015-Mar/9309
- ◆ DDB-ELE:2010-DEC/7890
- DDB-ELE:2008-JAN/6147
- ▲ DDB-ELE:2011-DEC/8439
- × DDB-ELE:2010-DEC/7806
- ✱ DDB-ELE:2008-JAN/1060
- DDB-ELE:2017/12065
- + DDB-ELE:2015/10063
- DDB-ELE:2017/12058
- DDB-ELE:2009-JAN/6740

Figure 79. References used in internal consistency of osmotic coefficient for CsCl